Design and Delivery of a Cryptic PrP^{C} Epitope for the Induction of a PrP^{Sc}-Specific Antibody Response.

A Thesis Submitted to the College of Graduate Studies and Research
in Partial Fulfillment of the Requirements for the
Degree of Doctor of Philosophy in the Department of Biochemistry at the
University of Saskatchewan, Saskatoon

By

Peter D. S. Hedlin

PERMISSION TO USE

In presenting this thesis in partial fulfillment of the requirements for a postgraduate degree from the University of Saskatchewan, I agree that the Libraries of this University may make it freely available for inspection. I further agree that permission for copying of this thesis in any matter, in whole or in part, for scholarly purposes may be granted by the professors who supervised my thesis work, or in their absence, by the Head of the Department or the Dean of the College in which my thesis work was done. It is understood that any copying or publication or use of this thesis or parts thereof for financial gain shall not be allowed without my written permission. It is also understood that due recognition shall be given to me and to the University of Saskatchewan in any scholarly use which may be made of any materials in my thesis.

Requests for permission to copy or make other use of material in this thesis in whole or in part should be addressed to:

Head of the Department of Biochemistry
University of Saskatchewan
Saskatoon, Saskatchewan S7N 0W0

ABSTRACT

Transmissible spongiform encephalopathies (TSEs) represent a unique category of diseases known as protein misfolding diseases. Pathogenesis is dependent on the misfolding of normal cellular prion protein (PrP^{C}), which is thought to occur following physical interaction with the infectious conformation PrP^{Sc} and a yet unknown cofactor molecule(s). Most common immunotherapeutic strategies involve targeting an immune response against the PrP^{C} protein since evidence has shown that functional membrane-expressed PrP^{C} is an absolute requirement for the development of a prion infection. As of yet, however, the true function of PrP^{C} is not known, therefore, stimulating such an immune response against this widely-expressed cell membrane protein may have harmful consequences. Targeting the PrP^{Sc} conformation avoids the potential initiation of an autoimmune response and may circumvent PrP^{C} tolerance mechanisms allowing for a greater Ab mediated immune response; thus representing a safer, and more effective, immunotherapeutic strategy.

A weakly immunogenic PrP^{C} epitope (YYR), which induces antibodies specific for the PrP^{Sc} conformation, was used as the starting point for the development of a prion vaccine. By optimizing epitope design, as well as vaccine formulation and delivery, immunogenicity was enhanced while PrP^{Sc}-specificity was retained. One epitope in particular, QV**YYR**PVDQYSNQN, when created as a genetic fusion with the leukotoxin carrier molecule, appeared to be an immunogenic vaccine candidate. The immune response following two vaccinations with this construct induced a robust and sustained serum PrP^{Sc}-specific IgG antibody response. Specific antibody was also detected in the nasal secretions and cerebral spinal fluid of vaccinated animals. Allowing for the possibility that epitope spreading may occur, resulting in the production of auto-reactive anti-PrP^{C} antibodies, both ELISA and immunoprecipitation experiments were performed and were unable to detect the presence of anti-PrP^{C} antibodies. Altogether the evidence suggests that this epitope may be a good candidate for the development of a TSE vaccine.

ACKNOWLEDGEMENTS

I would like to thank my supervisor Dr. Scott Napper for the chance to work on this exciting project. You have been extremely supportive of all of the opportunities that have arisen and the career path I have chosen to follow. In addition, you have shown great dedication and generosity during my time here, which has made it a truly enjoyable and productive experience. I also extend gratitude to Dr. Philip Griebel who has provided thought-provoking and insightful feedback throughout the entirety of the project. To my advisory and examining committee you have all been tremendously helpful by keeping me on track, giving me direction, showing me where I need to improve, and providing me with prompt feedback to facilitate my timelines, for all of that I thank you.

To everyone at the Vaccine and Infectious Disease Organization (VIDO), you have been like a second family. You have created such a wonderful environment that it was truly a pleasure coming to work every day. A special thanks to: Gordon Crockford for all of his help with the vaccine preparations; Dr. Jyotsana Gupta for her expertise in the molecular work; Dr. Sam Attah-Poku for his assistance in producing the peptides for our vaccine, and everyone in GMP. Because such a large part of this project involved animal trials, the support provided by Drs. Don Wilson and Stewart Walker, along with their entire Animal Care Staff, was absolutely invaluable. I must also thank my fellow graduate students Ryan Arsenault, Ryan Tashcuk, Kristen Marciniuk as well as technicians Kelli Bell, Erin Scruten and Kim Doig for all their assistance and camaraderie. In the Department of Biochemistry I have to thank Margaret Ross for all of her administrative assistance as well as the members of the teaching lab who made working as a teacher assistant a lot of fun.

I'm very privileged to have so many members of my family so close by. Thank you Mom and Dad for all your love, support and home-cooked meals. Congratulations to both of you on your recent retirement! Dad, those weekly squash matches have been a blast. Thanks to my younger brother Matt (aka Sunclef) for giving me a place to stay whenever in Toronto and for inspiring me with your music, it has been exciting watching you develop as an artist, I can't wait to see what your future holds. To my youngest brother Erik, I always look forward to our campus coffee/philosophy sessions. Your passion for wildlife and your innate ability as a photographer is a wonderful pairing, I'm always looking forward to seeing what interesting projects you are working on next. I wish you all the best as you venture out into the world of

graduate studies. To my beautiful wife Cherise, you are the most thoughtful, understanding and supportive person I know. Although it seems an unlikely prospect at the moment I assure you that some day I WILL have a job. You have been amazingly patient through this whole process!

Finally, I am thankful for all of the financial support provided by the Department of Biochemistry, the College of Medicine, PrioNet Canada, the Natural Science and Engineering Council of Canada as well as the operating grants obtained by Dr. Scott Napper.

TABLE OF CONTENTS

LIST OF FIGURES

LIST OF TABLES

LIST OF ABBREVIATIONS

AD	Alzheimer's disease
Ag	Antigen
ALS	Amyotrophic lateral sclerosis
Aβ	Amyloid-β
APC	Antigen presenting cell
BSE	Bovine spongiform encephalopathy
CWD	Chronic wasting disease
CJD	Creutzfeldt-Jacob disease
ENS	Enteric nervous system
ER	Endoplasmic reticulum
ERK	Extracellular signal-regulated kinase
FDC	Follicular dendritic cell
GABA	Gamma-aminobutyric acid
GnRH	Gonadotropin-releasing hormone
GPI	Glycosylphosphatidyl inositol
HD	Huntington's disease
IC	Intra-cranial
IgA	Immunoglobulin A
IgG	Immunoglubulin G
IgM	Immunoglobulin M
IP	Imunnoprecipitation
i.p.	Intra-peritoneal
KLH	Keyhole limpet hemocyanin
Lkt	Leukotoxin carrier molecule
MAPK	Mitogen-activated protein kinase
mAb	Monoclonal antibody
NMR	Nuclear magnetic resonance
PD	Parkinson's disease
PI3K	Phosphoinositide 3-Kinase

PK	Proteinase K
Prion	Proteinaceous infectious particle
Prnp	Gene encoding the prion protein
PrP	Prion protein
PrP^{C}	Cellular non-infectious prion protein
PrP^{Sc}	Infectious prion protein
ROS	Reactive oxygen species
sCJD	Sporadic Creutzfeldt-Jacob disease
SC	Sub-cutaneous
SOD	Superoxide dismutase
TNF	Tumor necrosis factor
TSEs	Transmissible spongiform encephalopathy
vCJD	Variant Creutzfeldt-Jacob disease
WT	Wild type

1.0 LITERATURE REVIEW

Although trillions of dollars have been invested in the development of antibiotics, antivirals and vaccines, infectious diseases are still responsible for 22% of all human deaths (http://apps.who.int/tdr/svc/publications/tdr-research-publications/globalization-infectious-diseases. Traditionally, these infectious diseases were limited to the categories of bacterial, viral, fungal and parasitic. Disease caused by each category of infectious agent reflects the unique biological interaction between the agent and the host. In spite of these differences, these agents are all unified by the utilization of genetic material for protein expression and replication of the agent. More recently, a novel infectious agent which lacks its own genome and is capable of causing devastating pathology in both humans and animals, has been identified. Specifically, following the efforts of anthropologists, pathologists and physicians in Papua New Guinea during the 1950's, a unique neurological disease, Kuru, afflicting the indigenous Fore tribes, was discovered. Initially described as being caused by a "slow" virus, further research in the 1970's revealed that this new agent lacked the qualifying features (nucleic acid) necessary for its classification as a virus. This was later termed by Stanley Prusiner as a proteinaceous infectious agent or "prion". Consequently, after much resistance from the scientific community, it was established that a new class of infectious agent had been discovered.

1.1 Prions

1.1.1 Prions as Infectious Agents

The discovery of Kuru stimulated research leading to the identification of a group of neurodegenerative disorders referred to as transmissible spongiform encephalopathies (TSEs). The concept of "slow viruses" was first described by Sigurdsson while researching neurodegenerative disease in sheep (Sigurdsson, 1954). Later, in 1959, a veterinary pathologist Hadlow, hypothesized that Kuru and Scrapie were related disorders. At the same time, similar assumptions about Kuru and another neurodegenerative disease that was called Creutzfeldt-Jacob disease were made (Klatzo *et al.*, 1959). The work by Gajdusek's group changed the

ideology regarding the cause of neurodegenerative disorders when they successfully transmitted Kuru to chimpanzees (Gajdusek *et al.*, 1966). This indicated that a transmissible agent was responsible for the disease (Gibbs *et al.*, 1968).

Following the logic that the observed neurodegeneration was due to an infectious agent, an exhaustive search for the traditional signs of an infectious agent began. Populations of T and B-cells were analyzed in both Scrapie-infected and control mice, but no differences between the experimental and control groups were detected (Garfin *et al.*, 1978). Experiments looking at the potential influence that B-cell maturation may have on Scrapie infections showed no difference in disease incubation or progression between infected wild-type mice and infected mice deficient in mature B-cells (Kasper *et al.*, 1982). Therefore, B-cell maturation did not appear to play a role in the Scrapie disease process. Attempts to detect a Scrapie-induced humoral response by immunofluorescence, neutralization and precipitation all failed (Kasper *et al.*, 1981). What was determined, however, was that Scrapie infections appeared to involve the lymphoreticular system (Stites *et al.*, 1979). Independent of the site of inoculation, high Scrapie titers were detectable in the spleen and other lymphoid organs (Dickinson and Fraser, 1969).

While many researchers had shown Scrapie was a transmissible disease, extensive research was indicating that the Scrapie agent behaved in a fashion that was distinct from known infectious organisms. With Scrapie infection studies producing perplexing results, Stanley Prusiner focused his work on characterizing the infectious component of these seemingly linked neurodegenerative disorders. Sedimentation experiments demonstrated that the Scrapie agent aggregated with cellular components (Prusiner *et al.*, 1980), and was stable in non-ionic and anionic detergents (Prusiner, 1982). Other experiments revealed it to be a hydrophobic molecule, a characteristic that complicates purification procedures and allows for extreme heat stability (Prusiner *et al.*, 1978). Several key pieces of evidence indicated that one of the required components of infectivity was a protein; digestion with proteinase K or protein denaturation via sodium dodecyl sulfate (SDS), trypsin, phenol, urea and chaotropic salts all led to a loss of infectivity (Prusiner *et al.*, 1981).

Early attempts to identify the genetic component associated with the Scrapie agent began with pH stability studies. Infectious material was inactivated at alkaline pH, whereas acidic treatments had no effect (Prusiner, 1982). Because alkali conditions disrupt both

proteins and nucleic acid, the results were unable to rule out the presence of nucleic acids in association with the Scrapie agent (Prusiner, 1982). Further experiments, in particular ones that determined the Scrapie agent was resistant to nuclease digestion and ultraviolet irradiation, suggested there was no nucleic acid content in the Scrapie agent (Prusiner, 1982). Collectively, the extensive molecular analysis determined that the Scrapie agent was different from plasmids, viroids, and viruses. Specifically, its resistance to nucleic acid degradation treatments, small size, and resistance to heat inactivation suggested the Scrapie agent to be a new type of infectious agent. Prusiner labelled these agents as "prions" which he defined as "small proteinaceous infectious particles which are resistant to inactivation by most procedures that modify nucleic acids" (Prusiner, 1982).

1.1.2 Cellular PrP

Human PrP^{C}, a 253 amino acid protein, is encoded by the prion gene *Prnp* located on the short arm of chromosome 20. In addition to regulatory regions such as heat shock elements, *Prnp* is composed of three exons (Haigh *et al.*, 2007). The discovery that the entire open reading frame is contained within a single exon (the third one) helped eliminate the possibility that PrP^{Sc} is produced by alternative RNA splicing (Basler *et al.*, 1986). Little is known regarding the regulation of this gene other than the entire first intron is required for full promoter activity (Inoue *et al.*, 1997) and that the heat shock elements are responsible for up-regulation of expression during periods of cellular stress (Shyu *et al.*, 2000). In 2007 it was shown that in the absence of intron 1, exon 1 decreased the activity of the promoter. This suggested that different control mechanisms may be utilized based on the cellular requirements, and that targeting intron 1, to reduce PrP^{C} expression in Scrapie infected animals, may help to slow disease progression (Haigh *et al.*, 2007).

1.1.2.1 PrP^{C} Structure

The cellular prion protein (PrP^{C}) is a membrane protein containing a glycosylphosphatidyl inositol (GPI) anchor and is highly conserved amongst mammalian species. PrP^{C} mRNA is constitutively expressed in many different tissues with the highest

levels of PrP^C mRNA expression in the neurons (Kretzschmar *et al.*, 1986) but there are also significant levels of expression in the heart (Brown *et al.*, 1990), skeletal muscle (Bosque *et al.*, 2002; Brown *et al.*, 1998), lymphoid tissue/white blood cells (Liu *et al.*, 2001; Paltrinieri *et al.*, 2004), gut tissues (Morel *et al.*, 2004), and reproductive tissues such as the testes and uterus (Tanji *et al.*, 1995). Before PrP^C is delivered to the outer cell membrane, it is targeted to the endoplasmic reticulum (ER) where the N-terminal signal peptide is cleaved and a GPI anchor is added to the C-terminus at serine 231, creating a 209 amino acid protein (Hope *et al.*, 1986). Once at the outer membrane, PrP associates with lipid rafts and is cycled between the cell surface and the endocytic compartment at approximately 60 minute intervals with 95% of the internalized protein getting recycled back to the cell surface (Shyng *et al.*, 1993). Nuclear magnetic resonance (NMR) studies have determined that PrP^C has a flexible N-terminal unstructured domain which contains four octapeptide-repeat regions, and a globular C-terminal domain consisting of three α–helices and two anti-parallel β–sheet structures [**Figure 1.1 a, b**](Riek *et al.*, 1996). There is a hydrophobic sequence in the middle of the protein from amino acids 113-135 which some suggest may serve as a transmembrane domain in some prion isoforms (Bartz *et al.*, 2000). Additionally, there is a single disulphide bond between cysteine residues 179 and 214 and two N-glycosylation sites at asparagine residues 182 and 198 (Cappai and Collins, 2004).

Prion structural comparisons among species (human, Syrian hamster and bovine) indicate great similarity, which is anticipated with 90% sequence homology (Alonso *et al.*, 2002). Cervid PrP, however, contains a unique and well defined rigid loop located between α-helix 2 and the connecting β-strand (amino acids 166-175) [**Figure 1.2 a, b**]. This same region in other species is flexible and disordered. Further investigations revealed that the rigidity of the loop in cervids is due to a two amino acid substitution S170N and N174T (Sigurdson and Aguzzi, 2007). Structural differences in PrP^C have been shown to influence species susceptibility to PrP^{Sc}. Consequently, it has been hypothesized that the rigid loop structure in cervid PrP may be a contributing factor to the rapid horizontal CWD transmission observed in wild populations (Sigurdson and Aguzzi, 2007).

a)

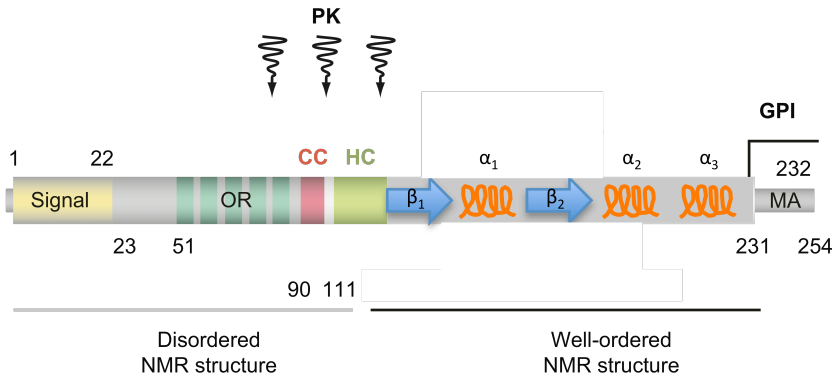

b)

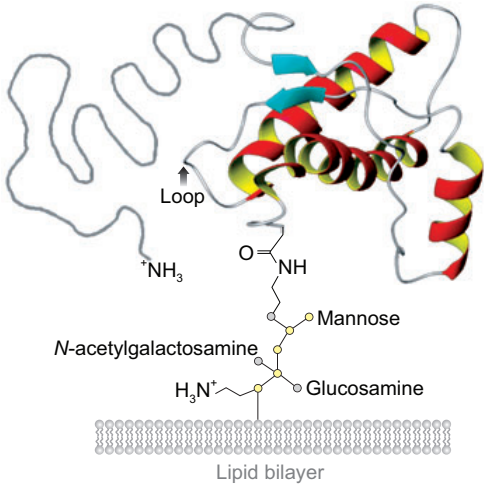

Figure 1.1: Structural features of PrP^C. a) Representation of the primary structure of PrP^C and its post-translational modifications. The numbers indicate amino acid position within the protein. OR (green) refers to the flexible octapeptide repeat region. CC (pink) shows the charged cluster. HC (green) is the hydrophobic core. The approximate cutting sites of proteinase K (PK) are indicated by the black arrows. Blue arrows represent the β-sheets while orange loops depict the α-helices. GPI is the glycosyl phosphatidyl inositol anchor and MA is the membrane anchor. b) Tertiary structure of PrP^C based on NMR spectroscopy including unstructured N-terminal and globular C-terminal domains. The α-helices are in red and the β-sheets are in blue. Adapted from references (Aguzzi and Heikenwalder, 2006). Permission from the publisher was granted for use of this material.

a)

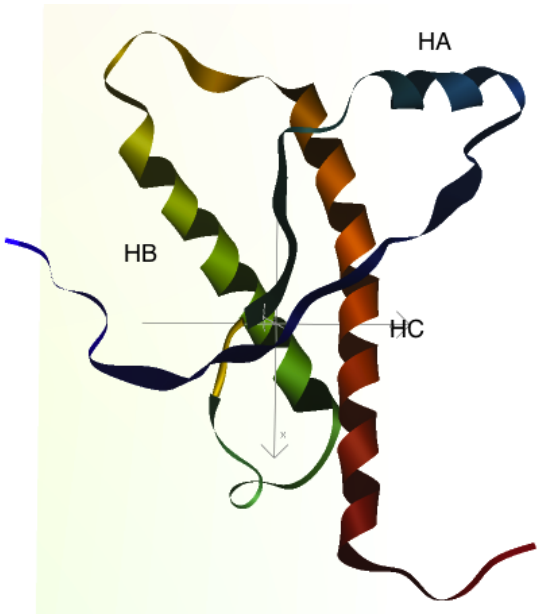

b)

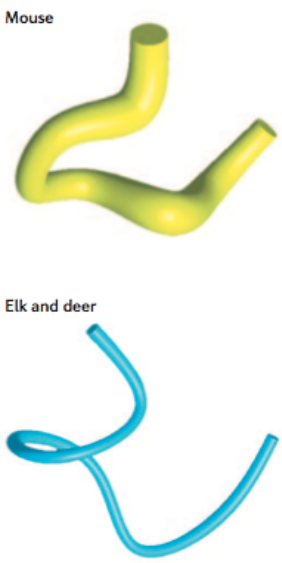

Figure 1.2: Cervid PrP^{C} structure. (a) NMR structure for elk prion protein. HA, HB and HC indicate the location α-helix 1, 2 and 3 respectively. Adapted from (Gossert *et al.*, 2005) using iMol. (b) Prion loop structural representations for both mice and elk corresponding to amino acids 165-174, a region between β-sheet 2 and α-helix 2. In most species the loop region is entirely flexible, however in elk and deer the same region is rigid. Adapted from (Aguzzi and Heikenwalder, 2006). Permission from the publisher was granted for use of this material.

1.1.2.2 PrP^C Function

Despite the highly conserved sequence across species and ubiquitous expression within the body, little is known about the actual function of PrP^C. It has been hypothesized, however, that the prion protein may be involved in the following biological processes: copper metabolism, due to its binding affinity of copper; neuroprotective function due to its anti-apoptotic activity (Bounhar *et al.*, 2001; Diarra-Mehrpour *et al.*, 2004); signal transduction (Koch *et al.*, 1991; Mouillet-Richard *et al.*, 2000); synapse formation/function (Aguzzi *et al.*, 2008a) and neuritogenesis (Graner *et al.*, 2000).

Copper has an important physiological role in all organisms, functioning as a cofactor in processes such as oxidative stress protection, blood clotting, normal cell growth and development, respiration, and iron transport (Puig and Thiele, 2002). Insufficient copper concentrations in humans have been linked to serious diseases which include Menkes syndrome (Harrison and Dameron, 1999), as well as various neurodegenerative disorders such as Alzheimer's disease (AD), amyotrophic lateral sclerosis (ALS) and transmissible spongiform encephalopathies (TSEs) (Waggoner *et al.*, 1999). Numerous studies have shown that the histidine-containing octapeptide repeat region of the PrP^C protein is capable of binding up to four Cu^{2+} ions (Walter *et al.*, 2006). These copper ions stimulate a conformational change in PrP^C, resulting in a structure that has some conserved characteristics similar to the infectious conformation, including a higher β–sheet content, increased protease resistance, a propensity for aggregation, but the structure is still distinct from the PrP^{Sc} isoform (Quaglio *et al.*, 2001). It was also found that micromolar concentrations of copper induce endocytosis of cell-surface associated PrP^C (Pauly and Harris, 1998). Consequently, it has been suggested that PrP^C has a role in copper uptake/efflux and may also serve as copper reservoir at the cell surface without stimulating endocytosis (Westergard *et al.*, 2007).

One model which has been used to explain the pathogenesis of several neurodegenerative disorders is chronic oxidative stress. Impairment of mitochondrial function, increased oxidative damage, defects in the ubiquitin-proteosome system, protein aggregation, altered iron metabolism, excitotoxicity and inflammation have all been linked to oxidative stress in the brain (Halliwell, 2006). Studies of oxidative stress in neurons found that PrP^C seems to protect against reactive oxygen species (ROS) (Milhavet and Lehmann, 2002).

Westergard *et al*. proposed three possible mechanisms by which this may occur. One explanation is that the PrP^C acts directly on the ROS via a copper-dependent superoxide dismutase (SOD) activity (Brown *et al.*, 1999). SOD's are enzymes which remove reactive oxygen species by converting them into more stable molecules (H_2O_2) (Halliwell, 2006). A second theory is that PrP^C acts indirectly by up-regulating activities of molecules like Cu-Zn SOD (Westergard *et al.*, 2007). The last hypothesis posits that PrP^C may prevent activation of ROS induced apoptosis (Halliwell, 2006).

In vitro signalling analysis and prion knockout ($PrP^{0/0}$) studies indicate PrP^C mediates the interaction between several signalling transduction pathways which include protein kinase A, Fyn, phosphatidylinositide 3-kinase (PI3K)/Akt, and mitogen-activated protein kinase/extracellular signal-regulated kinase (MAPK/ERK) known to induce neuronal survival (Chiarini *et al.*, 2002; Mouillet-Richard *et al.*, 2000). Through studies examining induced ischemic injuries in neuronal tissue of $PrP^{0/0}$ and wild type (WT) mice, it was demonstrated that the absence of PrP^C exacerbates ischemic brain injury. The authors hypothesized this was due to reduced activation of the anti-apoptotic pathway PI3K/Akt which in turn resulted in increased caspase-3 activity (Weise *et al.*, 2006).

Protein localization studies indicate the presence of PrP^C in the pre-synaptic region of the axon terminus (Fournier *et al.*, 1995). This observation is supported by the pathological changes such as synapse loss, PrP^{Sc} accumulation at the synaptic terminal (Jeffrey *et al.*, 2000), and abnormal electrophysiological recordings during prion disease progression (Barrow *et al.*, 1999). In the terminal stages of disease, accumulation of PrP^{Sc} in synaptosomes was found to coincide with alterations in the gamma-aminobutyric acid (GABA) system which is involved in the inhibition of excitatory glutamatergic transmission (Bouzamondo-Bernstein *et al.*, 2004). The synaptic involvement of PrP^C may also be responsible for the altered circadian rhythms (Tobler *et al.*, 1996) and impaired hippocampal-dependent spatial learning phenotype in PrP-deficient mice (Criado *et al.*, 2005).

With evidence that PrP^C function is linked to programmed cell death pathways (Kurschner and Morgan, 1995, 1996), it seems logical that studies have described a relationship between PrP^C and numerous cancer pathways. An important concept in tumorigenesis and the development of resistance to anti-cancer drugs is the ability of malignant cells to escape apoptotic death (Johnstone *et al.*, 2002). Consequently, cancer researchers have been

investigating strategies to overcome resistance and induce apoptotic death in cancer cells. While analysing genetic determinants of tumor cell resistance to the cytotoxic effects of tumor necrosis factor (TNF) in breast cell carcinoma cells, Diarra-Mehrpour *et al*. (2004) demonstrated that endogenous PrP^{C} mRNA and protein levels were 17-fold and 10-fold higher in TNF-resistant cells compared to TNF-sensitive cells. They further showed that ectopic expression of PrP^{C} produced TNF-resistance in previously sensitive breast adenocarcinoma cells (MCF7) via an alteration in cytochrome *c* release from nuclear condensation and mitochondria. This suggested that PrP^{C} has a role in the development of tumor resistance (Diarra-Mehrpour *et al.*, 2004). In a follow-up study, the same authors showed that silencing PrP^{C} in apoptotic resistant MCF7 cells activated the proapoptotic Bax by reducing Bcl-2 expression and consequently sensitized the cells to TNF induced apoptosis (Meslin *et al.*, 2007).

1.1.3 Infectious PrP

The infectious component of prion diseases appears to be an insoluble β–sheet-rich version of the normal non-pathogenic α–helical PrP^{C}. While the primary structures of the two isoforms are identical, differences in secondary and tertiary structure account for the unique properties of PrP^{Sc} (Zou and Cashman, 2002). Unlike PrP^{C}, the infectious isoform is resistant to proteinase K (PK) digestion and readily forms insoluble aggregates (Prusiner, 1998). These aggregates are composed of hydrolyzed fragments of the PrP^{Sc} protein, referred to as PrP 27-30 to reflect their molecular weights that range between 27 and 30 kDa. While crystal and NMR structures have been determined for PrP^{C}, the tendency for PrP^{Sc} to aggregate prevents the application of structural analysis. Through techniques such as circular dichroism, which offer less specific structural information, it has been determined that there is an increase in β–sheet content from 3% to 42% as the conformation changes from PrP^{C} to PrP^{Sc} (Pan *et al.*, 1993).

Although PrP^{Sc} is generally described as the infectious conformation, subtle variations exist which make identifying the exact infectious component more challenging. One variation, referred to as PrPSensitive (PrP^{Sen}), is more susceptible to PK digestion than another variation, PrPResistant (PrP^{Res}). While most PrP^{Sc} infected tissues contain PrP^{Res}, its presence in not an absolute requirement for infectivity (Bessen and Marsh, 1994; Lasmezas *et al.*, 1997). PrP^{Sen}

has also been identified in Scrapie-infected tissue, making it difficult to discern which version is truly responsible for infectivity (Caughey *et al.*, 1995; Safar *et al.*, 1998). While data are inconclusive in this regard, there is evidence for the existence of multiple PrP^{Sc} isoforms, also referred to as strains, which possess unique infectivity, pathology, neurotropism and biophysical traits. The concept of prion strains will be discussed later.

1.1.3.1 Pathogenesis

The formation of PrP^{Sc} is thought to occur via interaction between PrP^{C} and an infectious PrP^{Sc} particle whereby PrP^{Sc} induces refolding of PrP^{C} to PrP^{Sc}. PrP^{C} is an absolute requirement for conversion and infection. Infection of PrP deficient mice with PrP^{Sc} material produces no accumulation of infectious material or disease. When PrP^{C} expression was restored, typical prion disease pathology was observed (Mallucci *et al.*, 2003). Transgenic mice, engineered such that PrP is produced without the GPI anchor, resist clinical symptoms following inoculation with Scrapie. Unlike PrP knock-out mice, however, the GPI anchor transgenic mice still produced PrP^{Sc} and amyloid plaque aggregation (Chesebro *et al.*, 2005). This experiment illustrates the need for PrP^{C} to be membrane-anchored for Scrapie pathology to develop.

One research group investigated whether PrP^{C} expression was necessary on all types of brain cells (neurons, astrocytes and oligodendrocytes) for susceptibility to prion disease, formation of PrP^{Sc} and transmission of infectivity. Several transgenic mouse lines were created to selectively express PrP^{C}. Mice with exclusive neuronal PrP expression supported prion infection and development (Race *et al.*, 1995) while mice with only oligodendrocyte expression lacked signs of prion disease (Prinz *et al.*, 2004). Mice with astrocyte PrP expression showed disease symptoms despite the lack of neuronal PrP^{C} (Raeber *et al.*, 1997). It was suggested that deposition of PrP^{Sc} in close proximity to neurons and their processes was sufficient to induce pathology (Jeffrey *et al.*, 2004).

Because the definitive function of PrP^{C} has yet to be determined, the pathological mechanisms of PrP^{Sc} are also uncertain. One argument offers that PrP^{Sc} causes a 'gain of function' whereby the presence of the misfolded protein adds a neurotoxic function. The opposing argument hypothesises that PrP^{Sc} causes a "loss of function". This is derived from the

belief that PrP^{C} has a neuroprotective effect and as prion pathogenesis progresses, PrP^{Sc} converts more and more of the cellular isoform into the infectious conformation resulting in reduced neuroprotection. Some research has also shown that PrP^{Sc} itself is not neurotoxic due to the lack of correlation between PrP^{Sc} deposition and disease severity. It has been suggested instead that the conversion from PrP^{C} to PrP^{Sc} is the key component in pathogenesis rather than its accumulation (Trevitt and Collinge, 2006).

There are two main theories to explain the mechanism by which PrP^{Sc} induces the misfolding of PrP^{C}: the template-directed refolding model and the nucleated polymerization model [**Figure 1.3**]. The first model postulates that incoming PrP^{Sc} starts a catalytic cascade using PrP^{C}, or a PrP intermediate, as a substrate for conformational conversion into a new β–sheet-rich protein. This new PrP^{Sc} protein then serves to convert the next PrP^{C} molecule as the cycle continues. The re-folding mechanism is kinetically controlled by a high activation energy barrier which prevents spontaneous conversion at detectable rates. It is thought that this energy barrier is lowered by the formation of an intermediate PrP^{C}-PrP^{Sc} heterodimer complex which facilitates the full conversion of PrP^{C}, with the help of a chaperone molecule, into the new PrP^{Sc} conformation (Aguzzi *et al.*, 2008b).

The second model is based on a thermodynamically controlled nucleated polymerization reaction. This is a non-catalytic event whereby conversion of PrP^{C} to PrP^{Sc} is technically a reversible process. At equilibrium however, the natural cellular PrP isoform is highly favoured. The isoform conversion only occurs when a native PrP protein monomer comes into contact with an already formed PrP^{Sc} crystal seed or aggregate. Successful refolding into the PrP^{Sc} isoform is stabilized once the new protein adds onto the preformed seed. This model therefore, implies that infectivity requires the presence of PrP^{Sc} in oligomer form and that monomers consequently are not infectious (Aguzzi *et al.*, 2008b).

1.1.3.1.1 Peripheral Amplification

TSE infections are usually established following oral ingestion of infectious PrP^{Sc} material. Once in the digestive tract, it is proposed that PrP^{Sc} crosses the mucosal barrier via three potential mechanisms. The first utilizes a specific subset of intestinal epithelial cells

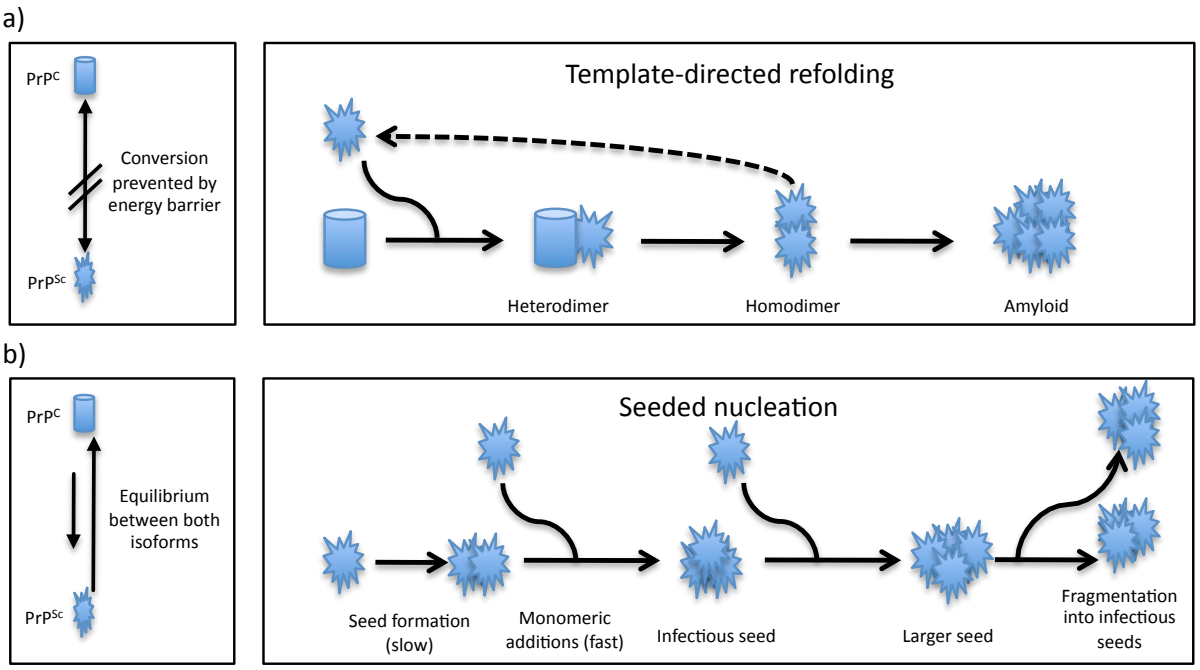

Figure 1.3: Two Models for the Conversion of PrP^{C} into the PrP^{Sc} isoform. a) The template directed model suggests the interaction between an exogenous PrP^{Sc} and endogenous PrP^{C} are required to facilitate the conversion. The spontaneous formation of PrP^{Sc} from PrP^{C} is prevented by high activation barrier. b) The seeded nucleation postulates that PrP^{C} and PrP^{Sc} are in equilibrium such that the PrP^{C} conformation is favoured. In the PrP^{Sc} conformation, monomers can act as seeds for the accumulation of other PrP^{Sc} proteins leading to the formation of amyloids and other infectious seeds. Figure adapted from (Aguzzi and Heppner, 2000). Permission from the publisher was granted for use of this material

called microfold cells or M-cells. These cells consist of a thin apical membrane made up of mircofolds, and an invaginated basal membrane which houses various immune cells. The thin membrane allows for the transport of many types of bacteria, viruses, and proteins including prions, across the epithelial layer where they encounter lymphocytes and dendritic cells (Neutra, 1999). This interaction between the immune cells and pathogenic antigen serves to stimulate a mucosal immune response. While the M-cells facilitate uptake and transfer of Ag to the immune system, they may also serve as a portal of entry for pathogens like prions which do not stimulate an immune response and are left to continue on their route of infection [**Figure 1.4**].

While in the intestinal lumen, PrP^{Sc} can be degraded by digestive enzymes into smaller protease resistant fragments. These fragments may form complexes with ferritin which are transported across the intestinal epithelium by a ferritin-dependent endocytosis mechanism (Mishra *et al.*, 2004).

A third mechanism of uptake has been proposed based on observations made during bacterial research and has yet to be directly linked to TSE transport. This involves direct sampling of prion Ag by migratory bone marrow-derived dendritic cells which can travel from the blood vessels to the inner surface of the intestinal wall. From here, the trapped Ag is transported to the lymphoreticular system which includes the mesenteric lymph nodes (Huang *et al.*, 2002).

Immunohistochemistry revealed that once across the mucosal barrier, PrP^{Sc} accumulation occurs in lymphoid tissues of the palatine tonsils, spleen, lymph nodes and Peyer's patches (Andreoletti *et al.*, 2000). More specifically, it is within the tingible body macrophages of the B-cell follicles and later on the plasmalemma of the follicular dendritic cells (FDC) that PrP^{Sc} replication and accumulation occurs (van Keulen *et al.*, 1996). This amplification phase, particularly within the Peyer's patches, is important for transfer of PrP^{Sc} to the nervous system.

Kitamota *et al*. (1991) were instrumental in establishing the relationship between B-cells, FDCs and prion disease progression. B-cell deficient mice were successfully infected with prion material via intra-cranial (IC) challenge, but failed to show any signs of disease following intra-peritoneal (i.p.) challenge. Further investigation of the i.p. inoculated mice

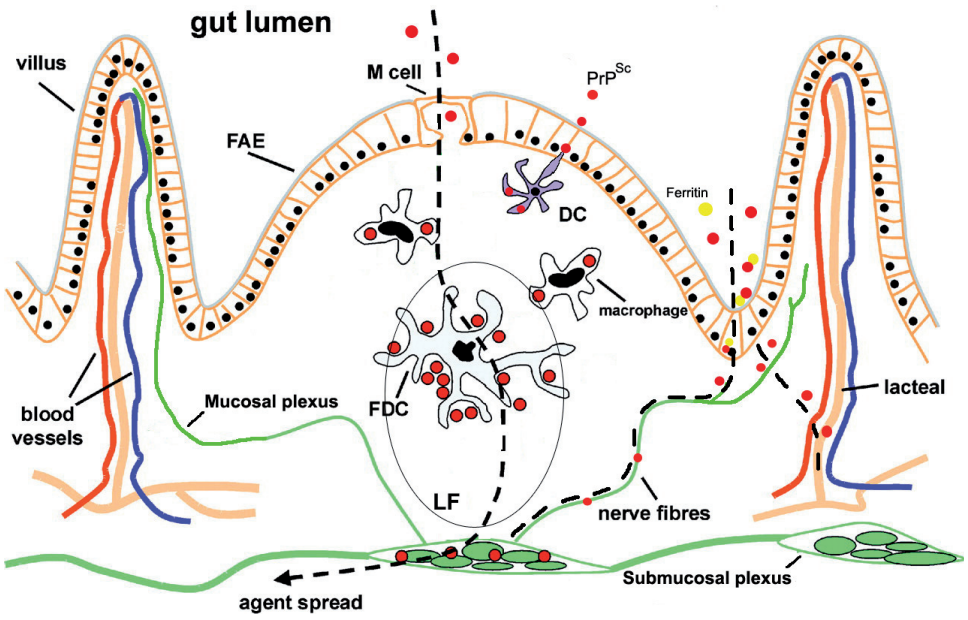

Figure 1.4: Representation of possible ways exogenous PrP^{Sc} could cross the intestinal epithelium and invade the enteric nervous system. M and dendritic cells are able to sample antigens and transport them to the lymphoid follicles (LF) of the Peyer's patches underlying the follicular-associated epithelium (FAE) where PrP^{Sc} then accumulates on follicular dendritic cells and follicular macrophages within the lymphoid follicles. An additional method of uptake may exist with ferritin-dependent trans-epithelial transportation pathway. Once PrP^{Sc} had crossed the epithelial layer, contact with the enteric nervous system leads to neural invasion. Figure from (van Keulen *et al.*, 2008). Permission from the publisher is granted for use of this material.

revealed that PrP^{Sc} failed to accumulate in the spleen and brain despite having normal levels of FDCs (Kitamoto *et al.*, 1991). Based on previous studies which illustrated that FDC development was a B-cell dependent process, the Kitamoto group concluded that by removing the B-cell population they prevented maturation of the present FDC population which, as it became evident, are essential for prion replication and disease progression. They were able to verify this by reconstituting B-cells in B-cell deficient mice, which had been given prion material i.p., which restored susceptibility to prion disease.

Following the linkage of FDCs and prion replication, studies discovered a link between the inflammatory process (involving FDCs, B-cells, macrophages and other immune cells associated with germinal centers) and accumulation of PrP^{Sc}. In the presence of inflammation, the upregulation of FDC cytokines such as lymphotoxin resulted in an ectopic induction of PrP^{C}-expressing FDCs (Aguzzi and Calella, 2009). As a result, non-lymphoid organs undergoing inflammation, such as nephritis, hepatitis or pancreatitis showed signs of prion accumulation. In contrast, they are prion-free under normal conditions (Heikenwalder *et al.*, 2005). Experiments have shown that in symptomatic and asymptomatic Scrapie-infected mice, with nephritis, prion infectivity was detectable in the urine (Seeger *et al.*, 2005). Similar experiments in sheep with mastitis showed that infectivity was shed in the colostrum and milk (Aguzzi and Calella, 2009). This is problematic in the context of wild/farmed animal populations where PrP^{Sc}-infected individuals suffering from inflammatory processes in excretory organs may shed PrP^{Sc} material into the environment and increase disease transmission.

1.1.3.1.2 Neuroinvasion

The mechanism by which PrP^{Sc} travels from lymphoid tissue to the nervous system is not well understood. Experimental conditions that either remove or increase lymphoid innervation show that increased lymphoid innervation correlates with faster neuroinvasion (Glatzel *et al.*, 2001). The proximity of PrP^{Sc} expressing FDC's to the sympathetic nerve endings has also been shown to influence rates of neuroinvasion. Whether there is passive diffusion of infectious PrP molecules or some sort of facilitated transport system from the FDCs to nerve endings is not known (Aguzzi, 2006).

The enteric nervous system (ENS) has been identified as the first neural tissue to be invaded by PrP^{Sc} following the amplification phase (Andreoletti *et al.*, 2000). The ENS, a member of the autonomic nervous system, innervates the gut and is made up of two main networks, Meissner's plexus, located in the gut submucosa, and Auerbach's plexus which runs between the circular and longitudinal muscle layer extending from the esophagus to the rectum (van Keulen *et al.*, 2008). As a component of the autonomic nervous system, the ENS is directed by the sympathetic and parasympathetic input from the central nervous system via efferent nerves which connect to the enteric plexi (van Keulen *et al.*, 2008). Following infection of the ENS, PrP^{Sc} travels to the brain using mainly the sympathetic pathway via the Vagus nerve to the dorsal motor nucleus in the medulla oblongata, or the parasympathetic pathway via the Splanchnicus nerve to the intermediolateral column of the spinal cord (van Keulen *et al.*, 2000).

1.1.3.1.3 Neurodegeneration

The mechanisms for prion-related neurodegeneration are closely related to the proposed functions of PrP^{C}. This is to be expected as the TSE disease process is essentially the conversion of PrP^{C} to PrP^{Sc} which leads to a reduction in the number of functioning cellular prion proteins, thus sparking the debate about whether prion pathology is due to a gain of a neurotoxic function or the loss of a neuroprotective function. Hur *et al*. proposed five mechanisms of prion neurodegeneration: increased oxidative stress and mitochondrial dysfunction; disruption of iron metabolism; altered calcium metabolism; increased inflammatory activity of cytokines, chemokines and nuclear factor-kappa; and finally apoptosis (Hur *et al.*, 2002).

It has been observed in TSE-infected animals that there is reduced activity of Manganese-SOD. This mitochondrial enzyme is responsible for converting superoxide anions into less reactive species. The resulting accumulation of ROS leads to ischemic cell injury and subsequently apoptosis or necrosis. Additional mitochondrial deficits, such as decreased cytochrome-c oxidase and ATPase activity, increased lipid peroxidation, and structural abnormalities, have been detected in hippocampal and cerebral cortical neurons of TSE infected hamsters (Choi *et al.*, 1998).

Increased iron metabolism within the brain (favouring a redox state of Fe^{+3}), as a result of a TSE infection, is involved in exacerbating ROS injury by converting harmful free radicals such as a superoxide anion into an even more highly reactive hydroxyl radical (Hur *et al.*, 2002). Hur *et al.* found that this change in iron content is linked to increased expression of two iron regulating proteins, IRP1 and IRP2, which play an instrumental role in iron metabolism. The abnormal IRP expression was particularly evident in the reactive astrocytes of the cerebral cortex and hippocampus.

Proper calcium regulation is essential for the normal functioning of the CNS. Variations in intracellular calcium concentrations facilitate the coordination of electrochemical signals, neurite growth, synaptogenesis, synaptic transmission, cell survival and plasticity (Sorgato and Bertoli, 2009). *In vitro* experiments showed that in PrP^{Sc} infected cells, there was a down-regulation of N-type voltage-gated Ca^{2+} channels resulting in reduced cytosolic Ca^{2+} (Sandberg *et al.*, 2004). PrP^{Sc} aggregates that accumulate in the synaptic cleft may physically interrupt synaptic transmission of electric potentials created by Ca^{2+}-activated potassium channels, or compromise the stability of newly formed synapses (Sorgato and Bertoli, 2009). This can result in excitotoxocity (Khosravani *et al.*, 2008), and ischemic brain damage (Spudich *et al.*, 2005). The interference with the development of long term potentiation also has negative effects on processes such as learning and memory (Sorgato and Bertoli, 2009).

1.1.3.2 Transmission of Infectious PrP

Natural transmission of TSEs likely occurs following ingestion of contaminated material such as skin, dirt, decomposed carcasses, urine, contaminated placentas, and faecal matter (Kruger *et al.*, 2009) or by direct contact between animals. These diseases can also be experimentally induced via intracerebral injection, a method that establishes neurdegenerative symptoms and pathology more quickly than either experimental oral or peripheral inoculation. Transmission of prion diseases between different species has been shown to be much less efficient than within the same species. This suggests TSEs are limited by a species barrier. Further trans-species experiments have demonstrated that transmission does occur but that incubation times may be greatly extended so that clinical disease may or may not occur during the natural lifespan of the affected animal (Race *et al.*, 2001). The concept of prion strains

complicates the understanding of TSE transmission in that certain strains of PrP^{Sc}, derived and transmitted within the same species, can result in the either the development of an asymptomatic carrier or the onset of clinical disease (Weissmann, 2004).

1.1.3.2.1 Strains

The term "strain", when used in the context of prion disease, refers to phenotypic differences such as variations in the pattern of aggregate deposition, incubation times, neuronal tissue tropism and pathological morphology (Falsig *et al.*, 2008). These differences are thought to result from the conformational flexibility of the PrP^{Sc} structure, which leads to exposure of distinct cleavage sites, differing stability in the presence of denaturing compounds (Peretz *et al.*, 2001a), and altered ratios of di-, mono- and unglycosylated forms (Aguzzi *et al.*, 2008b). The strain of an incoming infectious PrP^{Sc} molecule appears to be imprinted in all of the subsequent PrP^{Sc} proteins that are produced during the conversion of the host's cellular PrP (Aguzzi and Polymenidou, 2004).

Strains within traditional pathogens such as bacteria and viruses are determined by nucleic acid sequences in their genome. The mechanism of strain formation in prions is not attributable to differences in the primary PrP structure. It has been demonstrated that different strains can be passaged serially through inbred mice that have identical PrP gene sequences (Collinge and Clarke, 2007). Strains have also been be re-isolated in mice following passage through other species with differing PrP primary structures (Bruce *et al.*, 1994).

It has been shown that prion strain characteristics play a role in the establishment of a species barrier. Species barrier is a concept whereby the transmission of prion diseases between different species is much less efficient than within species (Collinge and Clarke, 2007). When species B is infected with prion from species A, the infectivity rate is low and the disease progression, in successfully infected animals, is slow and unpredictable. In contrast, when species A is infected with prions from species A, infection rates are high and progression is quick with a very similar disease course in each animal. Interestingly, following the passage of prion from species A to B, subsequent passages of the same prion to another B animal now has the same disease progression as if the prion had originated from a species B animal. The type of strain influences how easily this species barrier is broken. For example, the prion strain

responsible for the BSE crisis in England was very easily transmitted to a variety of species, including humans (Bruce *et al.*, 1994).

1.1.3.3 Prion Diseases

Since the earliest observation (around 1730) of a chronic neurodegenerative disease in Western Europe, several analogous neurodegenerative diseases have been identified in different species [**Table 1**]. In most cases, it was initially assumed that the causative agent was some sort of slow virus. It was not until Stanley Prusiner's work in the late 1970s and early 80s that these diseases were found to be caused by a misfolded prion protein. Different names were attributed to each of the diseases based on species: Scrapie in sheep, Creutzfeldt-Jacob disease (CJD) in humans, Bovine Spongiform Encephalopathy (BSE) in cattle, and Chronic Wasting Disease (CWD) in cervids.

In sheep and cattle, prion disease symptoms are very similar. The symptomatic phase of the disease initially presents with rubbing of the head, flanks and buttocks, a symptom which may last well into the later stages of the disease. Also evident at the early stages is the nibbling of hair on the lower legs. General weakness follows which progresses to the inability to rise. Wasting symptoms appear, such as a loss in body weight despite normal food and water intake. Neurological motor deficits affecting gait include wide-based stance of hind limbs and high stepping motions in the front limbs, which in severe cases makes the animals appear intoxicated. Further neurological changes include body tremors and personality/behavioural alterations which may manifest as uncooperativeness, excitability and extreme distress. Once an animal is symptomatic, Scrapie and BSE are slowly progressive and lethal within 2 to 6 months (Beghi *et al.*, 2004; Parry, 1962).

Sheep possess a unique attribute with regards to TSE transmission. Their susceptibility is influenced by polymorphisms at three different codons (136, 154 and 171) within the PrP sequence (Houston *et al.*, 2003). It has been observed that susceptibility to Scrapie strongly correlates with valine (V) at position 136, arginine (R) at 154 and glutamine (Q) at 171 (VRQ) (Goldmann *et al.*, 1994), whereas resistance is attributed to alanine (A) at 136, with R at 154 and 171 (ARR) (van Keulen *et al.*, 1996). Prion disease is rare in heterozygous ARR animals

Table 1.1: Summary of dates for when specific TSEs were first described. Adapted from (Vana *et al.*, 2007).

TSE	First Described	Reference
Creutzfeldt-Jakob disease	1920	(Creutzfeldt, 1989)
Sporadic Creutzfeldt-Jakob disease	1921	(Jakob, 1921)
Familial Creutzfeldt-Jakob disease	1924	(Kirschbaum, 1924)
Gerstmann-Straussler-Scheinker syndrome	1928	(Gerstmann *et al.*, 1936)
Kuru	1957	(Gajdusek and Zigas, 1957)
Chronic Wasting Disease	1967	(Williams, 2005)
Iatrogenic Creutzfeldt-Jakob disease	1974	(Duffy *et al.*, 1974)
New Variant Creutzfeldt-Jakob disease	1996	(Will *et al.*, 1996)

and virtually undetected in animals homozygous for ARR (Ikeda *et al.*, 1995). Knowledge of this led to a breeding strategy in Europe where sheep flocks were bred to attain the ARR genotype in an attempt to eradicate the transmission of Scrapie amongst their herds (Kao *et al.*, 2002).

1.1.3.3.1 Scrapie

Although Scrapie belongs to a group of diseases that were only recently classified, historical descriptions of Scrapie have been traced back to 1732. Some sources claim there is evidence, although less convincing, that corresponds to the Roman era (Schneider *et al.*, 2008). The term "Scrapie" was first seen in a manuscript from 1750 but a more common term for it at the time was "distemper" (Comber, 1772). The majority of written accounts were not produced by scientist or veterinarians, but by farmers, shepherds and government employees. The latter individuals were the ones immediately involved with the infected animals and actually went to great efforts to cover up the outbreaks because of the monetary/economic implications that would result (Schneider *et al.*, 2008). Similar to current management strategies, acknowledgment of a Scrapie infected animal meant the entire herd would be culled and pasture land quarantined indefinitely (Turner, 1795). This behaviour indicated a basic understanding of Scrapie as an infectious entity.

While historical descriptions of Scrapie symptoms were accurate, the beliefs of what caused the disease varied greatly. The range of hypotheses included: thunder, extreme atmospheric conditions, food/nutritional insufficiency, parasites, humidity in the sheep pen, tail docking, age during mating, cross-breeding and inbreeding (Schneider *et al.*, 2008). The method of transmission was equally debated with ideas ranging from sexual transmission (Comber, 1772), sporadic occurrence, and genetic inheritance. After 100 years of failed attempts to experimentally demonstrate Scrapie transmissibility, two French scientists, Cuille and Chelle in 1936, successfully infected sheep and goats intracerebrally, intraocularly, epidurally, and subcutaneously using brain and spinal cord suspensions from Scrapie-infected sheep (Cuille and Chelle, 1936). Their experiment was important for several reasons. First, they confirmed that Scrapie was indeed infectious; second, that the course of infection required a very long (18 month) incubation period; and third, that the incubation period was affected by

species. The infected sheep demonstrated a quicker symptom onset (11-22 months) than the goats (25-26 months) (Cuille and Chelle, 1938). Speculation as to what transmissible agent actually caused Scrapie evolved over the next 50 years, gaining momentum as human related prion diseases (CJD and Kuru) were identified in the 50's and 60's by Sigurdsson and Gajdusek.

1.1.3.3.2 Chronic Wasting Disease

CWD was first identified at a research station in Fort Collins, Colorado in 1967 (Williams, 2005). It was not until 1978 that the relationship between CWD and other TSEs was recognized following comparative analysis of neuronal lesions (Williams and Young, 1980) and accumulation of PrP aggregates (Browning *et al.*, 2004). During the 1970's and 80's, CWD existed primarily in the Colorado Rocky Mountains and an area extending along the river valleys to Wyoming (Miller *et al.*, 2000). In 1996, however, the disease was also detected in the Canadian prairies on an elk farm (Sigurdson and Aguzzi, 2007).

Strategies for containing CWD are extremely problematic because the afflicted animals primarily consist of wild, free-ranging populations. Other complicating factors are the scavenging of contaminated deer carcases by predators ranging from mountain lions to vultures, and a poor understanding of the natural routes of disease transmission (Sigurdson and Aguzzi, 2007). Although oral cross-species infection has not been directly observed, there have been suspicion in a few cases, which was later disproved, that human patients suffering from CJD may have contracted it from CWD infected deer meat (Belay *et al.*, 2004). CWD, being one of the most contagious of the TSEs, can reach a prevalence of 30% in wild populations and as high as 100% in captive cervids (Williams, 2005). This has created concern that infected wild populations of deer may serve as a reservoir leading to the transmission of CWD to farmed deer and cattle.

Symptoms of CWD are subtle and hard to detect in the early stages of disease. They include: weight loss, excessive drinking and urination as well as regurgitation. The motor deficits common to Scrapie and BSE are often absent in CWD cases (Sigurdson and Aguzzi, 2007). Despite the lack of easily observable symptoms, post-mortem histopathological examinations reveal neurological lesions similar to Scrapie, BSE and human prion diseases

(Williams and Young, 1993). It takes anywhere from several weeks to many months for the infected animal to succumb to the disease once it has spread to the nervous system.

1.1.3.3.3 Bovine Spongiform Encephalopathy

Since the first BSE diagnosis in 1986, more than 179,000 positive cases have been identified in Great Britain (Wells *et al.*, 1987). While the recycling of BSE-infected material into feed for cattle was likely the main factor of transmission, the actual source of the original BSE agent is still unknown (Baron and Biacabe, 2006). It has been suggested that BSE developed spontaneously in cattle via a somatic or germ-line mutation of PrP or that cattle may have been infected by another species such as sheep (Konold *et al.*, 2006). Twenty years of rigorous surveillance following the first BSE outbreak have indicated that disease transmission is under control in most of Europe (Editorial-team, 2007). Mass screening of bovine tissues as part of the surveillance initiatives has identified the presence of two new BSE strains, L-Type and H-Type which are distinct from the classic BSE (Cappai and Collins, 2004). These strains are more rare than classic BSE and are usually detected in older animals, thus representing a possible sporadic form of TSE in cattle (Biacabe *et al.*, 2008). Both strains are infectious, maintaining their original molecular phenotype upon transmission and cause distinct neuropathology. In mouse infection studies, the L-type has been observed to be more virulent, replicating faster than both classical BSE and the H-type strain (Cappai and Collins, 2004).

1.1.3.3.4 Creutzfeldt-Jacob Disease

In the 1950s, an epidemic spreading amongst the Fore people of Papua New Guinea gained the attention of health officials. At the peak of the epidemic, as many as 10% of the local Fore population was infected (Gajdusek and Zigas, 1957). The disease appeared to affect the central nervous system and displayed symptoms such as progressive ataxia or loss of motor coordination (Collinge, 2001). Derived from the appearance of these symptoms, the disease was given the name Kuru, which in the Fore language means “to shiver” (Collins *et al.*, 2004). William Hadlow, a veterinary pathologist specialising in TSEs, made the connection in 1959 between Scrapie and Kuru. He noted that epidemiologically, clinically and pathologically, the

two diseases were remarkably similar (Hadlow, 1959). This led to further investigations by Gajdusek who was able to prove Kuru to be transmissible after he successfully infected chimpanzees (Gajdusek *et al.*, 1966).

Epidemiological studies suggested that Kuru was transmitted by the cannibalistic Fore funeral rituals (Gajdusek, 1977). These ceremonies involved the children and women consuming nervous tissue from the deceased relative while men ingested tissue like muscle, which was much less likely than the nervous tissue to contain PrP^{Sc} material, although at that time the nature of the infectious agent was unknown (Klitzman *et al.*, 1984). The number of Kuru cases declined steadily following the discontinuation of the funeral ceremonies. However, complete eradication of Kuru has taken much longer than anticipated due to incubation periods lasting as long as four decades (Collins *et al.*, 2004).

The most common form of prion disease in humans in sporadic CJD (sCJD) with a frequency of approximately 0.5-1 case per million people (Coulthart and Cashman, 2001). Unlike the familial forms of CJD, which are caused by autosomal dominant traits linked to mutations on the *Prnp* gene (Hsiao *et al.*, 1989), it is unknown whether sCJD is caused by endogenous or exogenous factors (Aguzzi, 2006). Countries with active surveillance programs often report higher CJD incidence rates, such as Switzerland with 3 cases per million people (Glatzel *et al.*, 2003). Most of those cases, however, are due to iatrogenic spread rather than exposure to infected material (Aguzzi and Calella, 2009). Symptoms in sporadic cases usually appear around the age of seventy and are lethal within weeks or months. Symptoms often include rapidly progressing dementia, ataxia, muscle twitching and uncoordinated speech (Coulthart and Cashman, 2001).

Following the BSE crisis in the United Kingdom in the 1980s, a novel form of CJD emerged. Given the name "variant CJD" (vCJD), this new form of prion disease appeared to be linked to the consumption of BSE-contaminated meat products. The two main differences between sporadic and vCJD are the dramatic decrease in age at onset of symptoms (29 years), and increased duration of symptoms (16 months) prior to death (Will, 1999). Some additional symptoms, that are typically rare in sporadic CJD, like involuntary movements and sensory symptoms have been observed in 100% and 50% of symptomatic vCJD patients, respectively (Zeidler *et al.*, 1997).

As of 2003, the number of autopsy confirmed cases of vCJD was 153 and currently the number is estimated at 200 (http://www.bseinfo.org). While these numbers are low, the number of people actually infected with vCJD and not showing symptoms is likely much higher. Due to incubation times that can last decades, there may be a population of people that are harbouring the infectious PrP without a manifestation of observable symptoms. These people are often referred to as 'asymptomatic carriers'. Without accepted pre-mortem diagnostic tests, health professionals are not able to identify these asymptomatic individuals via routine screening. This creates a dangerous situation because researchers have found evidence that vCJD can be transmitted via contaminated blood products (Peden *et al.*, 2004), infectious cadaveric tissues, and contaminated surgical instruments (Brown *et al.*, 2000).

1.1.3.4 Prion Diagnostics

With the lack of accepted pre-mortem diagnostic tests available, health professionals have to rely on clinical examinations for the identification of TSE's (Soto, 2004). Definitive confirmation however, can only be made by post-mortem histological or biochemical analysis of brain (Ingrosso *et al.*, 2002). While histological assays are accurate, they are time-consuming, labour-intensive and low-throughput. Development of new biochemical tests has allowed multiple samples to be processed in a few hours. The majority of the tests have detection limits ranging from 0.5 pmol to 20 pmol and utilize immunodetection of the PrP^{Sc} isoform or proteolysis to distinguish PrP^{C} from the infectious conformation (Soto, 2004).

To enable the detection of preclinical peripheral PrP^{Sc}, Sabotio *et al*. developed a method of PrP^{Sc} amplification called protein misfolding cyclic amplification (PMCA) (Saborio *et al.*, 2001). Similar to the polymerase chain reaction method used to amplify DNA, PrP^{C} of the same species is added to a sample containing small quantities of PrP^{Sc} and incubated to allow for the expansion of PrP^{Sc} aggregates. These new aggregates are broken up using sonication to form more PrP^{Sc} seed molecules and are re-incubated in the presence of added PrP^{C}. After several amplification cycles, the amount of PrP^{Sc} has been shown to be several million fold higher than in the original sample (Saa *et al.*, 2006), allowing detection using standard molecular techniques like Western blots. Concerns were raised regarding the

specificity of this technique after it was shown that PrP^{Sc} can be generated from samples lacking PrP^{Sc} (Deleault *et al.*, 2007) which limits the usefulness of PMCA as a diagnostic test.

The discovery of PrP^{Sc} infectivity in blood from vCJD patients (Deleault *et al.*, 2007; Llewelyn *et al.*, 2004) created a great need for the development of a blood test for prions. The first detection system was developed in 1996 and consisted of capillary electrophoresis and a competitive immunoassay which detected a PK resistant C-terminal sequence of PrP (Schmerr *et al.*, 1998; Schmerr *et al.*, 1996; Schmerr and Jenny, 1998). Despite several revisions and improvements, the method was not suitable for routine testing (Everest *et al.*, 2007). More recent initiatives involve the use of a 15B3 prion antibody developed by Prionics (Korth *et al.*, 1999; Nazor *et al.*, 2005) and a Seprion resin manufactured by Microsense. Both systems concentrate PrP^{Sc} so it is detectable by ELISA and flow cytometry. One other group designed fluorescent labelled peptides to discriminate PrP^{C} from PrP^{Sc}. When the labelled peptide binds to PrP^{Sc}, a shift in conformation modifies the fluorescent properties of the label (Grosset *et al.*, 2005). Despite the advances in blood diagnostics, the strict guidelines governing diagnostic requirements prevent their acceptance for use in an official capacity.

1.2 Historical Approach to Prion Therapy

For the last fifty years there have been ongoing efforts to identify effective prion therapeutic agents. Typically these agents have targeted PrP^{C}, PrP^{Sc} or the conversion process. Research in this area increased dramatically with the emergence of vCJD in the 1990's and the discovery that prion infectivity can be transmitted via blood, surgical instruments and transplant tissues from asymptomatic carriers (Collinge, 1999). Investigations of potential therapies have been conducted primarily in three experimental systems which include cell-free *in vitro* conversion assays, cell-based models or animal models (Trevitt and Collinge, 2006). The cell-free method involves the addition of a PrP^{Sc} seed molecule to a PrP^{C} substrate in the presence of a potential therapeutic agent. Therapeutic potential is evaluated based on the ability of the molecule to interfere with the isoform conversion process. Cell-based research utilizes cell lines such as N2a (mouse neuroblastoma cells) to assess the ability of given therapeutic agent to either prevent prion infection of the cells, or clear a chronically prion infected cell line like ScN2a of PrP^{Sc}. These cell models allow for the analysis of some very basic aspects of prion

pathogenesis such as isoform conversion, cytotoxicity, apoptosis and abnormal cell signalling. Animal models make up the third type of commonly used experimental system. This tends to be the most expensive and complicated model, but it also has the potential to be the most informative. Many different aspects of an anti-prion therapeutic's potential can be analyzed such as its ability to influence incubation phase of infection, severity of symptoms, pathology, immune response, as well as survival time and rate. Several difficulties, however, exist within this type of model. Issues such as genetic variability between species such as sheep and mice, and inconsistent models of infection and lengthy incubation periods, are examples of the challenges facing researchers who utilize *in vivo* systems.

Dating back as far as the 1960's, the main area of research was focused on chemotherapeutic agents (Trevitt and Collinge, 2006). As it was initially thought that prion diseases were the result of a slow virus, this biased the nature of the therapeutic agents which were investigated. Typical TSE targets/goals for chemotherapeutic agents have been: sterilization of sources of infection; prion prophylaxis; interruption of PrP^{C} conversion during peripheral amplification; prevention of neuroinvasion; and reduction of PrP^{Sc} accumulation (Cashman and Caughey, 2004). Countless agents have been tested ranging in class from: polysulphated polyanionic compounds, glycosaminoglycans, sulphonated dyes, quinacrines, metal chelators, tetrapyrroles, polylene antibiotics, tetracyclic compounds and β–sheet breaker peptides (Cashman and Caughey, 2004; Trevitt and Collinge, 2006). Very few have shown significant success within an *in vivo* system, especially after symptoms have developed (Dormont, 2003). The blood-brain barrier serves as a substantial obstacle for most therapeutic agents. Due to the large size of most chemotherapeutic agents, they are unable to reach the CNS and consequently fail to interfere with prion related pathogenesis. Even compounds like curmunin, quinacrine, quinolones and polylene antibiotics, which are able to penetrate the CNS, fail to improve symptoms of late stage TSE disease (Cashman and Caughey, 2004).

1.2.1 Immunotherapy

1.2.1.1 *In vitro* Immune Therapy

The conversion of PrP^{C} to PrP^{Sc} occurs at or near the cell surface (Borchelt *et al.*, 1990; Caughey and Raymond, 1991). This provides an opportunity for antibodies to bind and prevent the interaction and conversion of PrP^{C} by PrP^{Sc}. Such a strategy might be used as immunoprophylaxis to prevent infection of animals exposed to PrP^{Sc} or as therapy to treat infected animals, helping to slow or stop the progression of disease and minimize the shedding of infectious PrP^{Sc} into the environment. The challenge with this approach is that PrP^{C} is a ubiquitously-expressed endogenous protein, making it very difficult to stimulate an immune response. This is the result of an immunological phenomenon known as tolerance. Tolerance occurs when the immune system recognizes a protein as being "self". Consequently, immune cells such as T and B-cells, which have receptors specific to a particular protein, are deleted or prevented from initiating an immune response towards that particular protein (Zinkernagel and Hengartner, 2001). This is a safety mechanism that ensures that the body's adaptive immune system does not attack itself. Situations where there is a malfunction in the process of self recognition result in autoimmune disorders such as rheumatoid arthritis, diabetes, and lupus. Overcoming tolerance to PrP^{C} remains one of the biggest challenges in prion vaccine research (Heppner and Aguzzi, 2004).

Early immunologic protection experiments in 1988 demonstrated that *ex vivo* incubation of a prion inoculum with anti-PrP^{C} polyclonal antibody, prior to inoculation, resulted in a 2-log reduction in infectivity (Gabizon *et al.*, 1988). Further work was done to identify the region of PrP involved in the interaction with PrP^{Sc} resulting in isoform conversion. This was done using mAb 3F4 (specific for amino acids 109-113) (Kascsak *et al.*, 1987) and polyclonal sera to peptides (corresponding to amino acids 23-33, 90-104, 143-156 and 219-232) to try and prevent PrP^{Res} formation in a cell free conversion system (Gabizon *et al.*, 1988). Abs to the region 219-232 were found to disrupt the formation of new PrP^{Res}. The same effect was not observed during incubation with PrP^{Res} seed. Furthermore, when PrP^{Sen} Abs and peptide 219-232 were co-incubated, the Ab bound to the peptide, allowing for the uninterrupted formation of PrP^{Res}.

This illustrated that the inhibition of PrP^{Res} formation was due to the direct binding of the Ab to the 219-232 region (Horiuchi and Caughey, 1999).

Preliminary immunotherapy research in 2001 showed that culturing ScN2a cells with mAb 6H4 (specific for amino acids 144-152 on the prion protein) continuously for 6 weeks resulted in the complete clearance of PrP^{Sc} (Enari *et al.*, 2001). In the absence of 6H4, however, the cells became susceptible to prion infection. This study, and similar *in vitro* investigations, offered evidence that anti-PrP Abs have the potential to interfere with the prion disease process. That same year Heppner *et al*. created transgenic mice that expressed 6H4 as a single chain Ab. To circumvent the issue of PrP tolerance, the mice used contained a heterozygous prion knockout ($Prnp^{+/-}$), thus allowing for the accumulation of high anti-PrP titers. The mice were infected with Rocky Mountain Laboratory (RML) strain of mouse adapted Scrapie via an intraperitoneal challenge and monitored for prion disease. The mice expressing 6H4 survived 120 days longer than the control mice (Heppner *et al.*, 2001).

That same year, Peretz *et al*. used recombinant antibody antigen-binding fragments (Fabs) to prevent PrP^{C} conversion in ScN2a cells infected with PrP^{Sc}. They observed a direct relationship between the amount of antibody binding to surface PrP^{C} and its inhibition of PrP^{Sc} formation. Their most effective Fab, D18, not only stopped PrP^{Sc} formation but also cleared pre-existing PrP^{Sc}. In challenge experiments, mice infected with Scrapie cells pre-incubated with the antibodies, survived more than three months longer than those that received untreated cells. The success of D18 had been attributed to its ability to bind to its specific epitope (132-156) as well as recognizing/binding to cell surface PrP^{C} molecules (Peretz *et al.*, 2001b).

In 2004, two antibodies, SAF34 (specific for the octarepeat PrP^{C} region) and SAF61 (specific for 144-152 of both PrP^{C} and PrP^{Sc}), were studied in neuroblastoma cells over-expressing PrP^{C} with and without PrP^{Sc} infection (Perrier *et al.*, 2004). When used independently, both antibodies decreased the levels of PrP^{C} in uninfected and PrP^{Sc} infected cells, however, SAF61 was more effective. When used cooperatively, they had a synergistic effect. The authors suggested that SAF61's mechanism of action was its quick clearance of PrP^{C}, which removes the substrate required for PrP^{Sc} production. Although treatment with SAF34 had a similar end result to SAF61, its mechanism is different. SAF34 was unable to clear PrP^{C} so it was hypothesized that it prevented interaction between PrP^{C} and PrP^{Sc}, as suggested by previous work (Enari *et al.*, 2001; Peretz *et al.*, 2001b). The epitopes recognized

by both SAF34 and SAF61 correspond to a region of PrP thought to be involved in an interaction with the laminin receptor (Hundt *et al.*, 2001). Consequently, the binding of SAF antibodies to PrP may interfere with this process (Perrier *et al.*, 2004).

Using $PrP^{-/-}$ mice, Kim *et al.* produced a panel of antibodies to either recombinant PrP or PrP^{Sc} (Kim *et al.*, 2004b). They then tested the ability of the antibodies to protect ScN2a cells from infection. From the results, they concluded that the criterium required for protection by antibody was not in the specificity of the epitope, but in the capacity of the antibody to bind cell surface PrP^{C} (Kim *et al.*, 2004a). At the end of its natural cycle, surface-expressed PrP^{C} becomes internalized via clarithrin vesicles and then enters the degradation pathway (Peters *et al.*, 2003; Shyng *et al.*, 1994). It is during this internalization process, at the level of the cell membrane, that the conversion from PrP^{C} to PrP^{Sc} is thought to occur (Borchelt *et al.*, 1992; Caughey and Raymond, 1991). Consequently, the authors suggested that the binding of mAb to surface PrP^{C} prevents internalization and thereby inhibits the conversion process (Kim *et al.*, 2004a).

In contrast to targeting of surface PrP, Cardinale *et al*. developed anti-prion single chain antibody fragments (scFv) with an endoplasmic reticulum (ER) retention signal KDEL to target intracellular PrP. Stable expression of these scFvs in nerve growth factor differentiating PC12 cells inhibited PrP^{C} translocation from the ER to the cell surface and prevented PrP^{Sc} accumulation (Cardinale *et al.*, 2005). They later applied this concept to an *in vivo* model. Lysates from wild-type and scFv (8H4)-expressing PC12 cells was injected intracerebrally into C57BL mice, 35 days after exposure to Scrapie. Mice that received wild-type PC12 cell lysate succumbed to prion disease whereas only 2/10 mice in the scFv (8H4) group were infected. At 300 days post-infection, the eight mice in the experimental group remained symptom free with no detectable histopathology (Vetrugno *et al.*, 2005).

1.2.1.2 *In vivo* Immunization

The necessity for extracerebral PrP^{Sc} to undergo amplification in the periphery prior to neuroinvasion provides an opportunity for prophylaxis. However, due to immunological tolerance to PrP^{C}, attempts to stimulate humoral responses against prion proteins *in vivo* has proven challenging. It was demonstrated in 1993 that it is possible to raise antibodies to PrP in

Prnp$^{-/-}$ mice (Prusiner *et al.*, 1993). Heppner *et al*. (2001) speculated that the use of genes encoding high-affinity anti-PrP antibodies produced in Prnp$^{-/-}$ mice might be able to redirect B-cell responses in mice expressing PrP^{C}. They took *Prnp*$^{-/-}$ and *Prnp*$^{+/-}$ populations of mice and transgenically introduced genetic sequences which encoded for the heavy and light chains of 6H4, a mAb specific for PrP^{C}. By four weeks of age, the *Prnp*$^{-/-}$ mice all produced consistently high anti-PrP titers. Mice expressing PrP (*Prnp*$^{+/-}$) developed anti-PrP antibodies more slowly than the control mice. Unresponsiveness of B-cells likely corresponds to the level of self-antigen presented (Adelstein *et al.*, 1991) and B-cell receptor avidity/affinity (Tiegs *et al.*, 1993). Therefore, the delay in production of anti-PrP in *Prnp*$^{+/-}$ mice may be due to negative selection of B-cells expressing 6H4 epitopes with high-avidity for PrP^{C} (Heppner *et al.*, 2001). Consequently, the 6H4 produced by *Prnp*$^{+/-}$ mice may have different binding properties than 6H4 produced by the *Prnp*$^{-/-}$ mice. All mice were inoculated i.p. with RML Scrapie. Following inoculation, spleen and brain were analyzed for the presence of PrP^{Sc}. Spleens from the nontransgenic *Prnp*$^{+/-}$ group showed PrP^{Sc} accumulation while the *Prnp*$^{+/-}$-6H4 group did not. Brain samples, used to assess the ability of PrP^{Sc} to spread to the CNS, showed identical results to that of the spleen. To rule out unintended mechanisms of PrP^{Sc} protection, the authors used Western blots to determine whether the presence of 6H4 was causing reduced expression of PrP^{C}. Equal levels of PrP^{C} protein in both the transgenic and nontransgenic *Prnp*$^{+/-}$ mice indicated this was not the case. It appeared that protection was mainly occurring via masking, by 6H4, of PrP^{C} sites critical for interaction with PrP^{Sc}. Because PrP^{C} is an abundant self protein the risk of inducing autoimmunity is always a concern, however, no obvious signs of autoimmune disease were detected in this study (Heppner *et al.*, 2001).

While the presence of anti-PrP antibodies in the peripheral compartments does not appear to have any negative consequences, Solforosi *et al.* (2004) investigated the effect of anti-PrP^{C} antibodies on neuronal cells *in vivo*. PrP^{C} D13 mAbs (1 mg/mL) were injected into the hippocampus of C57BL/10 mice. Within 24 hrs, cross-linking of cell-surface PrP^{C} by the antibodies resulted in rapid and extensive apoptosis of neurons in the hippocampal and cerebellar regions. Further investigation revealed that the administration of monovalent Fab fragments from D13, via the same methods, produced apoptosis at a much reduced rate. This suggested that the cross-linking event was most likely the cause of apoptosis. In contrast to the previous results, experiments with a D18 mAb specific for a region involved in PrP^{C}-PrP^{Sc}

interaction did not trigger apoptotic cell death. This may be because D18 was ineffective at cross-linking PrP^C or it obscured the region of PrP^C which binds to a cofactor molecule necessary for apoptosis signalling (Solforosi *et al.*, 2004).

1.2.1.2.1 Passive Immunization

Further enthusiasm for anti-prion immunotherapy developed following the experiments of White *et al*. in 2003. They were able to show that the passive transfer of anti-PrP IgG antibodies to wild type mice, which were subsequently i.p. challenged with PrP^{Sc}, resulted in a significant delay in prion symptoms (White *et al.*, 2003). The effects were most noticeable when a high antibody dose was administered biweekly during the splenic amplification phase. The treatment decreased splenic PrP^{Sc} at 60 days post-infection, and by 250 days, PrP^{Sc} was still undetectable in the brain. An unfortunate limitation, however, was the inability of the anti-PrP antibodies to effectively cross the blood-brain barrier which restricted protection by passive vaccination to the extraneural compartments. This conclusion was inferred from results showing that passive antibody transfer had no effect on prion disease progression following intracranial challenge.

Also in 2003, the ability of mAbs 8B4 (residues 34-52), 8H4 (175-185), and 8F9 (205-233) were tested to see if they provided passive protection against PrP^{Sc} challenge. Mice were inoculated intraperitoneally with Scrapie at either a 10-fold or 1000-fold dilution. Immediately after challenge, mice were injected with one of the three mAbs. Antibody treatment was repeated each week until death. In the group receiving the 1:10 diluted challenge material, both 8H4 and 8B4 provided a 10% incubation prolongation; with the 1000-fold dilution, disease prevention was observed in 10% of mice treated with 8B4. The ineffective response to 8F9 was likely due to its lower affinity for both PrP^C and PrP^{Sc}. While injected antibodies are rapidly cleared from the circulation, this experiment suggested further promise for antibody-based strategies (Sigurdsson *et al.*, 2003).

It appears that the effectiveness of passive immunization was restricted to the peripheral compartments, likely by the blood brain barrier, as several experiments have shown development of prion disease following intracerebral inoculation despite peripheral treatment with anti-PrP antibodies. There is, however, some potential application of antibody for

treatment of individuals accidentally exposed to prions. Although anti-PrP antibodies are rapidly cleared from the blood, their brief presence does not seem to stimulate any detectable autoimmune reaction. Whether this remains true for active vaccination strategies, where anti-PrP antibodies are present for much longer periods of time, is a question that needs to be addressed.

1.2.1.2.2 Active Immunization

Overcoming tolerance to PrP^C is one of the greatest challenges for active PrP immunization. Numerous investigations of different carrier systems [keyhole limpet hemocyanin (Hanan *et al.*, 2001a), bacterial heatshock protein DnaK (Koller *et al.*, 2002), multiple antigen peptide display (Sigurdsson *et al.*, 2002)] and adjuvants [CpG ODN (Rosset *et al.*, 2004), Freund's complete or incomplete adjuvant (Hanan *et al.*, 2001b; Polymenidou *et al.*, 2004), Montanide (Schwarz *et al.*, 2003), TitreMax (Gilch *et al.*, 2003)], have been employed as a way to compensate for the inherent lack of PrP^C immunogenicity. While many of the experiments use potent adjuvants, most are not suitable for use in humans or animals due to toxicity issues (Li *et al.*, 2010). Despite limitations posed by tolerance to PrP^C, experiments have shown a relationship between antibody titers and protection from disease, therefore exhibiting the potential benefit of immunotherapeutic approaches.

The first group to show a delay in prion disease onset following active immunization with recombinant PrP^C (residues 23-230) was Sigurdsson *et al*.. The results were modest with only a 10% increase in the incubation time in mice vaccinated (s.c.) at two week intervals starting 14 weeks prior to inoculation (i.p.). Despite a delay in symptom onset, all mice died as a result of disease progression. Those that were vaccinated at the time of inoculation did not benefit from the treatment. The authors noted that high titers corresponded to prolonged incubation times, but following disease onset, there was no discernable histopathological difference between groups (Sigurdsson *et al.*, 2002).

Other studies, which immunized against different regions of PrP^C, demonstrated that different epitopes of the protein may have unique therapeutic value (Li *et al.*, 2010). Experiments by Schwarz *et al*. (2003) compared the effectiveness of vaccinating with a short synthetic peptide (residue 105-125) to recombinant mouse PrP90-230 covalently linked to

keyhole limpet hemocyanine. Immunization with PrP105-125 significantly prolonged survival by an average of 23 days over the adjuvant control animals. Monoclonal antibodies with the same specificity had previously been shown to bind both PrP^{C} and PrP^{Sc}. They also prevented amyloid aggregation and dissolved preformed aggregates (Hanan *et al.*, 2001a; Hanan *et al.*, 2001b). In contrast to the previous work by Sigurdsson *et al.* with PrP23-230, the recombinant PrP90-230 immunization was not successful in delaying or preventing disease (Schwarz *et al.*, 2003). They followed up with epitope mapping experiments to determine which epitopes, within PrP90-230 produced antibodies with the highest reactivity. Antibodies to the region between 159-211 were the most highly detected by ELISA. The authors suggested that only antibodies specific for residues 105-125 and 144-152 were effective in preventing prion disease (Schwarz *et al.*, 2003).

1.2.1.2.3 Mucosal Immunization

The majority of TSEs are transmitted orally; consequently, mucosal immunization may be an effective immunotherapeutic strategy. Mucosal immunity is generally humoral and non-inflammatory in nature. Therefore, it is typically a safer alternative to subcutaneous or intramuscular immunization (Goni *et al.*, 2005). Immunological issues, such as those observed in a clinical trial of an Alzheimer's vaccine (AN1792), illustrate a potential complication for the use of systemic vaccine delivery for neurological protein misfolding diseases. The AN1792 vaccine stimulates an immune response to the misfolded Aβ protein found in amyloid plaques which are thought to be responsible for causing Alzheimer's disease symptoms/pathology. The case report published by Nicoll *et al*. described a patient in the trial who rapidly declined and died six weeks following her last vaccination. Post-mortem analysis revealed $CD4^{+}$ lymphocytic meningoencephalitis accompanied by extensive macrophage infiltration of the cerebral white matter, indicative of a significant cell-mediated (Th1) inflammatory response (Nicoll *et al.*, 2003). While only one patient died, 6% of participants experienced serious side-effects sufficient to bring the trial to a close. Experts suggested that the vaccine may have stimulated too strong an immune response which weakened the barriers that normally protect the CNS from bacterial or viral attack, or that T-cell and microglial overactivation may have induced neuroinflammation (Solomon, 2004).

Progress towards stimulating prion mucosal immunity was demonstrated by *in vivo* protection of mice following mucosal vaccination with PrP expressing *Salmonella typhimurium* (Goni *et al.*, 2008). The vaccination schedule consisted of weekly administration of four oral vaccinations using a live *Salmonella* construct followed by two injections of the same dead *Salmonella* construct. Seven weeks after the first vaccination, mice were exposed, via oral gavage, to 139A Scrapie strain. They found that 100% of mice expressing high IgA and IgG titers, and 33% of mice with high IgG and low IgA, were symptom-free 400 days after inoculation. Histological and Western blot analysis verified a lack of PrP^{Sc} in the brains of asymptomatic animals (Goni *et al.*, 2008). It was anticipated that the level of protection would be directly linked to the magnitude of IgA production, but the 33% survival rate observed in the low IgA/high IgG group suggested other factors may also be important in determining vaccine efficacy (Goni *et al.*, 2008). They concluded that anti-PrP IgA is likely important in preventing prion uptake in the gut while systemic anti-PrP IgG interferes with the isoform conversion process. One advantage of this system is the ability of *Salmonella* to target the key sites of prion uptake within the digestive tract, the M-cells (Li *et al.*, 2010). At the same time, the variation in *Salmonella* intra-gut survival, PrP expression, and level of gut penetration, pose significant challenges for stimulating the desired immunological response in each vaccinated animal (Goni *et al.*, 2008). Despite having only been tested in mice and not a larger animal model, the authors have provided insight into the type of immune response (non-inflammatory Th2) which may be necessary for providing protection against oral prion infections.

1.2.1.2.4 Immunization Using Plasmid and Viral Vectors

Tolerance is likely the greatest challenge for immunotherapeutic strategies targeting PrP^{C}. Despite anergy or deletion of most B and T-cell expressing receptors specific for PrP^{C}, experts believe it is possible to stimulate the limited anti-PrP^{C} antibody repertoire using potent immunogenic delivery systems (Gregoire *et al.*, 2005; Li *et al.*, 2010). Nikles *et al.* hypothesized that recombinant virus-like particles would function as more efficient B-cell immunogens than monovalent recombinant proteins, and consequently developed a retrovirus (murine leukemia virus) based PrP vaccine construct expressing residues 121-231 (PrP^{111}) (Nikles *et al.*, 2005). Using three different groups of C57BL/6 mice with PrP genotypes, (*Prnp*

$^{-/-, -/+, +/+}$) vaccination with PrP^{111} produced PrP^{C}-specific responses with titers inversely proportional to the number of PrP alleles expressed. The authors were surprised, however, by the similarity of IgM titers between the three genotypes in the early time points. While class switching of PrP^{C}-specific IgM to IgG antibodies was less pronounced in wild type animals compared to *Prnp*$^{-/-}$, use of the murine leukemia virus delivery system appeared to provide antigenic T-helper determinants allowing for class switching to occur in the wild-type animals despite tolerance to PrP (Nikles *et al.*, 2005). Whether the level of antibodies produced by this construct are sufficient to be of therapeutic value remains to be determined.

In 2007, Kirnbaur's group incorporated a PrP^{C} B-cell epitope (144-152) into a capsid protein component of the bovine papillomavirus type 1 which was expressed by recombinant baculovirus technology. Advantages of this carrier system are its ability to self-assemble into pentamers which further multimerize into virus-like particles and display the inserted PrP epitope at a density up to 360 copies per particle. Additionally, virus-like particle vaccines that continuously induce anti-PrP antibody result in a more constant antibody concentration over time, consequently, fewer vaccinations may be required (Handisurya *et al.*, 2007; Kirnbauer *et al.*, 1992). The epitope, also recognized by mAb 6H4 and other commercial antibodies, was selected based on previous studies linking that region with PrP^{Sc} induced conformational changes (Handisurya *et al.*, 2007). Rabbits and rats were vaccinated with the virus particles, along with either Freund's incomplete adjuvant or CpG, four times at 2-4 week intervals. Anti-PrP IgG antibodies were detected in both species two weeks after the last boost. *In vitro* experiments using ScN2a and rabbit anti-PrP IgG demonstrated the ability of the antibodies to prevent *de novo* formation of PrP^{Sc}.

Rosset *et al*. (2004) compared a plasmid expressing PrP as a vaccine in wild type and *Prnp*$^{-/-}$ C57BL/6 mice. On its own, PrP plasmid DNA stimulated anti-PrP antibodies directed against the N-terminal region in the knock-out mice but failed to induce a response in the wild-type animals. The addition of CpG oligodeoxynucleotides, an adjuvant that helps stimulate dendritic cells (Krug *et al.*, 2001) and B-cells (Krieg *et al.*, 1995), to the PrP plasmid DNA formulation helped to successfully induce anti-PrP antibodies in the wild-type mice (Rosset *et al.*, 2004). The epitopes recognized by these antibodies were unique to those produced in *Prnp*$^{-/-}$ mice and specific for the C-terminal portion of PrP. Another difference was that antibodies in *Prnp*$^{-/-}$ mice recognized membrane bound PrP^{C} whereas none of the antibodies from wild-type

animals did. The authors suggested that antibodies were specific for different locations on PrP despite identical immunizations because B-cells specific for native PrP^{C} epitopes are strongly tolerated (Gregoire *et al.*, 2005). It was also observed that *Prnp*$^{-/-}$ antibodies were primarily of the IgG1 isotype whereas antibodies from wild-type mice were mainly IgG2b, an indication that the immune response in wild-type animals was skewied toward a Th1 cell-mediated response. The authors concluded that antibodies stimulated by PrP plasmid DNA + CpG, while unable to bind PrP^{C}, might be effective in blocking PrP^{Sc} replication by targeting regions uniquely exposed in the PrP^{Sc} conformation (Gregoire *et al.*, 2005).

More recently it was suggested that the use of xenogenic antigens may be effective in circumventing tolerance to autoantigens such as PrP^{C}. Although 90% of the prion amino acid sequence is conserved among mammals, it was demonstrated that vaccination of mice with bovine PrP stimulated the production of anti-PrP antibodies (Ishibashi *et al.*, 2007). Tang *et al*. implemented xenogenic prion (human) expression via an adenovirus vector system which had been shown previously, in cancer studies, to be a potent generator of antibody ($CD4^{+)}$ and cell-mediated ($CD8^{+}$) responses to both the viral capsid proteins as well as the transgene (Tang *et al.*, 2004). In C57BL/6 wild-type mice, the authors compared dendritic cell mediated delivery with direct administration of the adenovirus vector. The dendritic cell mediated treatment, only, was able to break B-cell tolerance against murine PrP, producing antibodies which increased the survival of prion-infected mice by an average of 37 days (n=5) without stimulating T-cell directed autoimmunity (Rosset *et al.*, 2009).

1.2.1.2.5 PrP^{Sc}-specific Immunotherapy

The understanding about the physiological function of the PrP^{C} is still limited. For this reason, it may not be the safest strategy to target an immune response towards such a commonly expressed protein. It has previously been demonstrated that antibodies which crosslink PrP^{C} in neural tissue cause apoptosis (Solforosi *et al.*, 2004). The systemic presence of autoreactive PrP^{C} antibodies may also lead to an impairment of the natural function of PrP^{C}, inappropriate cell signal activation, or stimulation of suppressor T-cell lymphocytes (Li *et al.*, 2010). An alternative immunotherapeutic strategy is to stimulate an immune response specific for the PrP^{Sc} conformation. While this approach is challenged by the lack of PrP^{Sc} structural

information, it may present a more viable method for circumventing the body's tolerance mechanisms to PrP^{C} and avoid induction of autoimmunity.

In 2007, Pilon *et al*. (2007) created three peptide vaccine constructs ranging in length from 13 to 29 amino acids. One construct contained a tyrosine-tyrosine-arginine motif on α-helix 1 which was one of the two regions predicted by Paramithiotis *et al*. (2003) to be selectively exposed on the PrP^{Sc} conformation. Results from vaccination trials showed all three constructs to be moderately immunogenic, with the α-helix 1 group displaying higher median titers than the other two groups. In a Scrapie challenge experiment, the best result observed was a 20 day increase in survival when compared to the control group. There was, however, a lack of correlation between the longest surviving group and the group with the highest median titers. The authors concluded that a successful vaccine would need to address two main issues; overcoming self-tolerance and stimulating antibodies with high affinity for the PrP^{Sc} conformation (Pilon *et al.*, 2007).

One strategy for establishing an immune response to the infectious prion conformation would be to identity a cryptic epitope specifically exposed in the PrP^{Sc} conformation. In an attempt to address this issue, it was found that during the refolding process from PrP^{C} to PrP^{Sc}, there is increased solvent exposure of tyrosine (Y) side chains (Paramithiotis *et al.*, 2003). The majority of these residues are located in the structured C-terminal domain, a region linked to infectivity and protease resistance (Riek *et al.*, 1996). Of the 11 residues in the structured region, 6 are present in bi-tyrosine pairs, a motif that is conserved in human, sheep, mouse, hamster, cattle and deer [**Figure 1.5]**. Two pairs are in conjunction with a C-terminal arginine (R), one of which is located on α–helix 1 and the other on β-strand 2. It was hypothesized by Paramithiotis *et al*. that a YY-motif located on a β–sheet may present an epitope specific for the PrP^{Sc} conformation. Testing of this hypothesis resulted in the production of rabbit antiserum that selectively immunoprecipitated (IP) PrP^{Sc} from infected mouse brain and not PrP^{C} from uninfected brains (Paramithiotis *et al.*, 2003). These results indicate that the YYR epitope on β2–sheet may represent a strong vaccine target for the stimulation of a specific PrP^{Sc} immune response. Despite use of an aggressive vaccination protocol which utilises the commonly used vaccine carrier molecule KLH and potent adjuvants such as Freund's Complete, this strategy

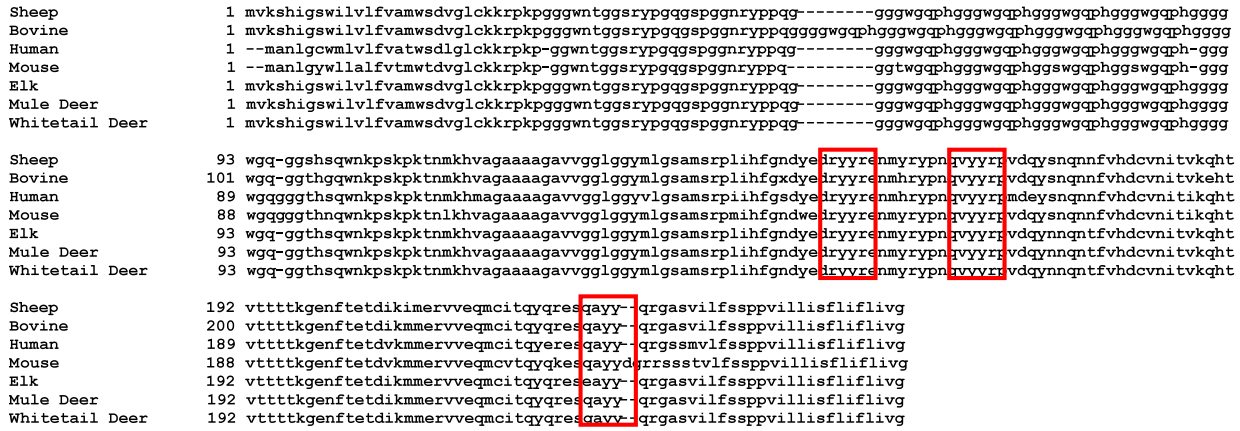

Figure 1.5: Conserved Tyr-Tyr-X motifs in aligned amino-acid sequences of sheep, bovine, human, mouse, elk, mule deer and whitetail deer PrP.

has been limited by poor immunogenicity where IgM was the only antibody isotype detected (Paramithiotis *et al.*, 2003).

1.2.1.2.5.1 Peptide-Based Vaccine Design

Traditional vaccines are often designed using attenuated live or inactivated microorganisms. Culturing these organisms can be difficult and even the safest attenuated vaccine systems can produce harmful immune responses. For diseases such as cancer, and protein misfolding diseases like TSEs, Parkinson's, Alzheimer's and Huntington's disease, pathology is linked to altered self-proteins. As a result, normal vaccine strategies are not applicable due to robust tolerance mechanisms. Extensive research has determined that short peptide fragments derived from residues found on the much larger self-proteins, can stimulate very specific immune responses (Purcell *et al.*, 2007). The ability to target only the 'rogue' self proteins may serve as a powerful tool in preventing the transmission of these diseases or progression of symptoms/pathology in already sick individuals, without stimulating autoimmunity.

Peptide vaccine technology offers advantages in terms of safety and ease of production. Peptide preparations can be freeze-dried, making their transportation and storage much easier than those vaccines requiring refrigeration. Their safety is derived from the ability to create an immune response without the requirement of infectious material such as that required for attenuated vaccines. Also, the absence of genetic material eliminates the risk of genetic integration or recombination with the patient's genome, a concern posed by DNA vaccines. Furthermore, large scale production of peptides is economical, and purity is easily analyzed using liquid chromatography and mass spectrometry (Purcell *et al.*, 2007).

Vaccinating with an exogenously administered peptide can be challenging because the exact pathway by which the peptide is processed and then presented to immune cells is thought to be different than for traditional antigens and not well understood (Purcell *et al.*, 2007). To successfully activate B-cells specific for a certain target, the peptide fragment has to represent the appropriate conformation. For this to be achieved, structural knowledge of the native antigen is very beneficial (Purcell *et al.*, 2003). Consequently, peptide vaccine design for TSEs is made more challenging due to the lack of structural data for the misfolded prion protein.

An additional challenge for peptide vaccine design is overcoming the weaker immunogenicity of the peptide fragments, a drawback attributed to their small size. This is particularly true of the cryptic YYR epitope identified by Paramithiotis *et al*. (2003) as a potential peptide target for prion immunotherapy. This three amino acid motif, due to its size, has the immunological characteristics of a hapten. A hapten is an antigen which on its own lacks sufficient immunogenicity to stimulate an immune response. Consequently, haptens are usually coupled to a larger immunogenic carrier molecule such as tetanus toxoid or KLH. When such an immunogenic complex is presented to the immune system, antibodies to the carrier, hapten and junction between the hapten and carrier, are produced. Successful activation of the humoral branch of the immune system against a given antigen "A" requires two components. The first is the activation of the T-helper (T_h) CD4+ cell which occurs via interaction with an antigen presenting cell (APC) (usually a macrophage, dendritic cell or B-cell) displaying the antigen A in the context of a surface MHC II molecule (Mond *et al.*, 1995). One of the main functions of an APC is to phagocytose cellular debris, degrade it into peptide fragments which attach to MHC II molecules and are translocated to the cell surface for presentation to the immune system (while both endogenous and exogenous peptide processing occurs, this discussion will focus on the exogenous component). If a T_h-cell recognizes antigen A, it binds to it (producing signal #1) and receives a costimulatory signal (signal #2) from the APC, completing the activation requirements of the T_h-cell. The second component requires a B-cell that has an Ig receptor on its surface specific for antigen A. This interaction alone is not sufficient to activate the B-cell. It needs authorization from a T_h-cell with the same specificity to antigen A. Once this occurs, the B-cell becomes activated and produces Abs specific for antigen A (Purcell *et al.*, 2007). Therefore, the goal of a successful vaccine carrier molecule is to provide T_h epitopes which will help activate a robust B-cell response to the poorly immunogenic hapten. By specifically testing for these different groups of antibodies using peptide-specific ELISAs it is possible to determine the effectiveness of the vaccine construct.

1.2.1.2.5.2 GnRH as a Model for Vaccine Design Against Endogenous Peptides.

There was a significant amount of work done in the 1990's on a vaccine strategy for targeting the gonadotropin-releasing hormone (GnRH). GnRH is an important hormone which

helps regulate the release of pituitary gonadotropins (Schally *et al.*, 1973). Immunological neutralization of GnRH has the potential for use in treatment of sex hormone-related malignancies (Meloen *et al.*, 1995) without the side effects caused by castration (Meloen *et al.*, 1994). Issues such as carrier molecule selection and antigen presentation were addressed to compensate for the weak immunogenicity of the GnRH peptide.

In an effort to find a effective carrier molecule, Manns *et al*. (1997) found they could stimulate significant GnRH peptide-specific responses using the carrier molecule Leukotoxin (Lkt), a truncated 96 kDa multiple repeat toxin containing many T_h-cell epitopes derived from *Pasteurella haemolytica*. Typically, the strategy used for coupling vaccine carrier molecules to weakly immunogenic peptides is through a chemical conjugation using carbodi-imide (Fraser *et al.*, 1974). This method, however, is labour intensive when used to produce a highly purified and homogenous protein and is not cost effective for use in a commercial vaccine (Manns *et al.*, 1997). Furthermore, this process can interfere with the biological activity of the carrier molecule by physically obstructing immunogenic epitopes. Consequently, a genetic construct was utilised, within a highly regulated bacterial expression system, to produce large amounts of identical chimeric Lkt-GnRH proteins (Manns *et al.*, 1997).

Antigen presentation is an important variable affecting the immunogenicity of an endogenous peptide. While trying to figure out how to alter the GnRH peptide to increase its immunogenicity, one research group speculated that creating tandem repeats of the original 10 amino acid sequence may help reduce the appearance of "self". Their experiments showed that all animals vaccinated with the tandem repeat responded to the treatment whereas only two out of five responded to vaccination with the non-repeated construct (Meloen *et al.*, 1994). Another group of researchers investigated the effect of epitope orientation on immunogenicity. Results indicated that the synthesis of an inverted repeat yielded an increase in immunogenicity similar to that seen in the repeated versus non-repeated constructs (Ghosh and Jackson, 1999). An example of an inverted repeat versus a linear repeat for a given hypothetical three residue epitope would be XYZZYX and XYZXYZ, respectively.

1.3 Importance of a TSE Vaccine

Discovering the link between BSE and the vCJD outbreak of 1996 brought TSEs to the attention of the public and health professionals. As many as 180,000 BSE cases were identified, triggering the culling of 750,000 animals (Donnelly *et al.*, 2002; Wilesmith *et al.*, 1988). Experts suggested that as many as 3 million BSE-infected animals entered the human and animal food chains undetected (Donnelly *et al.*, 2002). While confirmed cases of vCJD are only at 188 worldwide (Collee *et al.*, 2006), the potential spread via contaminated blood or tissue products taken from asymptomatic carriers is of great concern.

CWD is the most contagious of the TSE's and presents a significant threat to both wild and farmed deer populations with rates of infectivity as high as 30% and 100%, respectively (Williams, 2005). The possibility for cross-species infectivity with humans and farmed animals, as well as its ability to persist in the environment for years, and a poor understanding of CWD transmission, make containment using current resources unattainable (Sigurdson and Aguzzi, 2007).

As a group, TSE's have had undeniable economical impact, leaving many countries with billions of dollars in lost revenue due to border closures and weakened consumer confidence. While key historical TSE events have provided the momentum for research initiatives aimed at understanding PrP^{C} function, PrP^{Sc} infectivity and designing effective pre-mortem diagnostics and therapeutic strategies, definitive answers in these areas remain elusive. Despite the research initiatives that have been underway for a few decades, there are still large deficits in key areas of understanding such as PrP^{C} function and pre-mortem diagnostics. Identifying a disease-specific epitope may have significant applications in more than one of these TSE research areas. These events have provided the momentum for research initiatives aimed at understanding PrP^{C} function, PrP^{Sc} infectivity and designing effective diagnostic tests and therapeutic strategies.

1.4 Other Protein Misfolding Diseases

The development of a successful vaccine strategy for prion disease, using cryptic epitopes, may shed light on how similar approaches can be used in the battle against other

protein misfolding diseases such as ALS, Alzheimer's, and Parkinson's. ALS is a neurodegenerative disease most commonly associated with pathology within the upper and lower motor neurons of the spinal cord (Bruijn *et al.*, 2004). Pathogenesis has been linked to the intracellular accumulation of aggregates consisting of a misfolded version of the endogenous protein superoxide dismutase (SOD1) (Nordlund and Oliveberg, 2008). Non-pathogenic SOD1 is a soluble homo-dimer expressed in neurons which helps to reduce oxidative damage from free radical species (Rakhit *et al.*, 2006). The mechanism causing the misfolding of SOD1 is not well understood but is hypothesized to be a result of mutations in the SOD1 gene (Shaw and Valentine, 2007). Research on identifying a conformational epitope specific for the pathological conformation began in 2006 when Rakhit *et al*. reported that they identified an epitope on misfolded SOD1 monomers that is normally buried in native SOD1 dimers.

Like TSEs, Alzheimer's is a neurodegenerative disease and typically causes dementia in the form of memory loss, and impairment of language, reasoning, and judgment in the elderly population (Hooper and Turner, 2008). Alzheimer's disease, however, has a much higher prevalence rate with 29.3 million people worldwide currently suffering from the disease (Wimo *et al.*, 2007) and no acceptable therapeutic agents are currently available (Roberson and Mucke, 2006). Symptoms are caused by the deposition of neuronal plaques consisting primarily of insoluble amyloid-β (Aβ) peptides that are 40-42 amino acids in length (Mattson, 2004). Unlike the pathological misfolding of PrP^{C} to produce PrP^{Sc}, the formation of Aβ results from the proteolytic cleavage of the amyloid precursor protein (APP) by the enzyme β-secretase (Hooper and Turner, 2008). Normally, APP is cleaved by α-secretase to produce a soluble isomer called sAβ which is readily detectable in serum and cerebrospinal fluid (Walsh and Selkoe, 2007). Analysis of the proteolytic pathway producing Aβ has shown it to have a physiologic function that responds to neurological activity. Increased activity results in increased Aβ formation which reduces excitatory synaptic transmission. In the diseased state, overproduction of Aβ peptide and/or failure of the degradation enzymes leads to oligomerization and aggregation which over time results in senile plaque formation (extracellular amyloid deposits) and symptom development (Ghochikyan, 2009).

Parkinson disease (PD) is a neurodegenerative disorder that typically affects movement. Symptoms result from a tropic loss of dopaminergic neurons located in the substantia nigra, an

area responsible for the initiation of intentional movements (Kazantsev and Kolchinsky, 2008), and the formation of cytoplasmic inclusions referred to as Lewy bodies (Emadi *et al.*, 2009). The main therapeutic strategy is dopamine replacement using a dopamine precursor molecule called levodopa; however, after prolonged use this strategy becomes ineffective (Kazantsev and Kolchinsky, 2008). Research has shown that PD-associated neuronal damage results from an accumulation of misfolded α-synuclein, which forms neurotoxic aggregates. The presence of these aggregates interfere with cytoskeleton components as well as mitochondrial and cellular membranes (Kazantsev and Kolchinsky, 2008). They have also been detected in extracellular compartments such as plasma and cerebrospinal fluid of PD patients (El-Agnaf *et al.*, 2006). Non-pathogenic α-synuclein is 14 kDa and is most often found in the presynaptic terminals of neurons (Iwai *et al.*, 1995). Existing normally as an unfolded protein, α-synuclein can adopt many different conformations such as fibrils, oligomers, small aggregates, spherical and linear protofibrils (Conway *et al.*, 1998; Serpell *et al.*, 2000). The oligomeric conformation has been linked to the neurodegenerative effects seen in PD (Volles and Lansbury, 2003; Volles *et al.*, 2001). Work by Emadi *et al*. has shown it is possible to detect the different morphological conformations of α-synuclein using single chain variable domain antibody fragments. This allows for the possibility that the stimulation of a conformation specific immune response may be a realistic therapeutic strategy (Emadi *et al.*, 2009).

1.5 Hypothesis and Objectives

Using the YYR epitope, unique to the infectious conformation of the prion protein, it is hypothesized that through epitope optimization, significant antibody responses can be stimulated in mice, cows and cervids as a result of sequence homology between species.

The objectives of this project were to:

1) Design a series of vaccine constructs based on different lengths of YYR motif to test their capacity to stimulate specific Ab responses *in vivo* (using sheep and mice).

2) Develop enzyme-linked immunoabsorbent assays (ELISA) to assess epitope-specific Ab titres.

3) Determine what vaccine dose is most immunogenic for each species being used in the vaccine trials.

4) Determine if there is an immunological advantage to increasing the number and orientation of the YYR repeats incorporated into the vaccine construct.

5) Evaluate the specificity of the antibody responses for PrP^{C} and PrP^{Sc}

6) Evaluate vaccine immunogenicity in cervid species.

7) Assess safety of the vaccine by screening for antibodies which may cross react with PrP^{C}.

2.0 MATERIALS AND METHODS

2.1 Animals

Mice were obtained from Charles River (Wilmington, MA) and housed in the animal care facilities at the Vaccine and Infectious Disease Organization (VIDO). Mice were typically four to six weeks of age at the start of each experiment.

Sheep were obtained from the University of Saskatchewan breeding program associated with the Animal Science Department. Sheep have genetic polymorphisms within the PrP gene (at codons 136, 154 and 171) which influence susceptibility to prion disease. The most common phenotypes in the order of susceptible to resistant are: valine, arginine, glutamine (VRQ); alanine, arginine, glutamine (ARQ) and alanine, arginine, arginine (ARR). Of the prion susceptible phenotypes, VRQ is very rare. The majority of sheep used in these studies were bred from ARQ homozygous breeding pairs. The lambs typically consisted of mixed sex and breed (Suffolk and Arcott) and ranged from 1-6 months in age at the beginning of a trial. For each trial, however, the groups of animals being used were aged matched, to allow for better comparison among experimental groups. Sheep were housed in outdoor pens, fed a standard ration at VIDO, and all experimental procedures were performed by VIDO Animal Care technicians during trials.

Sheep used in the Norwegian Scrapie challenge trial were from the Rygia breed and ranged in age from 0-7 years of age. Animals were housed in dedicated Scrapie isolation pens at the Sheep and Goat Research Station in Sandes, Norway. Experimental procedures were supervised by Dr. Martha Ulvund, and sheep were handled by the Animal Care staff at the research station in Sandes.

Elk and Whitetail deer were puchased by the University of Saskatchewan and housed at the Goodale Research farm located 9 miles South East of Saskatoon. The animals ranged in age from 1-5 years of age. Experimental procedures were supervised by Dr. Trent Bollinger, Western College of Veterinary Medicine, and the deer were handled by the Goodale staff.

2.2 Epitope Design and Construction

2.2.1 Peptide Synthesis for ELISA

To detect peptide-specific antibody responses, peptides of the same sequence as the epitopes were chemically synthesized on a Pioneer solid-phase peptide synthesizer (PerSeptive Biosystems, Foster City, CA) using Fmoc (9-fluorenylmethoxy carbonyl) chemistry. The peptide chains were synthesized from the carboxyl terminus to the amino terminus onto [5-(4-Fmoc-aminomethyl-3,5-dimethyloxyphenoxy) valeric acid]-polyethylene glycol-polystyrene (PAL-PEG-PS) resin. Fmoc-protecting groups at the amino terminus were deprotected with piperidine. The peptides were cleaved from the resin with concurrent deprotection of the side chain-protecting groups by treating the resin-bound peptide with trifluoroacetic acid (TFA) (9.3 parts) in the presence of scavengers (anisole-ethyl-methyl sulfide-1, 2-ethanedithiol [3:3:1]), for 7 h. The crude peptides were filtered from the resin, and the TFA was evaporated. Diethyl ether was added to the residues to precipitate the crude peptide. The peptides were isolated and purified by high-performance liquid chromatography (HPLC) on Vydac protein C_4 columns (1.0 by 25 cm) eluting with a linear gradient of 10% buffer A (H_2O-0.1% TFA)-90% buffer B (acetonitrile-H_2O [90/10]-0.01% TFA) for 40 min at a flow rate of 3 mL/min. The purity and molecular weight of the respective peptides were confirmed by matrix-assisted laser desorption ionization (MALDI)-time of flight mass spectrometry on a PE Biosystems Voyager system 4068 (National Research Council, Plant Biotechnology Institute, Saskatoon, Canada).

2.2.2 Recombinant Lkt-YYR Constructs

Genes corresponding to the desired epitopes were synthesized with flanking *BamH*I and *Nco*I restriction sites by Codon Devices (Cambridge, MA) and BioBasic (Markham, ON) to facilitate their insertion into the Lkt expression vector pAA352 (Potter AA and Manns JG, 2000). The appropriate fragments were sub-cloned, via *Nco*I and *BamH*I restriction sites, into pAA352 [**Figure 2.1**] which contains a gene encoding a 96 kDa version of the Lkt protein such that the antigens are expressed as C-terminal fusions. A series of plasmid constructs were

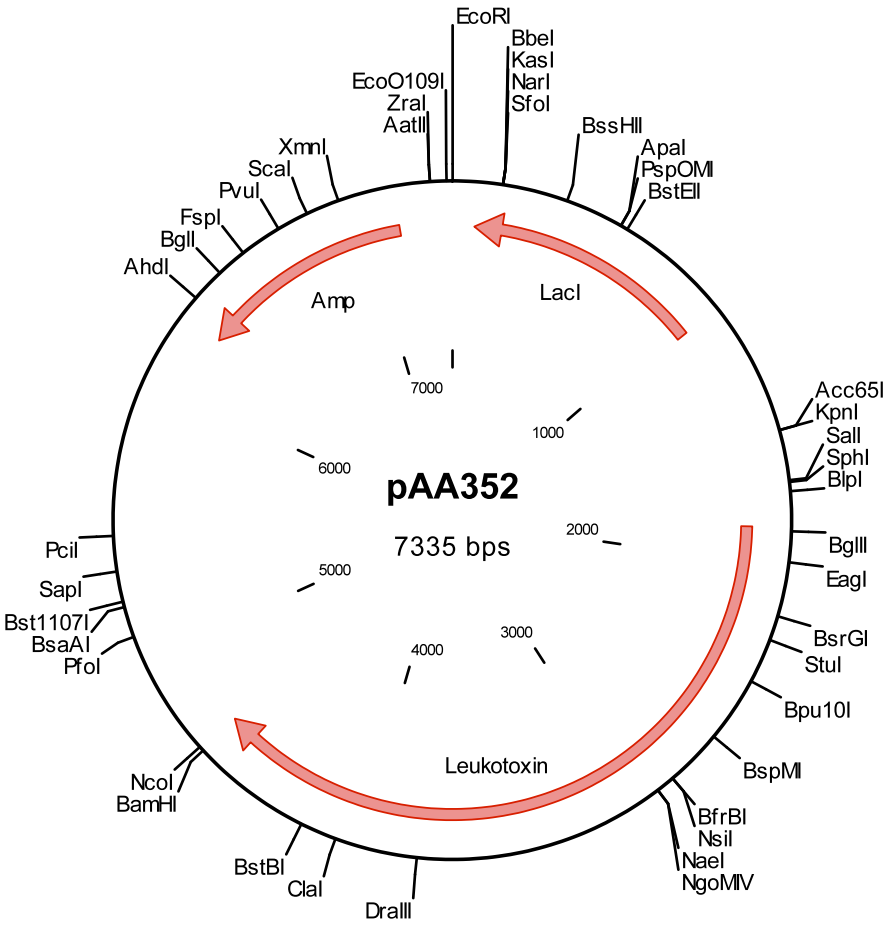

Figure 2.1: Map of pAA352 Lkt expression vector. The plasmid contains an ampicillin (Amp) resistance gene to allow for plasmid screening. YYR constructs were inserted at the C-terminal end of the Lkt gene using the restriction sites BamHI and NcoI. Leukotoxin expression is under regulations of a hybrid trp::lac promoter from *E.coli.*

created representing different expansions of the YYR epitope as well as different presentations (either linear or inverted repeats) [**Table 2.1**]. All plasmids were sequenced verified in-house using the Beckman Coultier CEQ 2000XL DNA Analysis System and manufacturer's specifications for the CEQ Dye Terminator Cycle Sequencing with Quick Start Kit (Beckman Coulter).

2.2.2.1 Growth and Induction of Lkt expression Vectors

Eschericia coli DH5αF5 cells were transformed with chimeric Lkt expression vectors and incubated overnight at in 10 mL of Luira-Bertani (LB) broth with 100 μg of ampicillin shaking at 220 rpm at 37 °C. The overnight culture was used to inoculate 500 mL of pre-warmed LB broth containing ampicillin. Incubation at 37 °C with shaking was continued until an OD600 of 0.6 was achieved. Cells were then induced using sterile isopropyl beta-D-1-thiogalactopyranoside (IPTG) to a final concentration of 1 mM and incubated for 3 h at 37 °C. Cells were harvested by centrifugation at 10,000 x *g* for 15 minutes at 4 °C. The supernatant was discarded and cell pellets were re-suspended in 25% sucrose, 50 mM Tris pH 8.0 (4 mL/L of culture) and then frozen at -80 °C.

2.2.2.2 Lysis and Purification/Solubilization of Lkt fusion proteins

Cells were thawed at room temperature and 1 mL of lysozyme (10 mg/mL) was added per 4 mL of re-suspended pellet. This solution was mixed, set on ice for 15 minutes before adding 20 mL RIPA:TET buffer (5:4; RIPA containing 20 mM Tris-HCl pH 8.0, 200 mM NaCl and 2% sodium deoxycholate; TET containing 100 mM Tris-HCl 8.0, 50 mM EDTA and 2% Triton X-100), inverted quickly, vortexed for 20 seconds, and then placed on ice for 20 minutes. The cell mix was then sonicated three times with a 3/4 inch probe at 50% for 20 seconds. Cells were centrifuged at 25,000 x *g* for 20 minutes, the supernatant discarded and tubes were inverted on tissue to drain supernatant off the pellet. The pellet was resuspended in 1 mL of 4 M guanidine-HCl per 30 mg pellet and then stored at 4 °C overnight. Particulates were removed by centrifugation at 1,300 x *g* for 10 minutes and the supernatant was decanted. Protein purity and quantity in the supernatant was determined using electrophoresis in SDS

Table 2.1: PrP Peptide Sequences and Presentations. Constructs were created, based on the ovine PrP sequence, as C-terminal fusion to the Lkt protein. Nomenclature indicates YYR from alpha helix 1 (α1) or beta sheet 2 (β2), the direction and magnitude of epitope expansion and the presentation as either linear (L) or inverted (I) epitopes represented graphically by the arrows in the "Presentation" column.

	Construct Notation	Peptide Sequence	Presentation
1	β2(YYR)L	YYR	(➡➡)$_4$
2	β2(YYR)I	YYR	(➡⬅⬅)$_4$
3	β2(1+YYR+1)L	VYYRP	(➡➡)$_4$
4	β2(1+YYR+1)I	VYYRP	(➡⬅⬅)$_4$
5	β2(1+YYR+1)I x 4	VYYRP	(➡⬅⬅)$_{16}$
6	β2(2+YYR+2)L	QVYYRPV	(➡➡)$_4$
7	β2(2+YYR+2)I	QVYYRPV	(➡⬅⬅)$_4$
8	β2(3+YYR+1)L	NQVYYRP	(➡➡)$_4$
9	β2(3+YYR+1)I	NQVYYRP	(➡⬅⬅)$_4$
10	β2(2+YYR+3)I	QVYYRPVD	(➡⬅⬅)$_4$
11	β2(2+YYR+4)I	QVYYRPVDQ	(➡⬅⬅)$_4$
12	β2(2+YYR+5)I	QVYYRPVDQY	(➡⬅⬅)$_4$
13	β2(2+YYR+6)I	QVYYRPVDQYS	(➡⬅⬅)$_4$
14	β2(2+YYR+7)I	QVYYRPVDQYSN	(➡⬅⬅)$_4$
15	β2(2+YYR+8)I	QVYYRPVDSQYSNQ	(➡⬅⬅)$_4$
16	β2(2+YYR+9)I	QVYYRPVDSQYSNQN	(➡⬅⬅)$_4$
17	β2(9+YYR+2)I	NMYRYPNQVYYRPV	(➡⬅⬅)$_4$
18	α1(2+YYR+2)I	DRYYREN	(➡⬅⬅)$_4$

PAGE with Coomassie Blue staining and compared relative to BSA standards. The isolated protein was determined to be greater than 85% pure.

2.2.3 Recombinant Lkt-PrP^C

Recombinant Lkt-PrP^C constructs were synthesized using the same protocol as the Lkt-YYR constructs but with the following modifications: full-length ovine PrP^C was synthesized with flanking restrictions sites by BioBasic to facilitate its insertion into pAA352 at the C-terminal end as a non-repeated, linear sequence.

2.2.4 Bacterial Strains

Competent DH5αF5 *E. coli* cells (VIDO) were transformed by our pAA352 Lkt-YYR based constructs.

2.2.4.1 Competent Cells

Competent *E. coli* DH5αF5 cells were prepared by treating a log phase culture that had been centrifuged at 5,000 x *g* for 5 minutes at 4 ºC with sterile 0.1 M $CaCl_2$ and cooling on ice for 20 minutes. Cells were centrifuged again as above and resuspended in chilled 0.1 M $CaCl_2$ with 17.5% glycerol on ice for 20 minutes and then stored at -80 ºC (Sambrook and Russell, 2001).

2.2.5 Bacterial Growth Media

To facilitate growth of *E. coli* bacteria containing specific plasmids for mini-preps, cultures were inoculated into LB broth (BD Biosciences) which consists of 10 g tryptone, 5 g yeast, and 10 g NaCl for every 1 L of water. Once necessary ingredients are added the medium is sterilized in the autoclave at 121 ºC for 15 minutes. Once cooled, ampicillin was added to make a final concentration of 100 μg/mL (LB-amp^{100}) which allowed for selection of bacteria containing plasmid DNA following transformation.

2.2.6 Vectors

Three different vectors were used throughout this project. The majority of the molecular experiments involved the use pAA352 which was made at VIDO. Epitope constructs synthesized by BioBasic were sent in generic pUC57 vectors allowing for the extraction of the sequence of interest using restriction digestion with *BamH*I and *Nco*I for the Lkt fusion constructs. Double digestions were carried out for the pAA352 and pUC57 vectors as follows: 10 Units (U) of *Nco*I and 20 U of *BamH*I were added to 1 μL of plasmid, 5 μL of NEbuffer 3, 0.5 μL BSA, 1 μL RNase and 36 μL ddH_20. The reaction mix was incubated at 37 ºC for 60 minutes and then heat inactivated at 65 ºC for 20 minutes. Samples (pUC57) were run on an agarose gel to visualize and excise the portion of the gel containing the fragments of interest, which was then processed with the Wizard SV gel and PCR cleanup system (Promega) according to manufacturers specifications. For ligation, 30 μL of insert was added to: 2 μL of pAA352 (the ratio of insert to plasmid, 15:1, was established by the difference in the number of base pairs between the two), 3 U of T4 DNA ligase and 3.5 μL ligase buffer. Samples were incubated at room temperature for 10 minutes and then inactivated at 65 ºC for 10 minutes. A description of the amino acid and nucleic acid sequence for the β2(YYR)L construct is provided in **Table 2.2** with the rest of the construct descriptions are included in the Appendix A.

2.2.7 Transformation

Competent cells were thawed on ice for 30 minutes. Plasmid DNA (2 μg) was added to 20 μL of cells and placed on ice for 30 min. The culture was heat-shocked at 42 ºC for 90 seconds and put on ice for 2 minutes. Pre-warmed LB broth (100 μL) was added and incubated at 37 ºC for one hour. Cells were then plated on LB-amp^{100} plates overnight at 37 ºC and screened for viable colonies.

Table 2.2: The amino acid and nucleic acid sequence of the β2(YYR)L construct (Sequences for all the other constructs used in this project have been included in Appendix A).

Construct	β2(YYR)L
Amino Acid Sequence	GSYYRSGSYYRGSSYYRSGSYYRGSSYYRSGSYYRGSSYYR SGSYYRGSSHHHHHH
Nucleotide Sequence	GGA TCC TAC TAT CGT AGC GGT TCT TAC TAT CGC GGC TCT AGC TAC TAT CGT AGC GGT AGC TAC TAT CGC AGC GGT TCT TAC TAT CGT GGC TCT AGC TAC TAT CGC AGC GGT TCT TAC TAT CGT AGC GGT TCT TAC TAT CGC GGC TCT AGC CAC CAC CAC CAC CAC CAC TGA CCA TGG

2.2.8 SDS-PAGE Analysis

Samples were loaded with 5x SDS loading dye onto a 10% acrylamide gel with a pre-stained low range molecular weight marker (Biorad). Gels were run in SDS-PAGE buffer at 100 V for 2 hours or until the dye beyond the end of the gel. Gels were then stained for 30 minutes with Coomassie blue and then de-stained overnight.

2.2.9 Western Blot

Lkt-YYR chimera proteins were resolved through a 10% SDS-PAGE gel. Following electrophoresis, the proteins were transblotted onto polyvinylidene difluoride membranes (PolyScreen; Perkin Elmer Life Sciences). The membranes were blocked with 3% molecular grade fat-free skim milk powder in phosphate-buffered saline containing 0.02% Tween 20. Primary and secondary washes were carried out using this sample buffer. The 6H4 mAb was used to detect prion protein.

2.2.10 Mini-prep Isolation of Plasmid DNA

Following transformation, individual colonies were selected from the LB-amp^{100} overnight plates and inoculated into 5 mL of fresh LB-amp^{100} broth for overnight incubation in a 37 ºC shaker. The cultures were centrifuged at 18,000 x *g* for 5 minutes and then DNA was isolated using the Wizard Plus SV Miniprep DNA Purification System by Promega. Pellets were resuspended in 250 μL of the provided solution (50 mM Tris-HCl (pH 7.5), 10 mM EDTA and 100 μg/mL of RNase A) and vortexed. Cell lysis solution (250 μL) containing 0.2 M NaOH and 1% SDS was added and gently mixed using tube inversion followed by a 5 minute incubation at room temperature. 10 μL of alkaline phosphatase was added and mixed by inversion 4 times and then incubated for 5 minutes. Neutralization solution (350 μL) containing 4.09 M guanidine hydrochloride, 0.759 M potassium acetate and 2.12 M glacial acetic acid was added and mixed by inversion. Samples were centrifuged at 18,000 x *g* for 10 minutes at room temperature. The supernatant was transferred to a spin column and centrifuged at maximum speed for one minute. The column was transferred to a new tube and washed with

750 μL of 60 mM potassium acetate, 8.3 mM Tris-HCl (pH 7.5), 0.04 mM EDTA (pH 8.0) and 60% Ethanol. Following a second centrifugation, another 250 μL of column wash solution was added. Samples were centrifuged at 18,000 *g* for two minutes and the column was transferred to a new tube where 50 μL of Nuclease-Free Water was added and incubated for one minute and then centrifuged for one minute as above. The DNA in the bottom of the microcentrifuge tube was then ready to be run on an agarose gel for visualisation.

2.2.11 Agarose Gel Electrophoresis

Plasmids were analysed for the presence of an insert using 1% agarose gel electrophoresis and a DNA supercoiled ladder to identify the molecular weight of the plasmid DNA. Gels were run at 100 V for 30-45 minutes in 1x TAE buffer (40 mM Tris, 20 mM acetic acid, 1 mM EDTA).

2.3 Immunization

2.3.1 Mice

Balb/c and C57BL/6 mice were immunized subcutaneously with 10 μl of Lkt recombinant fusions prepared in 60 μl of PBS (0.188 M Na_2HPO_4, 0.012 M NaH_2PO_4, 0.137 M NaCl, pH 7.8) and 30 μl of Emulsigen-D (MVP Technologies) for a final injection volume of 100 μl/ vaccine dose. Emulsigen-D contains the immunostimulant dimethyl dioctadecyl ammonium bromide. Vaccines were administered at three-week intervals by the Animal Care staff at VIDO. Initial vaccination experiments, demonstrated that vaccination at three-week intervals was the minimum amount of time required between boost to stimulate maximal antibody responses.

2.3.2 Deer/Elk

Deer and elk were immunized subcutaneously with 50 µl of the Lkt recombinant fusions prepared in 650 µl of PBS (0.188M Na_2HPO_4, 0.012M NaH_2PO_4, 1.8% NaCl, pH 7.8) and 300 µL Emulsigen-D for a final injection volume of 1 mL/vaccine dose. Vaccines were administered at six-week intervals by Dr. Trent Bollinger and the Goodale farm staff.

2.3.3 Sheep

2.3.3.1 University of Saskatchewan

Sheep of mixed sex and breed (Suffolk and Arcott) were immunized subcutaneously with 50 µg of the Lkt recombinant fusions prepared in 650 µl of PBS (0.188M Na_2HPO_4, 0.012M NaH_2PO_4, 1.8% NaCl, pH 7.8) and 300 µL Emulsigen-D for a final injection volume of 1 mL/vaccine dose. Vaccines were administered at six-week intervals (with the exception of the dose titration study which used four week intervals) by the Animal Care staff at VIDO. Although the ideal vaccination interval was determined to be six weeks, it was felt that the four-week interval used in the dose titration study was sufficient to answer our specific objective for that experiment.

2.3.3.2 Norwegian School of Veterinary Science

Pregnant female ewes were used for the Scrapie challenge experiment. They were immunized SC at 6 weeks and 3 weeks prior to delivery of their lambs. Vaccinations, inoculations and sample collections were conducted by the Animal Care staff at the Sheep and Goat Research division of the Norwegian School of Veterinary Science in Sandnes, Norway.

2.4 Characterization of Antibody Immune Response

2.4.1 Sample Collection

2.4.1.1 Serum

Serum samples were collected from the jugular vein in 10 mL SST vacutainer tubes (BD) and centrifuged at 1,000 x *g* for 10 minutes. Serum was then archived at -80 ºC for ELISA testing.

2.4.1.2 Nasal Secretions

Nasal secretions were collected using cotton tampons as described by (Raggo *et al.*, 2000).

2.4.1.3 Cerebrospinal Fluid

The cerebrospinal fluids (CSF) were collected from the subarachnoid space (cisterna magna) between the arachnoid and pia mater layers of the meninges surrounding the brainstem at the level of the atlanto-occipital joint. For this study, the sheep were placed in sternal recumbency and the neck fully flexed immediately following euthanasia. At the centre of the triangle formed by the caudal aspect of the occipital protuberance and the wings of the atlas (C1), a 1 1/2 inch 19 gauge needle was slowly advanced along a plane parallel to the horizontal ramus of the mandible. The needle was passed through the skin, subcutis, nuchal ligament, dura mater and finally the arachnoid mater. It was possible to aspirate 2 to 10 mL/sheep. Samples were visually inspected for contamination by blood.

2.4.2 ELISAs

PrP epitope, Lkt and PrP^{C}-specific antibody responses were quantified by ELISA. The 96-well Immulon 2HB polystyrene microtiter plates (Thermo Fisher) were coated overnight with either 0.5 µg per well of synthetic peptide, 0.125 µg per well of PrP-Pure, a recombinant protein (Allprion) or 0.1 µg per well of purified 96 kDa Lkt protein diluted to the proper concentration in coating buffer (0.05 M carbonate-bicarbonate, pH 9.6). Plates were washed six times with distilled water (dH_20) then blocked with 200 µL per well of TBST (TBS: Tris-

buffered saline, 10 mmol/L Tris, 150 mmol/L NaCl, 0.05% Tween 20) and 1% skim milk. Plates were incubated for one hour at room temperature then washed 6 times with dH_20. Serum samples were diluted 1:10 in TBST with 1% skim milk and then serially diluted 1:4 in TBST plus 1% skim milk. Plates were incubated for 2 h then washed 6 times with dH_20. 100 µL of alkaline phosphatase (AP)-conjugated rabbit anti-sheep immunoglobulin gamma (IgG) or AP-conjugated goat anti-mouse IgG (Kirkgaard and Perry Laboratories; 1:2500) were added to each well to detect bound ovine and murine antibodies, respectively. [For the IgG subtype ELISAs AP-conjugated goat anti-mouse IgG1, IgG2a or IgG2b was used instead. (Kirkgaard and Perry Laboratories; 1:2000).] After a 1 h incubation, plates were washed 6 times with dH_20 then 100 µL *p*-nitrophenyl phosphate (PNNP) (Sigma) was added to each well for 2 h. ELISA titers were expressed as the reciprocal of the highest serum dilution resulting in a reading exceeding two standard deviations above the negative control.

2.4.3 Immunoglobulin Purification

IgG antibody was purified from sera on protein A-Sepharose columns which bind to the F_c portion of IgG molecules (Amersham Pharmacia).

2.4.4 Brain Homogenate Preparation

2.4.4.1 Immunoprecipitation Experiments at University of British Columbia

Brain homogenates containing either Scrapie-infected or uninfected hamster brains were produced as described by Paramithiotis *et al*. (2003).

2.4.4.2 Scrapie Challenge Trial at the Norwegian School of Veterinary Science

Brain homogenates containing Scrapie-infected sheep brains were produced by suspending 1 g of frozen sheep brain tissue (-20 C; transverse section of cerebrum anterior to hippocampus) in 4 mL of PBS solution (pH 7.4) and mixed in a stomacher (Heggebo *et al.*, 2000). The 4 mL preparations were administered to the newborn lambs via a stomach tube immediately after birth, prior to their first colostrum feed.

2.4.5 Coupling of YYR Antibody to Dynabeads for Immunoprecipitation

Tosylactivated Dynabeads (Invitrogen) beads (175 μL) were added to PBS (pH 7.4) to make a volume of 1 mL. The beads were washed with 1 mL 2x PBS and 50 μg of purified sheep YYR monoclonal antibody along with PBS up to 1 mL in a 2 mL cylindrical tube was added. Tubes were rotated for 20 h at 37°C and then washed with 1 mL 2x 0.1% BSA/PBS. 1 1 mL of blocking buffer: 0.2 M Tris-HCl, pH 8.5/0.1% BSA was added. Samples were rotated for 4 h at 37°C, washed with 1 mL 2x PBS/0.1% BSA and then store at 4°C in 1 mL PBS.

2.4.6 Immunoprecipitation

Sera from immunized sheep were evaluated for a specific interaction with PrP^{Sc} and PrP^{C}. Prior to running the immunoprecipitation experiment, immunoglobulin was separated from the serum using column-affinity purification to reduce background. To 10 μL of mAb-beads, 89 μL of binding buffer (3% Tween 20 and 3% NP40 in PBS) was added with 1 μL of 10% (w/v) brain homogenate (RML/WT CD1). Samples were rotated for 3 h at RT and washed with PBS (2% Tween20, 2% NP40) 3x. After the last wash, 80 μL was removed, vortexed, and spun for 30 sec. Tubes were placed in a magnet rack where all remaining liquid was removed and 20 μL of 2x loading buffer was added. Samples were vortexed before heating for 5 min at 95°C, spun down and placed in a magnet rack for the loading of the supernatants onto gels. (All experiments described in section 2.4.3 – 2.4.6 were performed by the laboratory staff of Dr. Neil Cashman, our collaborator, at the University of British Columbia)

2.5 Genotyping of the University of Saskatchewan Sheep Flock

Genotype analysis was conducted by the DNA Sequencing and Gene Synthesis department at the Plant Biotechnology Instutute.

2.6 Chemicals and Reagents

A list of the chemicals and enzymes used in this project are listed in **Table 2.3**.

2.7 Statistics

Data presented were non-parametric in their distribution. Comparisons between treatment groups were conducted using Mann-Whitney analysis (GraphPad Prism 5.0 software, CA, USA). *P* values less than 0.05 were considered significant.

Table 2.3: List of chemicals, enzymes and proteins used and the suppliers' addresses.

Chemical	Supplier
Acrylamide	Sigma-Aldrich
Ampicillin	Shelton Scientific
Agarose	EMD
BSA	New England Biolabs
Coomassie-Brilliant blue R250	Biorad
Diethanolamine	Sigma
Emulsigen-D	MVP Laboratories
Ethidium bromide	Pharmacia Biotech
Glycerol	EMD
LB broth	Difco
LB agar	Difco
Magnesium chloride	Sigma-Aldrich
Methanol	EMD
PNPP (4-Nitrophenyl phosphate di(tris) salt	Sigma-Aldrich
Skim milk powder	Difco
Sodium acetate	Sigma-Aldrich
Sodium dodecyl sulfate	EMD
Tween 20	Biorad

Enzymes	Suppliers
BamHI	New England Biolabs
NcoI	New England Biolabs
T4 DNA Ligase	USB

Antibodies	Supplier
Goat anti-mouse IgG (H+L) Alkaline Phosphatase (AP) conjugated	Kirkgaard & Perry Laboratories
Rabbit anti-sheep IgG (H+L) AP conjugated	Kirkgaard & Perry Laboratories
Rabbit anti-deer IgG (H+L) AP conjugated	Kirkgaard & Perry Laboratories
6H4 mAb	Prionics
Tosylactivated Dynabeads M-280	Invitrogen

Supplier	Address
Allprion	Allprion AG Schlieren, Switzerland.
Amersham Pharmacia	Amersham Biosciences, Pittsburgh, PA, USA.
BD Biosciences	BD Bioscience, Mississauga, ON, Canada.
Beckman Coulter	Beckman Coulter Canada Inc., Mississauga, ON, Canada

Biorad	Bio-Rad Laboratories Ltd., Mississauga, ON, Canada
EMD Bioscience	VWR Canlab, Mississauga, ON, Canada.
Eppendorf	Eppendorf Canada, Mississauga, ON, Canada.
Invitrogen	Invitrogen Canada, Inc., Burlington, ON, Canada.
Kirkgaard & Perry Laboratories	KPL, Inc., Gaithersburg, MD, USA.
MVP Laboratories	MVP Laboratories, Omaha, NE, USA.
New England Laboratories	NEB Ltd., Pickering, ON, Canada.
PerkinElmer Life Sciences	PerkinElmer, Waltham, MA, USA.
PerSeptive Biosystems	Global Medical Instruments Inc., Ramsay, MN, USA.
Prionics	Prionics AG, Schlieren-Zurich, Switzerland.
Promega	Fisher Scientific, Ltd., Nepean, ON, Canada.
Sigma-Aldrich	Sigma-Aldrich Canada Ltd., Oakville, ON, Canada.
Shelton Scientific	VWR Canlab, Mississauga, ON, Canada.
Thermo Scientific	Thermo Fisher Scientific, Waltham, MA, USA.
usb	GE Healthcare Bio-Sciences, Baie d'Urfe, Quebec, Canada.

3.0 RESULTS

3.1 Sheep Genotyping

One of the risks during vaccine development is that the test vaccine, if not properly designed, may induce immunopathology. This has been observed previously with traditional vaccines such as the live-attenuated viruses or inactivated bacteria, rather than for peptide vaccines. From a safety perspective, it was essential that we investigated the possibility that the PrP constructs might induce prion disease or immunopathology. Due to the existence of several prion genoptypes (VRQ, ARQ and ARR) within sheep, each with a distinct Scrapie phenotype, it was important to know the genotype of sheep used in our studies. Clinical manifestation of prion disease can either be observable as in the VRQ and ARQ genotypes or be asymptomatic as in the ARR genotype. Consequently, sheep in the University of Saskatchewan flock were genotyped and only animals of the ARQ genotype were used for vaccine trials. Although VRQ would have been the ideal genotype, it is very rare and none of the local sheep contained those particular residues within *Prnp* **[Table 3.1]**. Of the 55 sheep genotyped, two of the four rams were homozygous for the ARQ genotype with the other two being heterozygous ARQ/ARR. Of the ewes, 28 were homozygous for ARQ, 4 were homozygous for ARR and the remaining 19 were heterozygous ARQ/ARR. Only animals of the ARQ/ARQ genotype were bred to produce the sheep used in the vaccine trials for this project.

3.2 Analysis of Carrier Molecules KLH and Lkt

Previous studies in mice demonstrated the limited immunogenicity of the YYR epitope when chemically coupled to the KLH carrier molecule (Paramithiotis *et al.*, 2003). Due to the published success using the Lkt carrier protein with the GnRH peptide, it was hypothesized that Lkt may be an effective carrier for the YYR peptide. To address this, four experimental groups of mice (n=10) were vaccinated SC at week 0. 3 and 6. One group was vaccinated with 100 μg of KLH chemically coupled to the β2(YYR)L peptide. The other three groups received either 1, 10, or 100 μg of the Lkt-β2(YYR)L chimera because immunogenicity of Lkt has been shown

Table 3.1: Genotyping of the Prnp gene for the University of Saskatchewan sheep flock.

# of Animals	Sex	Codon 136	Codon 154	Codon 171	Phenotype
2	M	AA	RR	QQ	ARQ
2	M	AA	RR	RQ	ARR/ARQ
25	F	AA	RR	QQ	ARQ
20	F	AA	RR	RQ	ARR/ARQ
5	F	AA	RR	RR	ARR

to be dose-dependent (Potter and Manns, 2000). The vaccine formulation contained 10 μL of the adjuvant Emulsigen-D in each dose to enhance immunogenicity of the constructs.

Within 24 hours of the primary vaccination, all of the mice in the group receiving 100 μg Lkt-β2(YYR)L chimera had died. Possible explanations for this acute death may be the amount of guanidine toxicity, or Lkt over-stimulation of the murine immune system causing systemic shock and consequently death. Over the course of the experiment, 2 animals in the KLH group and 1 animal in the Lkt 1 μg group also died. Results for the KLH group showed a maximum β2(YYR)L-specific titer of 1,000 reached at week eight with the exception of two animals which achieved titers of 3,000 and 3,500 [**Figure 3.1a**]. The β2(YYR)L-specific titers for the Lkt 10 μg group reached peak titers between 3,000-4,200 at week eight [**Figure 3.1b**]. The lowest concentration of Lkt-β2(YYR)L chimera created a broader range of titers following each vaccination at week 0, 3 and 6 [**Figure 3.1c**]. As observed in the previous two groups, peak titers were achieved at week eight and ranged between 1,000 to 3,300 following the third vaccination. Both the KLH 100 μg and Lkt 10 μg groups displayed a drop in titers by week 10 following the peak titers at week eight. The similar reduction in titers was not observed in the Lkt 1 μg group where titers remained relatively constant between week eight to ten. A comparison of median titers for each group at week eight revealed that the β2(YYR)L-specific antibody response for the Lkt 10 μg group was significantly higher than both the KLH ($p < 0.0018$) and Lkt 1 μg groups ($p < 0.0006$) [**Figure 3.2**].

3.3 Antibody Response to the Lkt-β2(YYR)L Chimeric protein in Sheep

After determining that the Lkt carrier protein significantly improved β2(YYR)L-specific antibody responses relative to the KLH carrier in mice, we then tested the Lkt carrier system in sheep, a relevant species for TSE. Seven sheep were immunized with 50 μg of Lkt-β2(YYR)L formulated in 30% Emulsigen-D and 0.1 M PBS solution. The sheep were immunized three times at 6 week intervals.

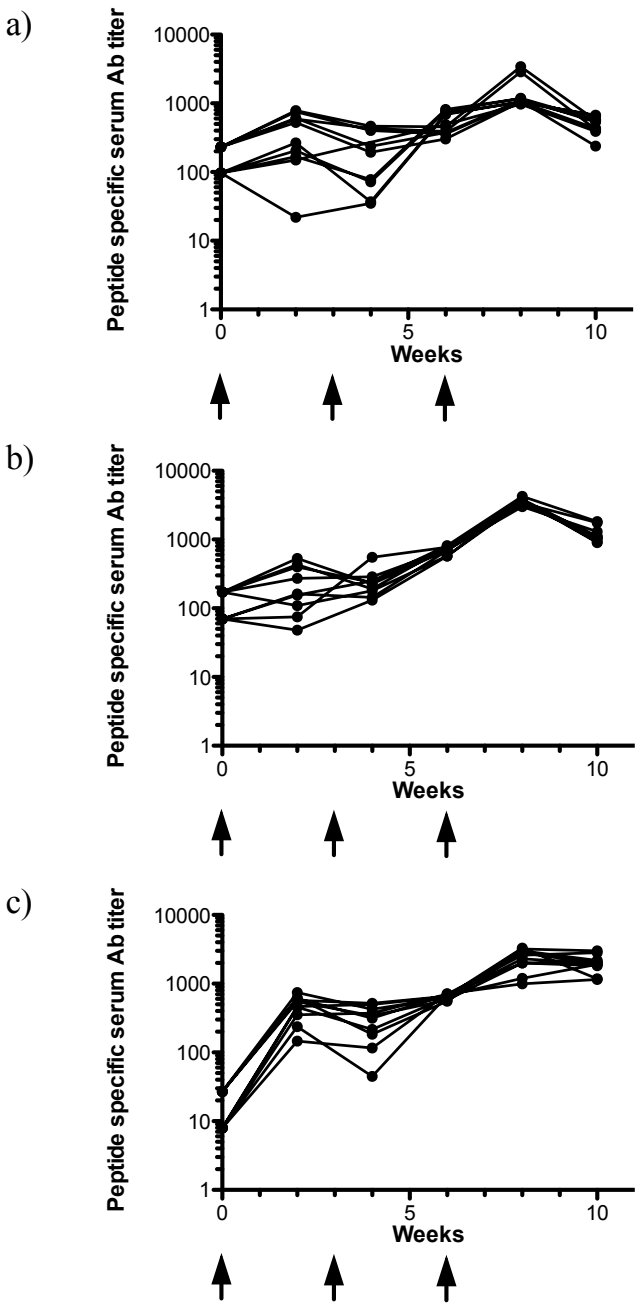

Figure 3.1: Peptide-specific murine serum Ab titers for KLH-β2(YYR)L and three different doses of Lkt--β2(YYR)L. a) Mice (n=8) were vaccinated with 100 μg of KLH chemically coupled to the β2(YYR)L epitope. **b)** Mice (n=9) were vaccinated with 10 μg Lkt-β2(YYR)L produced as a genetic fusion to the β2(YYR)L epitope. **c)** Mice (n=10) were vaccinated with 1 μg Lkt-β2(YYR)L produced as a genetic fusion to the β2(YYR)L epitope Vaccines were formulated with 10% Emulsigen-D and administered SC at weeks 0, 3 and 6. Antibodies were detected using peptide-specific ELISAs and data presented represents individual animals. Arrows indicate immunization intervals.

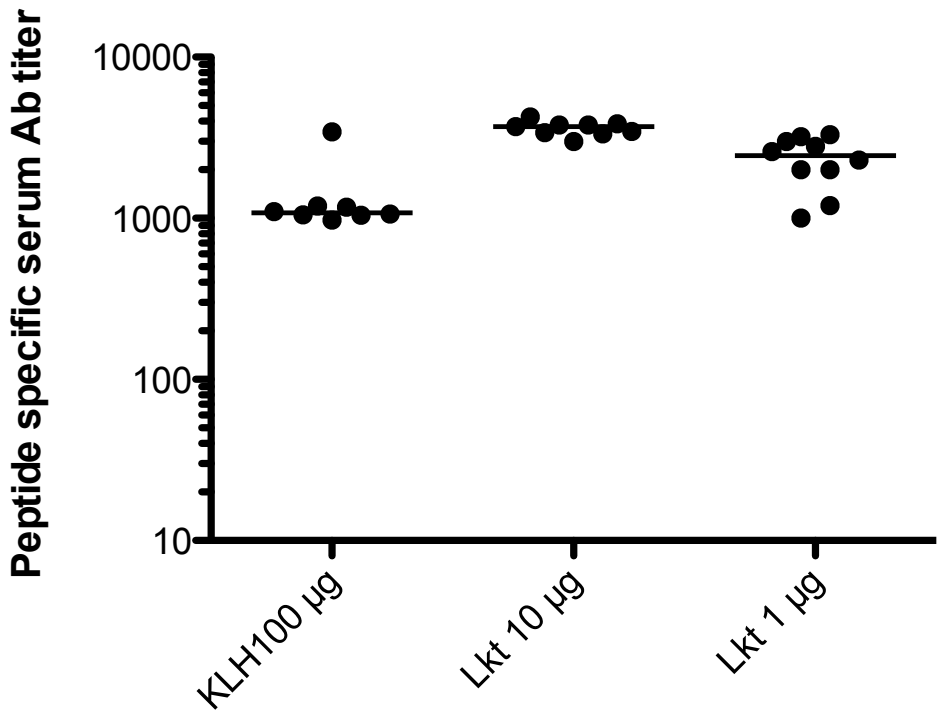

Figure 3.2: Comparison of week 8 β2(YYR)L peptide-specific serum Ab titers among all three groups of mice. Mice were vaccinated SC at 0, 3, and 6 with the indicated carrier protein conjugated with β2(YYR)L peptide and formulated in 10% Emulsigen-D. Each dot represents the titer of individual mice within each group and the horizontal bars indicate group median values. The Lkt 10 µg group was significantly higher than both the KLH ($p < 0.0018$) and Lkt 1 µg groups ($p < 0.0006$).

ELISA analysis of peptide-specific titers revealed no detectable antibody response following all three vaccinations in all animals [**Figure 3.3**]. To determine if the absence of an antibody response was the result of ineffective vaccine delivery, an ELISA was performed to analyze antibody responses to the LKT carrier. Lkt-specific antibody titers increased following each vaccination which confirmed effective delivery of the carrier protein [**Figure 3.3**]. Therefore, we concluded there may be species variability in recognition of the β2(YYR)L epitope and that epitope modifications may be required to improve antibody responses.

3.4 Symmetrical Expansion of the β2(YYR) Epitope to β2(1+YYR+1) in Linear and Inverted Presentations

We postulated that increasing the length of the YYR epitope to include more of the naturally surrounding residues from the PrP protein might enhance B-cell recognition of the peptide. It has also been reported that epitope orientation and the number of epitope tandem repeats can influence antibody production (Jinshu *et al.*, 2004). Consequently the original YYR was expanded to VYYRP (β2(1+YYR+1)) and synthesized as both linear and inverted repeats and presented as C-terminal fusions on Lkt. Each construct was expressed in *E. coli*, purified, and formulated with 30% Emulsigen-D in a 0.1 M PBS solution. Four groups of sheep were injected SC with each vaccine formulation [β2(YYR)L, n=5; β2(YYR)I, n=7; β2(1+YYR+1)L, n=5; β2(1+YYR+1)I, n=7] and the vaccine was injected three times at six week intervals. Due to constraints of animal availability, the linear and inverted YYR constructs were tested in separate trials.

Results for both presentations of the YYR epitope reflected the previous YYR study with no detectable increase in antibody following any of the three vaccinations [**Figure 3.4 and 3.5**]. Furthermore, the inverted peptide orientation provided no increase in immunogenicity when compared to the linear form. This suggested that the limited immunogenicity of the three amino acid motif was not altered by orientation within the recombinant protein.

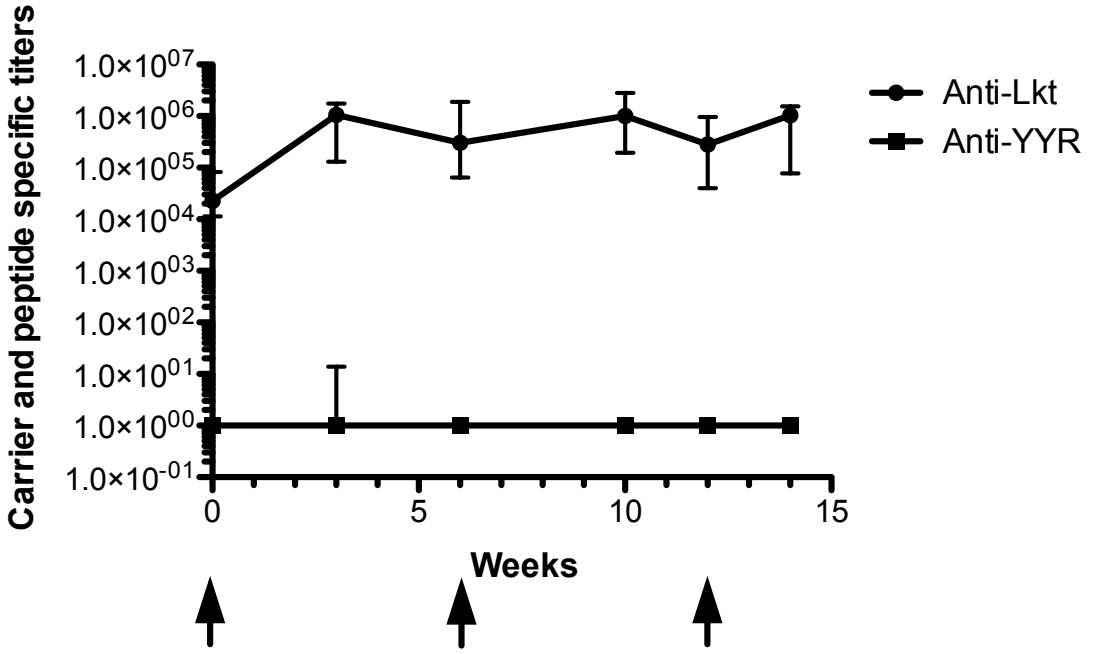

Figure 3.3: Immunogenicity of Lkt-β2(YYR)L in sheep. Sheep (n=7) were vaccinated with 50 μg of Lkt produced as a genetic fusion to the β2(YYR)L epitope. Vaccines were formulated with 30% Emulsigen-D and administered SC at week 0, 6 and 12. Antibodies to Lkt and YYR were detected using peptide-specific ELISAs and data are presented as median values. Arrows indicate immunization intervals.

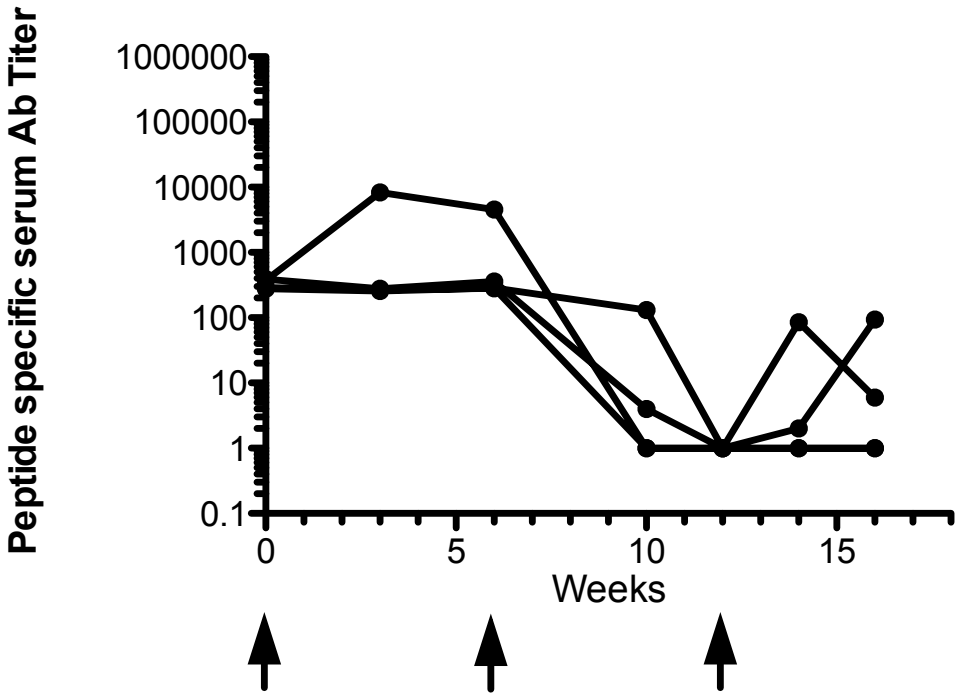

Figure 3.4: β2(YYR)L-specific Ab titers in sheep serum following immunization with recombinant Lkt-β2(YYR)L. Sheep (n=4) were vaccinated with 50 μg Lkt produced as a genetic fusion to the β2(YYR)L epitope. Vaccines were formulated with 30% Emulsigen-D and administered SC at weeks 0, 6 and 12. Antibodies were detected using peptide-specific ELISAs and data presented represents individual animals. Arrows indicate immunization intervals.

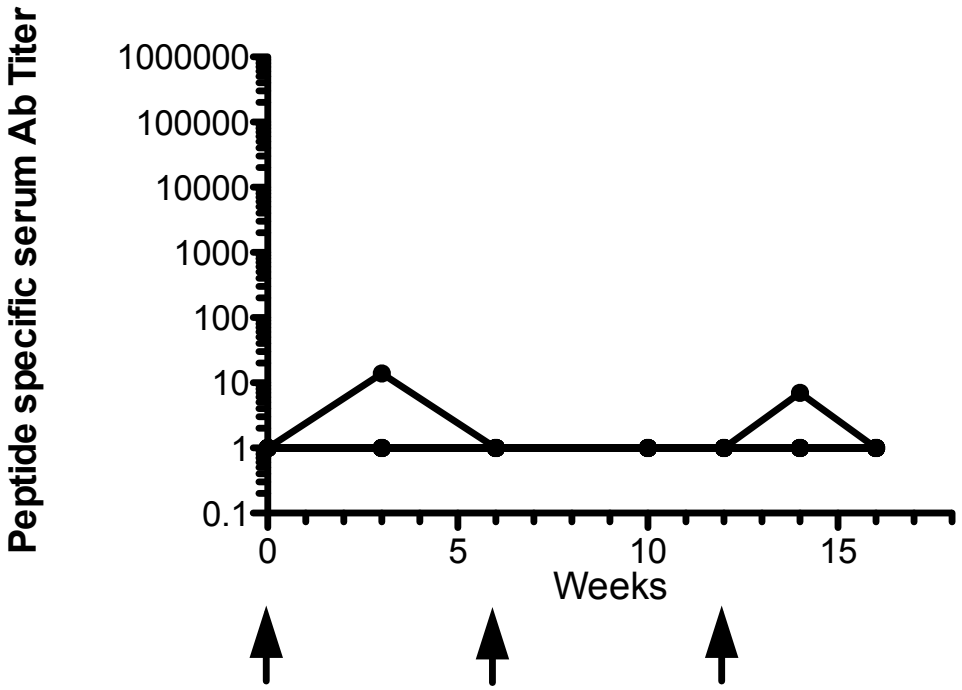

Figure 3.5: β2(YYR)I-specific Ab titers in sheep serum following immunization with recombinant Lkt-β2(YYR)I. Sheep (n=7) were vaccinated with 50 μg Lkt produced as a genetic fusion to the β2(YYR)I epitope. Vaccines were formulated with 30% Emulsigen-D and administered SC at weeks 0, 6 and 12. Antibodies were detected using peptide-specific ELISAs and data presented represents individual animals. Arrows indicate immunization intervals.

The addition of a single amino acid to the C- and N-terminal portions of the tandemly repeated YYR epitope in its linear orientation had no significant effect on immunogenicity. Two sheep showed a response with titers of 6,000 at week 6, with an additional two animals responding by week 12 with titers of 5,300 [**Figure 3.6**]. The two animals which responded significantly after the initial vaccination at week 0 displayed a drop in titer following the vaccination at week 6. One animal had peptide-specific antibody titers which were detectable prior to vaccination. That same animal failed to respond to any of the subsequent vaccinations.

The inverted presentation of the expanded epitope produced consistent and sustained antibody responses in 6 of 7 animals throughout the experiment, with peak titers ranging between 1,000 to 18,000 by week 16 [**Figure 3.7**]. Unlike the linear version of this construct, titer increases followed booster vaccinations time points and no decrease in titers was observed until week 15 following the third vaccination. Analysis of median titers at week 16 showed β2(1+YYR+1)I to be significantly more immunogenic than the inverted form of the basic YYR construct ($p < 0.0106$) [**Figure 3.8**].

3.5 Vaccine Dose Titration with Lkt-β2(1+YYR+1)I

The effectiveness of the Lkt carrier is dose-dependent in a species-specific manner (Potter AA and Manns JG, 2000). Having designed a chimeric Lkt construct which stimulates detectable PrP peptide-specific antibody responses in sheep, the next step in the project was to identify a carrier protein dose which optimized β2(1+YYR+1)I-specific antibody responses in sheep. Five doses (12.5, 25, 50, 100 and 200 μg) of the Lkt-β2(1+YYR+1)I construct were formulated with 30% Emulsigen-D and administered SC to 5 groups of sheep (n=5) at four week intervals.

Using a β2(1+YYR+1)I-specific titer of 1,000 as a cut-off to define a positive Ab response, the lowest dose of Lkt-peptide induced a positive antibody response in only two animals by week twelve [**Figure 3.9a**]. Doubling the Lkt-peptide dose to 25 μg induced a minimum positive antibody response in 4/5 animals with one animal achieving an antibody titer of 5,300 at week 6 and another animal achieving a titer of 19,000 by week 10 [**Figure 3.9b**]. At 50 μg, all five animals exceeded Ab titers of 1,000 with one animal achieving a peak titer of

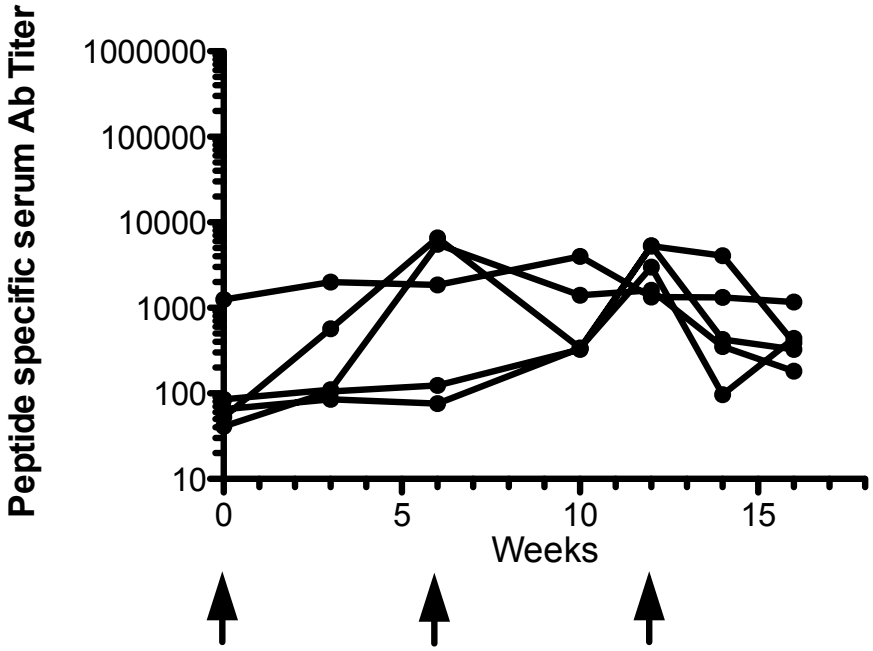

Figure 3.6: β2(1+YYR+1)L-specific Ab titers in sheep serum following immunization with recombinant β2(1+YYR+1)L. Sheep (n=5) were vaccinated with 50 μg Lkt produced as a genetic fusion to the β2(1+YYR+)L epitope. Vaccines were formulated with 30% Emulsigen-D and administered SC at weeks 0, 6 and 12. Antibodies were detected using peptide-specific ELISAs and data presented represents individual animals. Arrows indicate immunization intervals.

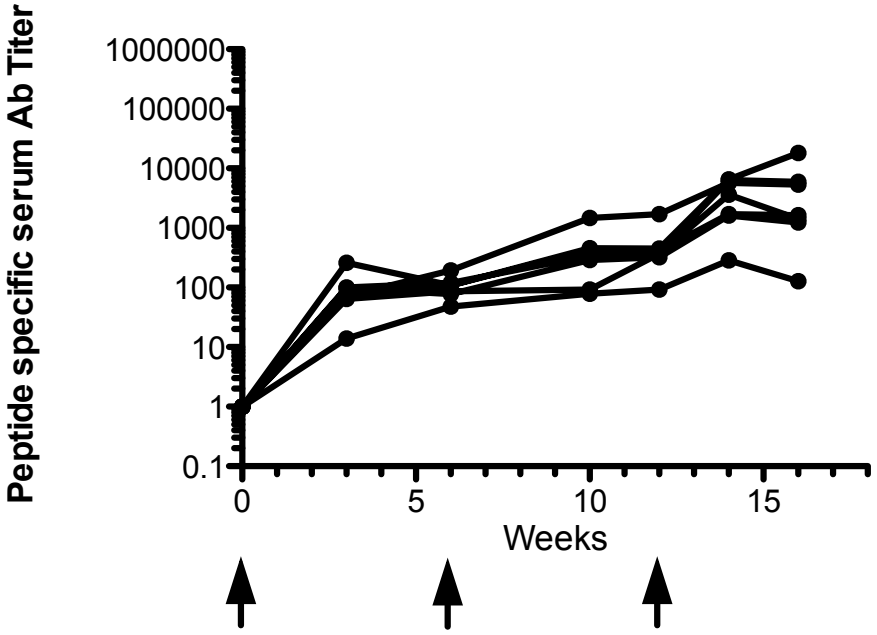

Figure 3.7: β2(1+YYR+1)I-specific Ab titers in sheep serum following immunization with recombinant Lkt-β2(1+YYR+1)I. Sheep (n=5) were vaccinated with 50 μg Lkt produced as a genetic fusion to the β2(1+YYR+)I epitope. Vaccines were formulated with 30% Emulsigen-D and administered SC at weeks 0, 6 and 12. Antibodies were detected using peptide-specific ELISAs and data presented represents individual animals. Arrows indicate immunization intervals.

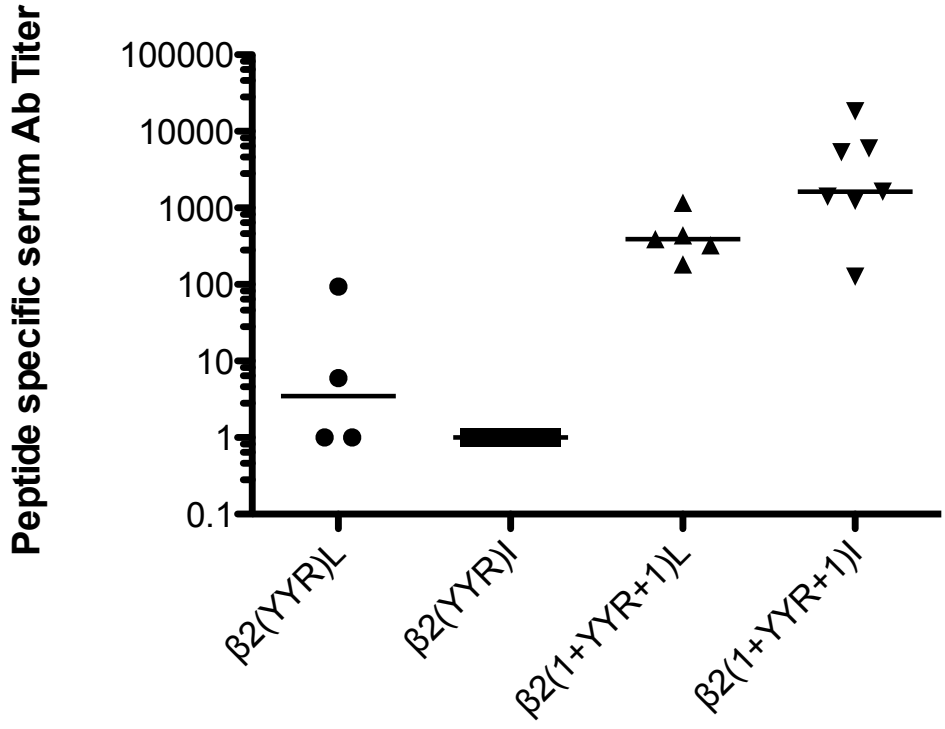

Figure 3.8: Comparison of week 16 β2(YYR) and β2(1+YYR+1) peptide-specific serum Ab titers in their linear and inverted orientations. Sheep were vaccinated SC at 0, 6, and 12 weeks with 50 μg of the indicated Lkt chimeric protein and formulated in 30% Emulsigen-D. Each dot represents the titer of individual sheep within each group and the horizontal bars indicate group median values. The median β2(1+YYR+1)I titers were significantly greater than that of β2(YYR)I and β2(YYR)L ($p < 0.011$). Arrows indicate immunization intervals.

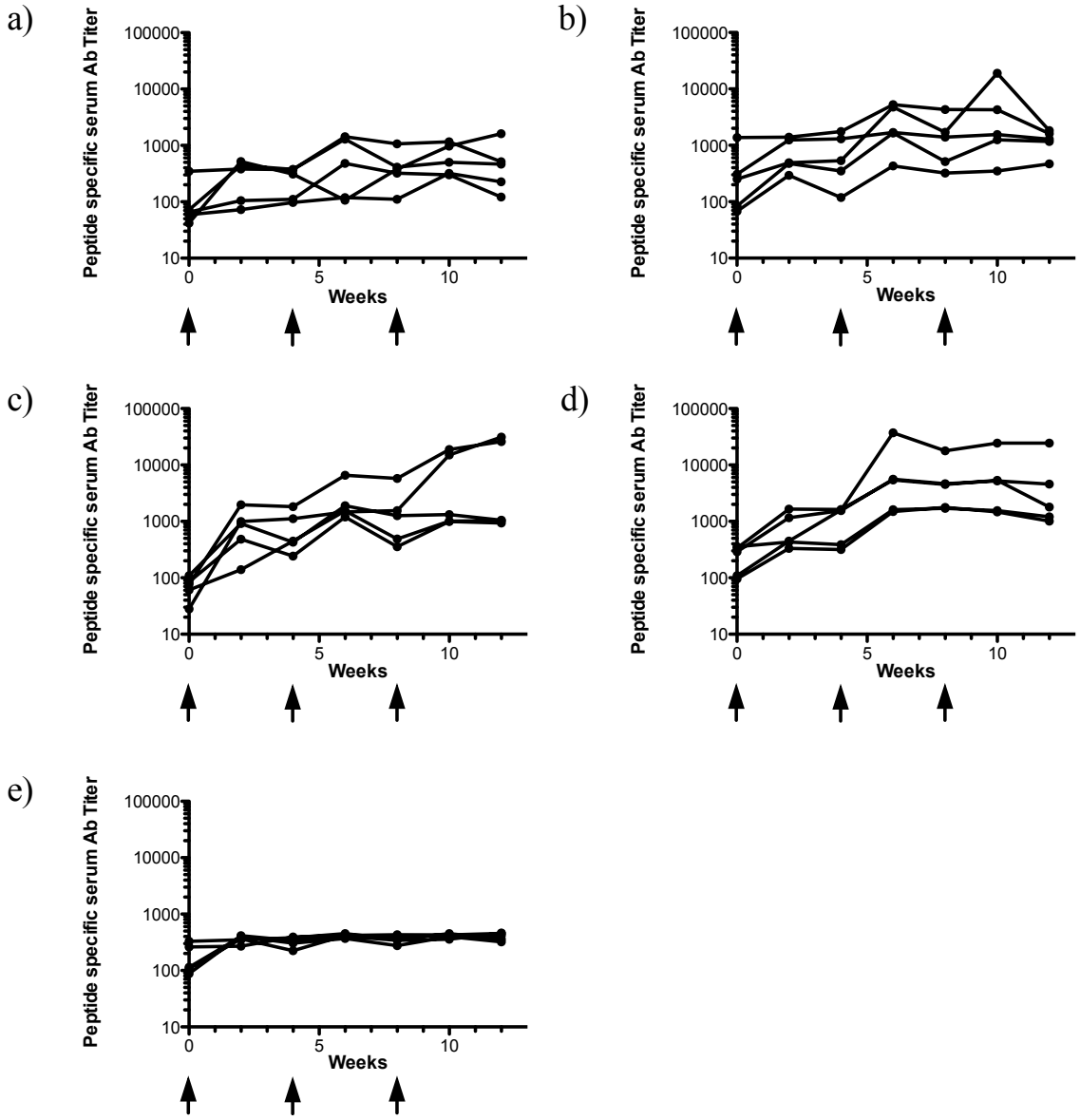

Figure 3.9: Peptide-specific sheep serum Ab titers for five different Lkt-β2(1+YYR+1)I doses. a) Sheep (n=5) were vaccinated with 12.5 µg Lkt-β2(1+YYR+)I. **b)** Sheep (n=5) were vaccinated with 25 µg Lkt-β2(1+YYR+)I. **c)** Sheep (n=5) were vaccinated with 50 µg Lkt-β2(1+YYR+)I. **d)** Sheep (n=5) were vaccinated with 100 µg Lkt-β2(1+YYR+)I. **e)** Sheep (n=5) were vaccinated with 200 µg Lkt-β2(1+YYR+)I. Vaccines were formulated with 30% Emulsigen-D and administered SC at weeks 0, 4 and 8. Antibodies were detected using peptide-specific ELISAs and data presented represents individual animals. Arrows indicate immunization intervals.

26,000 and another had a peak titer of 31,000 [**Figure 3.9c**]. All animals in the 100 μg group surpassed a titer of 1,000, with two animals developing titers of 5,000 and one animal had an antibody titer of another 37,000 [**Figure 3.9d**]. Further increasing the Lkt-peptide dose to 200 μg resulted in decreased peptide-specific antibody responses, with all five animals attaining titers less than 500 [**Figure 3.9e**].

Therefore, the magnitude of the peptide-specific antibody response was dependent on the dose of the carrier protein, with the highest and lowest doses of the carrier protein inducing the weakest peptide-specific antibody titers. A comparison of median peptide-specific titers at week 10 revealed no statistically significant difference among the three intermediate Lkt doses of 25, 50 and 100 μg [**Figure 3.10**]. There was, however, a significant difference when comparing the 100 μg and 200 μg Lkt groups (p <0.0079) but no significant difference when comparing the 12.5 μg and 25 μg Lkt groups (p < 0.095). At weeks 6 and 10, there was a significant difference between 50 μg and 12.5 μg Lkt groups (p < 0.032), and at 6 and 8 weeks there was a significant difference between 50 μg and 200 μg Lkt groups (p < 0.032 and p < 0.0079, respectively). While the 100 μg Lkt dose stimulated a marginally higher median antibody titer than the 50 μg dose, the difference was outweighed by the economical advantages of the lower dose.

3.6 The Effect of Epitope Tandem Repeat Number [β2(1+YYR+1)I x 4]

In an effort to further enhance the immunogenicity of the β2(1+YYR+1)I, we hypothesized that increasing the physical size of the construct through the addition of more tandem repeats may improve immunogenicity based on the concept of T-cell independent (TI) activation. Typically, antibody responses require T_h-cells for the activation of an Ag-specific B-cell, however, there is an alternative method of B-cell activation which is much quicker and can occur in the absence of T_h-cells (Mond *et al.*, 1995). TI inducing Ags are usually large, multivalent molecules present on bacteria, viruses and fungal pathogens. It is the multivalency of these proteins which enable them to induce multiple domains of highly cross-linked membrane Ig and consequently produce high levels of B-cell activation (Humphrey, 1981). Due to the enhanced membrane Ig cross-linking, low TI Ag concentrations are sufficient to achieve the threshold level of activation required for B-cell induction. These low TI Ag

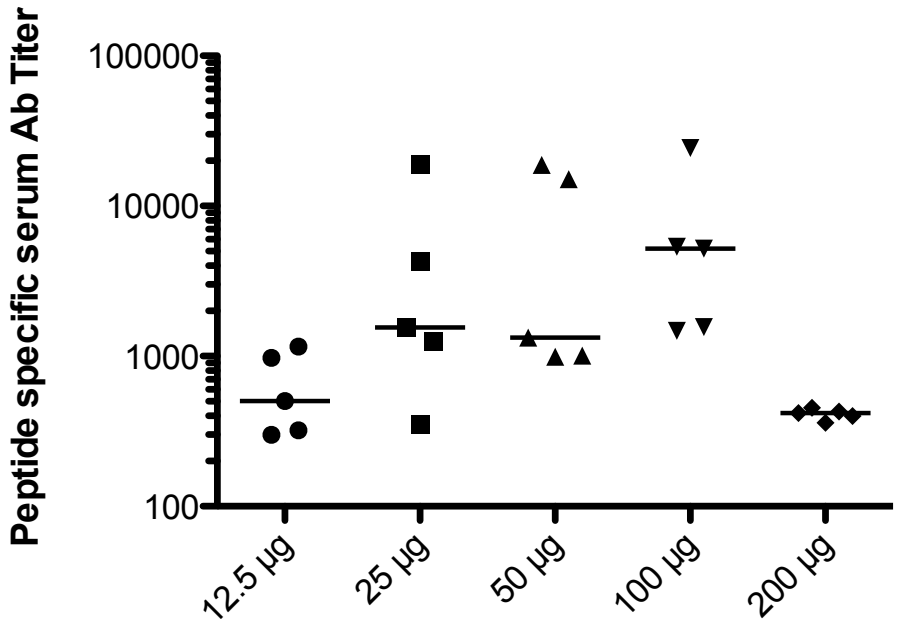

Figure 3.10: Comparison of week 10 β2(1+YYR+1)I peptide-specific sheep serum Ab titers among the 12.5, 25, 50, 100 and 200 µg Lkt groups. Sheep were vaccinated SC at 0, 4, and 8 weeks with the different indicated doses of Lkt-β2(1+YYR+1)I protein formulated in 30% Emulsigen-D. Each dot represents the titer of individual sheep within each group and the horizontal bars indicate group median values. There was a significant difference in the median titers between the 100 µg and 200 µg groups ($p < 0.0079$).

concentrations minimize the degree of modulation and disappearance of Ig from the surface of Ag-specific B-cells, allowing for prolonged contact between the Ag and membrane Ig resulting in persistent B-cell signalling (Brunswick *et al.*, 1988). With the concept of TI activation in mind, a β2(1+YYR+1)I gene was created with a combination of restriction sites that facilitated the insertion of multiple repeats into the pAA352 vector. Fusing four copies of the gene produced a total of 48 β2(1+YYR+1)I epitopes and sequence analysis confirmed all the inserts were in-frame.

Two groups of sheep (n=7) were injected SC with 50 μg of either the Lkt-[β2(1+YYR+1)I x 4] or the regular β2(1+YYR+1)I construct formulated in 30% Emulsigen-D. The sheep were immunized at 6 week intervals. The antibody response to the β2(1+YYR+1)I construct were similar to the previous experiments [**Figure 3.3 and 3.11**] with the antibody response at week 14 ranging between a titer of 300 to 6,500. Six of 7 animals had peptide-specific titers exceeding 1,000. At week 14, in the [β2(1+YYR+1)I x 4] group, titers ranged from 0 to 5,000 with 5/7 animals exceeding 1,000 [**Figure 3.12]**. A comparison of median titers at week 14 indicated, however, that doubling the number of peptide epitopes in the Lkt chimeric protein did not significantly enhance peptide-specific antibody responses ($p < 0.073$) [**Figure 3.13**]. There was actually a decrease in the median titers of the [β2(1+YYR+1)I x 4] group compared to the β2(1+YYR+1)I group.

3.7 Further expanding the PrP epitope from β2(1+YYR+1) to β2(2+YYR+2) and β2(3+YYR+1)

Having observed an increase in immunogenicity following the symmetrical addition of a single amino acid to the YYR epitope, four more constructs were designed to further expand the YYR epitope. Building on results from the previous symmetrical expansion, where increased immunogenicity was observed, an additional symmetrical construct β2(2+YYR+2) in both linear and inverted presentation was synthesized. Another construct consisted of a non-symmetrical expansion towards the N-terminus [β2(3+YYR+1)] in both linear and inverted forms. Based on PrP^{C} structural data (Riek *et al.*, 1996), expansion of the YYR epitope in the N-terminal direction incorporates residues postulated to be contained within the PrP^{Sc} cryptic

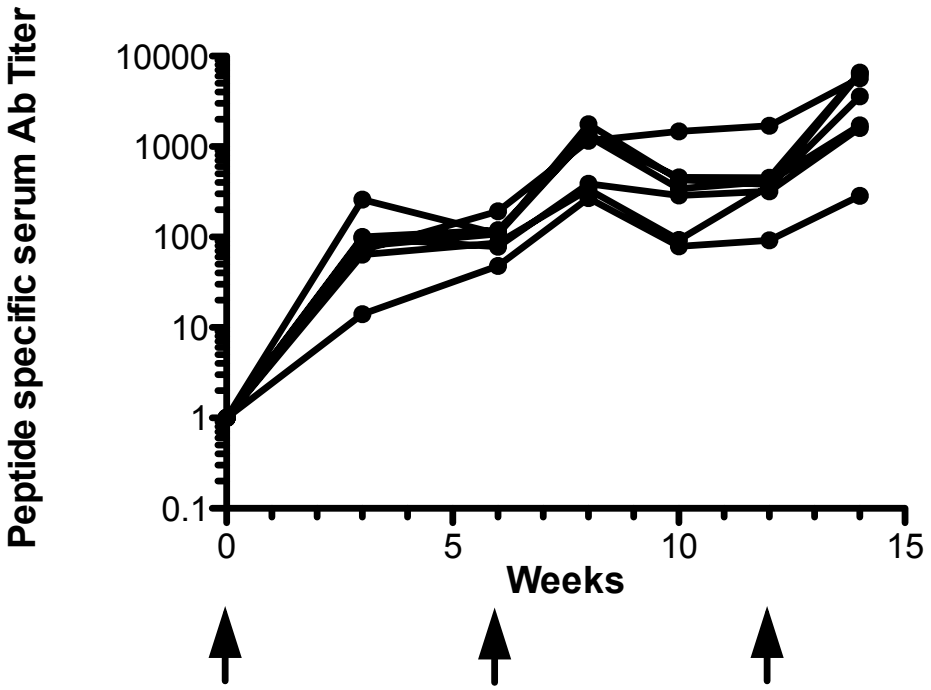

Figure 3.11: β2(1+YYR+1)I peptide-specific sheep serum Ab titers for the 50 μg Lkt-β2(1+YYR+1)I group. Sheep (n=7) were vaccinated with 50 μg Lkt produced as a genetic fusion to the β2(1+YYR+)I epitope. Vaccines were formulated with 30% Emulsigen-D and administered SC at weeks 0, 6 and 12. Antibodies were detected using peptide-specific ELISAs and data presented represents individual animals. Arrows indicate immunization intervals.

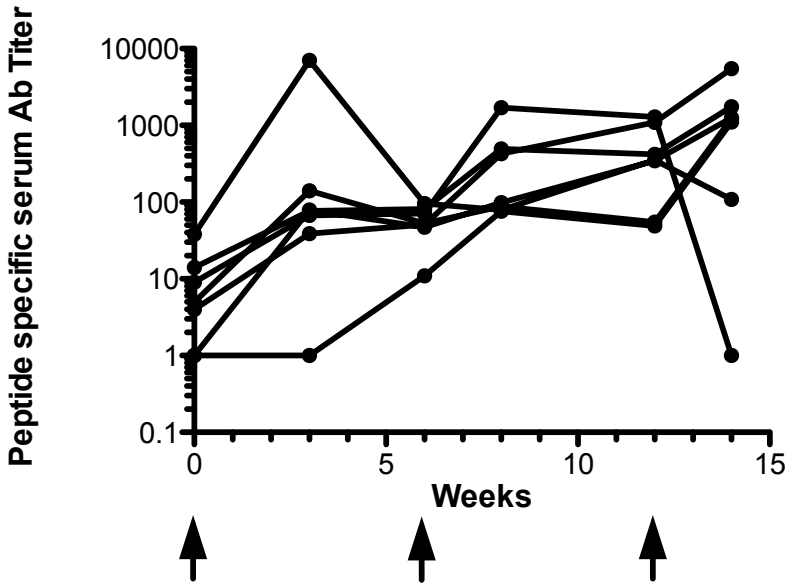

Figure 3.12: [β2(1+YYR+1)I x 4] peptide-specific sheep serum Ab titers for the 50 μg Lkt-[β2(1+YYR+1)I x 4] group. Sheep (n=7) were vaccinated with 50 μg Lkt produced as a genetic fusion to the [β2(1+YYR+1)I x 4] epitope. Vaccines were formulated with 30% Emulsigen-D and administered SC at weeks 0, 6 and 12. Antibodies were detected using peptide-specific ELISAs and data presented represents individual animals. Arrows indicate immunization intervals.

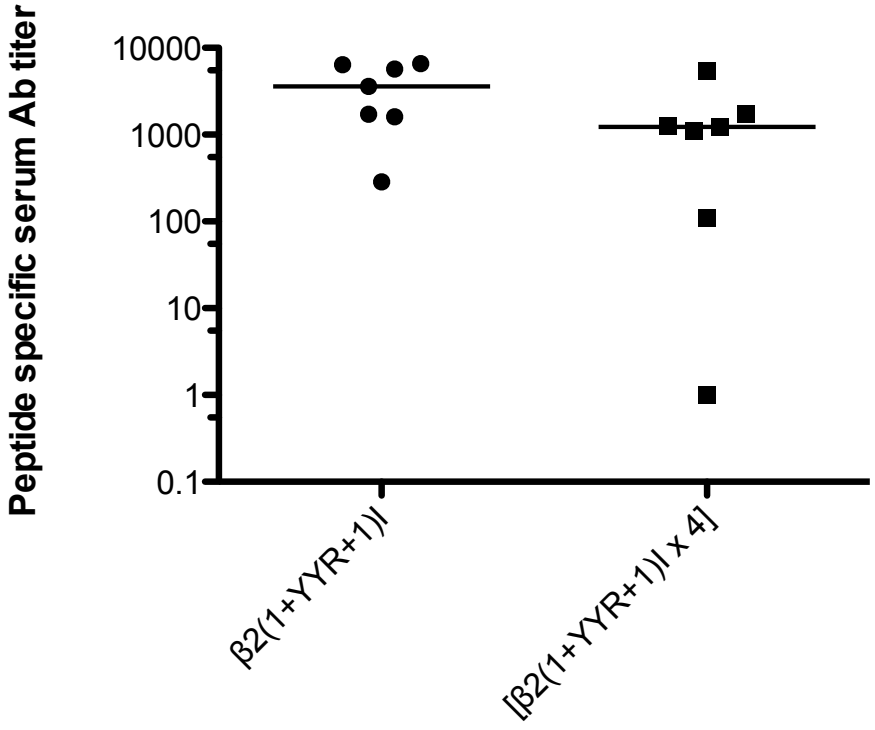

Figure 3.13: Comparison of week 14 β2(1+YYR+1)I and [β2(1+YYR+1)I x4] peptide-specific serum Ab titers for the two groups of sheep. Sheep were vaccinated SC at 0, 6, and 12 weeks with 50 μg of the indicated Lkt chimeric protein formulated in 30% Emulsigen-D. Each dot represents the titer of individual sheep within each group and the horizontal bars indicate group median values.

epitope. Expansions in the C-terminal direction would contain residues that may be surface-exposed and risk induction of antibodies that could cross-react with PrP^C. Four groups of sheep (n=7) were injected SC three times at 6 week intervals with the four constructs formulated in 30% Emulsigen-D. All groups had 7 animals with the exception of the β2(3+YYR+1)L group which had 5. Six of the 7 animals in the β2(2+YYR+2)L group developed peptide-specific titers exceeding 1,000; 5 animals had titers exceeding 5,000 and two animals had titers greater than 100,000 [**Figure 3.14**].

This was the first trial in which peptide-specific antibody responses exceeded 100,000. The inverted orientation of β2(2+YYR+2) induced antibody responses which peaked at 15,000 by week 16. As with the linear construct, 5 animals had titers exceeding 5,000 [**Figure 3.15**]. Three of 5 animals in the linear version of the non-symmetrical expansion β2(3+YYR+1)L also achieved titers of 5,000, with responses at week 16 ranging between 800 to 6,800 [**Figure 3.16**]. Despite a smaller range in antibody responses, when compared to the other peptide expansions, β2(3+YYR+1)L induced antibody titers exceeding 1,000 in 6/7 immunized animals. Similarly, the inverted asymmetrical construct stimulated an immune response in all animals. Seven animals had antibody titers of 1,000 with 6 animals developing titers of 5,000 and 3 animals exceeding 20,000 [**Figure 3.17**]. A comparison of median antibody titers at week 16 indicated that only the β2(3+YYR+1)L and β2(3+YYR+1)I ($p < 0.0049$) groups were significantly different [**Figure 3.18**].

3.8 Immunization of Deer and Elk with β2(1+YYR+1)I and β2(3+YYR+1)I

Following the identification of immunogenic PrP peptide constructs, the opportunity arose to test cross-species reactivity in white-tail deer and elk, two very important target species for CWD. Due to the limited number of available animals, a decision was made to test only the 50 μg vaccine dose. The chimeric Lkt-peptide vaccines were formulated with 30% Emulsigen-D and injected SC at 6 week intervals. Sample collection was complicated due to the use of semi-domesticated animals which required careful restraint during blood collection. Consequently, some samples are missing at time points when not all the deer or elk were captured.

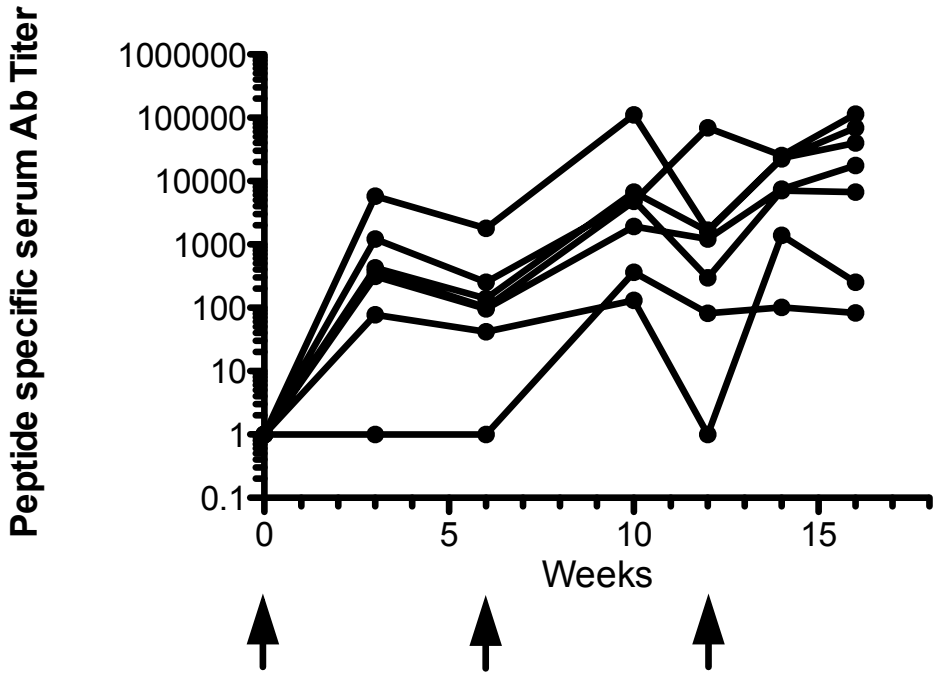

Figure 3.14: β2(2+YYR+2)L peptide-specific sheep serum Ab titers for the 50 μg Lkt-β2(2+YYR+2)L group. Sheep (n=7) were vaccinated with 50 μg Lkt produced as a genetic fusion to the β2(2+YYR+2)L epitope. Vaccines were formulated with 30% Emulsigen-D and administered SC at weeks 0, 6 and 12. Antibodies were detected using peptide-specific ELISAs and data presented represents individual animals. Arrows indicate immunization intervals.

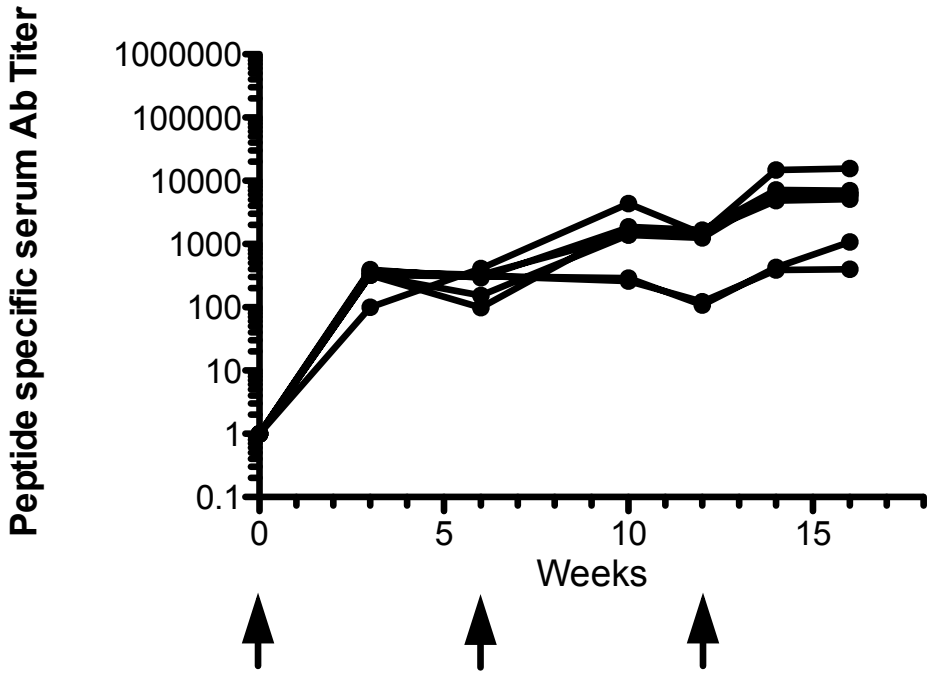

Figure 3.15: β2(2+YYR+2)I peptide-specific sheep serum Ab titers for the 50 μg Lkt-β2(2+YYR+2)I group. Sheep (n=7) were vaccinated with 50 μg Lkt produced as a genetic fusion to the β2(2+YYR+2)I epitope. Vaccines were formulated with 30% Emulsigen-D and administered SC at weeks 0, 6 and 12. Antibodies were detected using peptide-specific ELISAs and data presented represents individual animals. Arrows indicate immunization intervals.

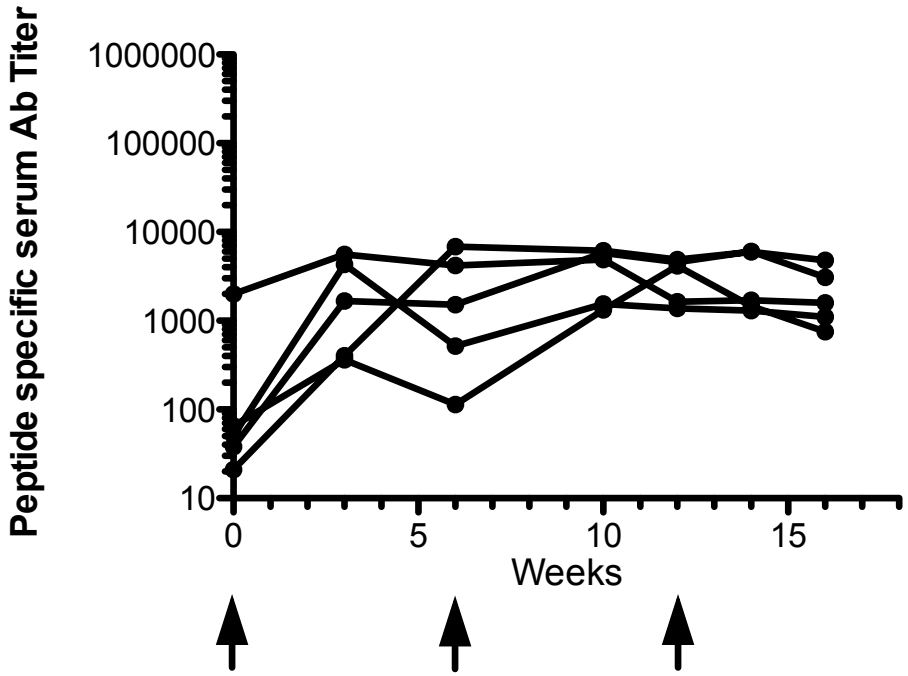

Figure 3.16: β2(3+YYR+1)L peptide-specific sheep serum Ab titers for the 50 μg Lkt-β2(3+YYR+1)L group. Sheep (n=5) were vaccinated with 50 μg Lkt produced as a genetic fusion to the β2(3+YYR+1)L epitope. Vaccines were formulated with 30% Emulsigen-D and administered SC at weeks 0, 6 and 12. Antibodies were detected using peptide-specific ELISAs and data presented represents individual animals. Arrows indicate immunization intervals.

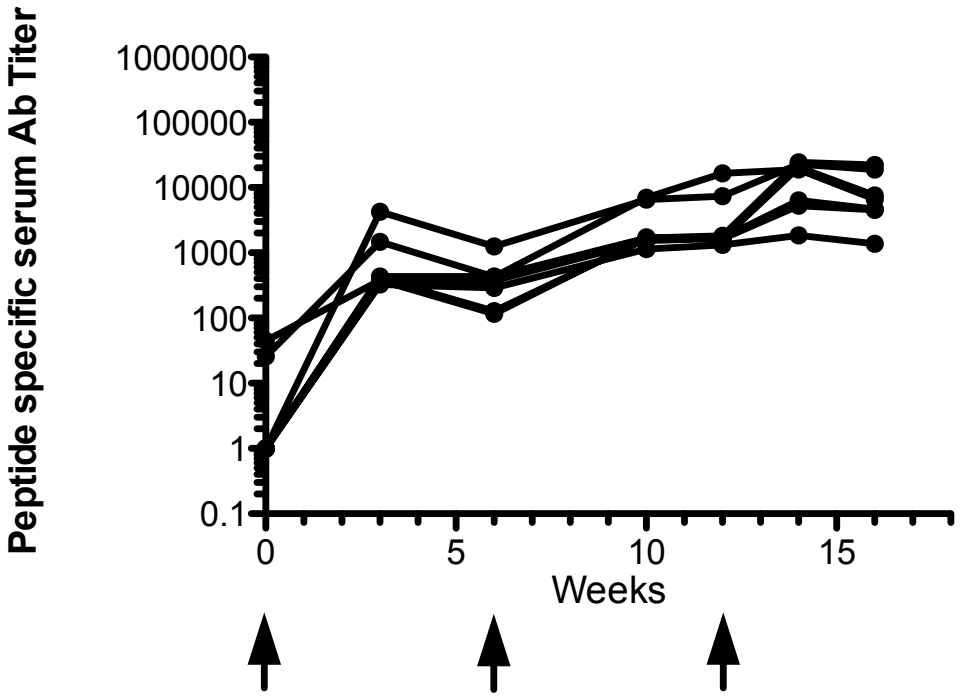

Figure 3.17: β2(3+YYR+1)I peptide-specific sheep serum Ab titers for the 50 μg Lkt-β2(3+YYR+1)I group. Sheep (n=5) were vaccinated with 50 μg Lkt produced as a genetic fusion to the β2(3+YYR+1)I epitope. Vaccines were formulated with 30% Emulsigen-D and administered SC at weeks 0, 6 and 12. Antibodies were detected using peptide-specific ELISAs and data presented represents individual animals. Arrows indicate immunization intervals.

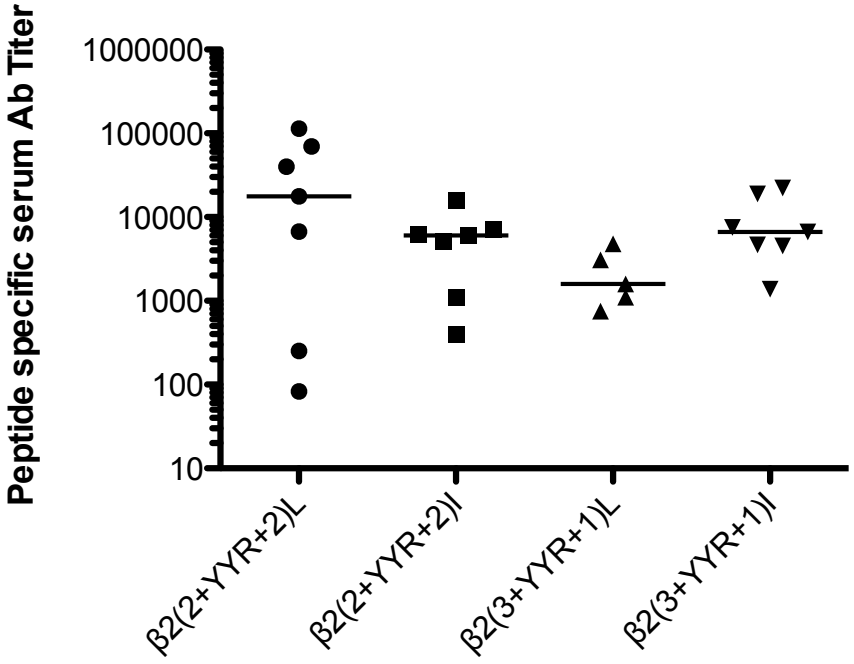

Figure 3.18: Comparison of peptide-specific titers at week 16 for sheep immunized with Lkt-β2(2+YYR+2) and Lkt-β2(3+YYR+1) constructs in their linear and inverted orientations. Sheep were vaccinated SC at 0, 6, and 12 weeks with 50 μg of the indicated Lkt chimeric protein formulated in 30% Emulsigen-D. Each dot represents the titer of individual sheep within each group and the horizontal bars indicate group median values. There was a statistically significant difference between the linear and inverted versions of the β2(3+YYR+1) epitopes ($p < 0.0049$).

Deer vaccinated with the β2(1+YYR+1)I construct developed peptide-specific antibody titers between 0 to 5,000 with titers in only 2/5 animals exceeding the 1,000 threshold [**Figure 3.19**]. The expanded construct β2(3+YYR+1)I produced a greater range in antibody responses (0-76,000), with 4/5 animals developing titers greater than 1,000 [**Figure 3.20**]. Both constructs induced lower antibody responses in elk. The β2(1+YYR+1)I construct failed to induce antibody responses, with titers greater than 1,000 in any of the animals [**Figure 3.21**]. While the expanded construct produced stronger antibody responses, there was not a significant difference ($p < 0.095$) between vaccine groups, and the antibody titers were less than those observed in deer. Two elk developed titers greater than 1,000 [**Figure 3.22**].

A comparison of the two PrP peptide constructs within the two cervid species indicated that in both deer and elk, the β2(3+YYR+1)I construct induced higher median titers than β2(1+YYR+1)I [**Figure 3.23**]. Analysis of the median titers at week 18, however, revealed no statistically significant difference between the two epitopes in either species [**Figure 3.24**]. The dose of vaccine used in this trial had previously been optimized in sheep for which the average female/male weighs 140/160 lbs. The average weight for a female/male whitetail deer and female/male elk is 140/165 and 500/700 lbs, respectively (http://www.antelope.org/weights/estimate_weights.htm). Factors such as body weight, vaccine dose, sex and interspecies genetic variation may have a significant impact on vaccine immunogenicity (Van Loveren *et al.*, 2001). Therefore, additional studies such as dose titrations in each species should be conducted before making conclusions regarding the immunogenicity of individual PrP peptide constructs.

3.9 Addition of Multiple C-Terminal Amino Acids [β2(2+YYR+9)]

Previous experiments indicated that expansion of the YYR epitope increased immunogenicity with enhanced antibody responses. To further investigate the limits of this concept, a much larger YYR epitope was constructed. Nine amino acids were added to the C-terminus, extending the amino acid sequence away from the YYR epitope on the α-helix 1, a region that had already been examined by other research groups (Muller-Schiffmann and Korth, 2008). The goal of this expansion was not only to develop a construct with improved

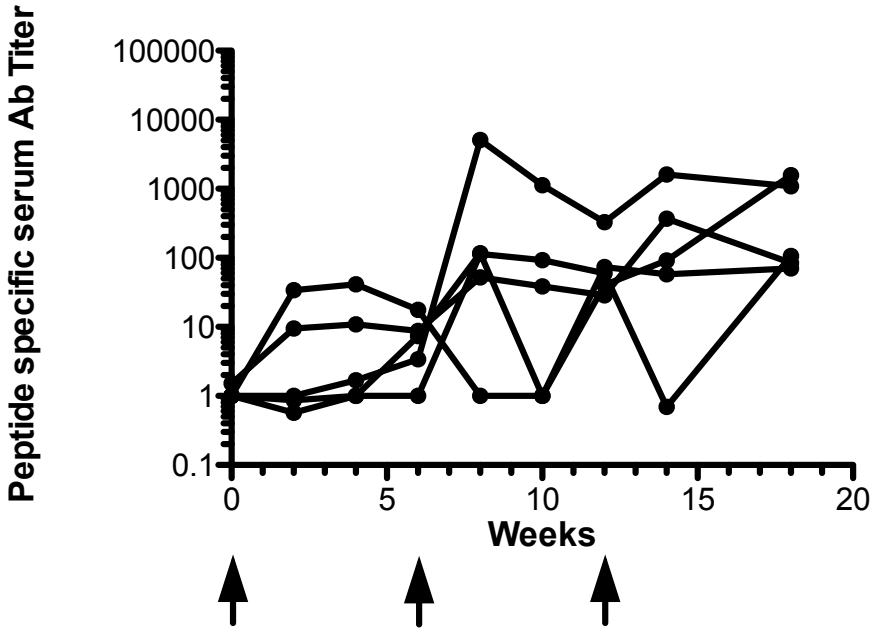

Figure 3.19: β2(1+YYR+1)I peptide-specific whitetail deer serum Ab titers for the 50 μg Lkt-β2(1+YYR+1)I group. Deer (n=5) were vaccinated with 50 μg Lkt produced as a genetic fusion to the β2(1+YYR+1)I epitope. Vaccines were formulated with 30% Emulsigen-D and administered SC at weeks 0, 6 and 12. Antibodies were detected using peptide-specific ELISAs and data presented represents individual animals. Arrows indicate immunization intervals.

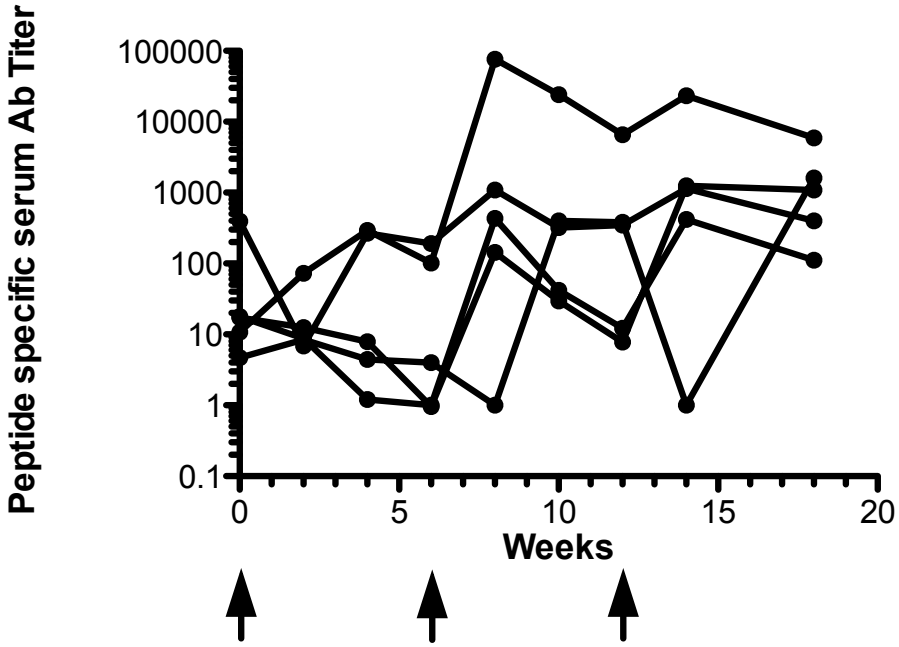

Figure 3.20: β2(3+YYR+1)I peptide-specific whitetail deer serum Ab titers for the 50 μg Lkt-β2(3+YYR+1)I group. Deer (n=5) were vaccinated with 50 μg Lkt produced as a genetic fusion to the β2(3+YYR+1)I epitope. Vaccines were formulated with 30% Emulsigen-D and administered SC at weeks 0, 6 and 12. Antibodies were detected using peptide-specific ELISAs and data presented represents individual animals. Arrows indicate immunization intervals.

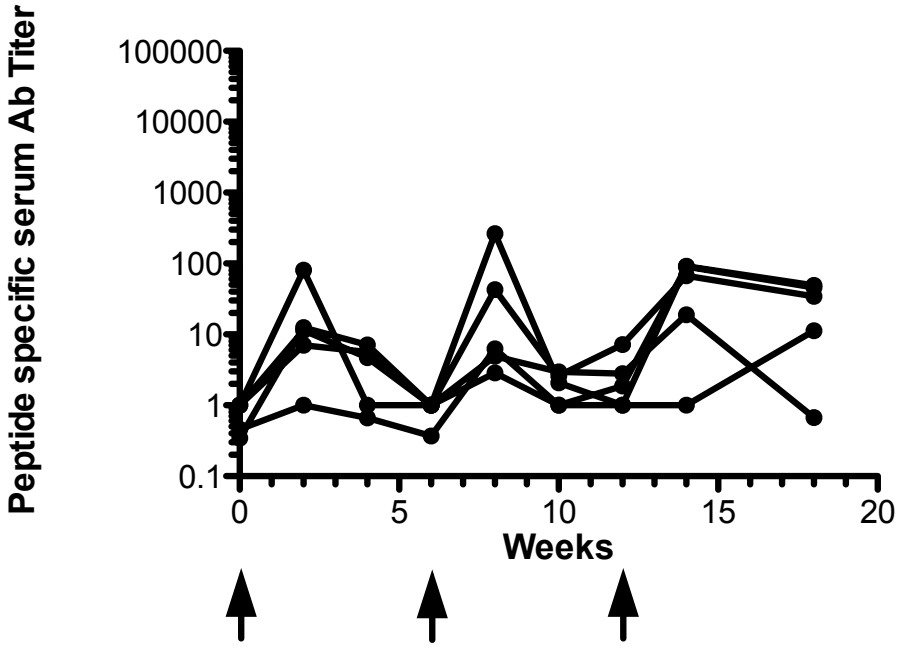

Figure 3.21: β2(1+YYR+1)I peptide-specific elk serum Ab titers for the 50 μg Lkt-β2(1+YYR+1)I group. Elk (n=5) were vaccinated with 50 μg Lkt produced as a genetic fusion to the β2(1+YYR+1)I epitope. Vaccines were formulated with 30% Emulsigen-D and administered SC at weeks 0, 6 and 12. Antibodies were detected using peptide-specific ELISAs and data presented represents individual animals. Arrows indicate immunization intervals.

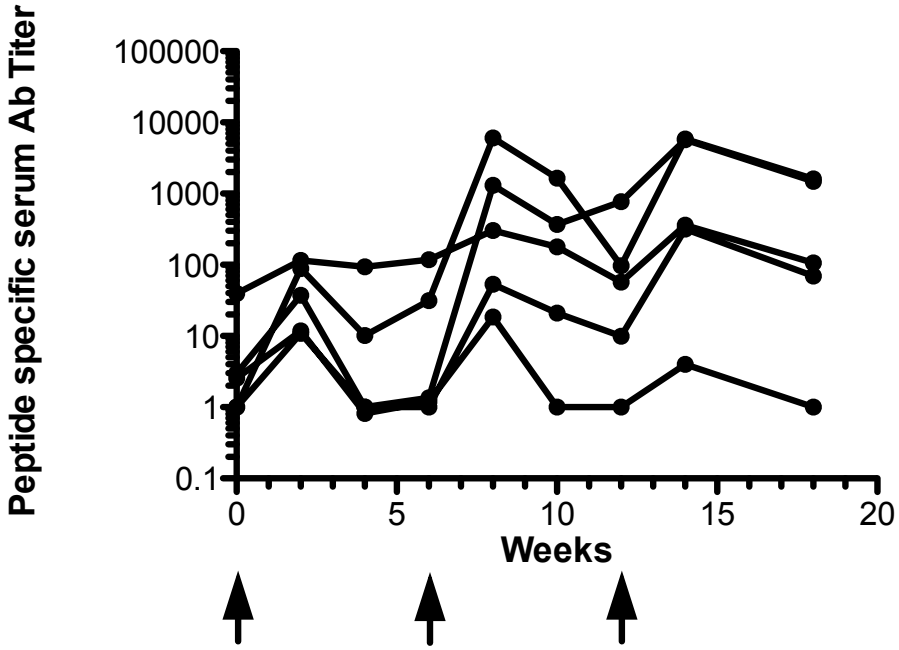

Figure 3.22: β2(3+YYR+1)I peptide-specific elk serum Ab titers for the 50 μg Lkt-β2(3+YYR+1)I group. Elk (n=5) were vaccinated with 50 μg Lkt produced as a genetic fusion to the β2(3+YYR+1)I epitope. Vaccines were formulated with 30% Emulsigen-D and administered SC at weeks 0, 6 and 12. Antibodies were detected using peptide-specific ELISAs and data presented represents individual animals. Arrows indicate immunization intervals.

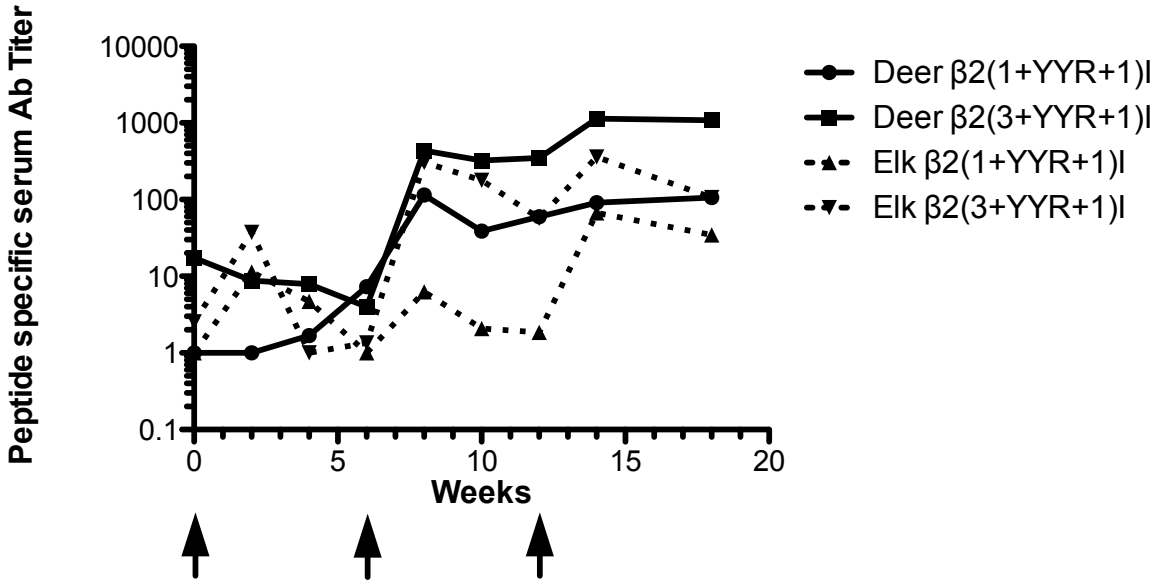

Figure 3.23: Median β2(1+YYR+1)I and β2(3+YYR+1)I peptide-specific whitetail deer and elk serum Ab titers for the 50 µg Lkt-β2(1+YYR+1)I and Lkt-β2(3+YYR+1)I groups. Elk (n=10) and deer (n=10) were vaccinated SC at 0, 6, and 12 weeks with 50 µg of the indicated Lkt chimeric protein formulated in 30% Emulsigen-D. Antibodies were detected using peptide-specific ELISAs and data is presented as the median values for the four groups. Arrows indicate immunization intervals.

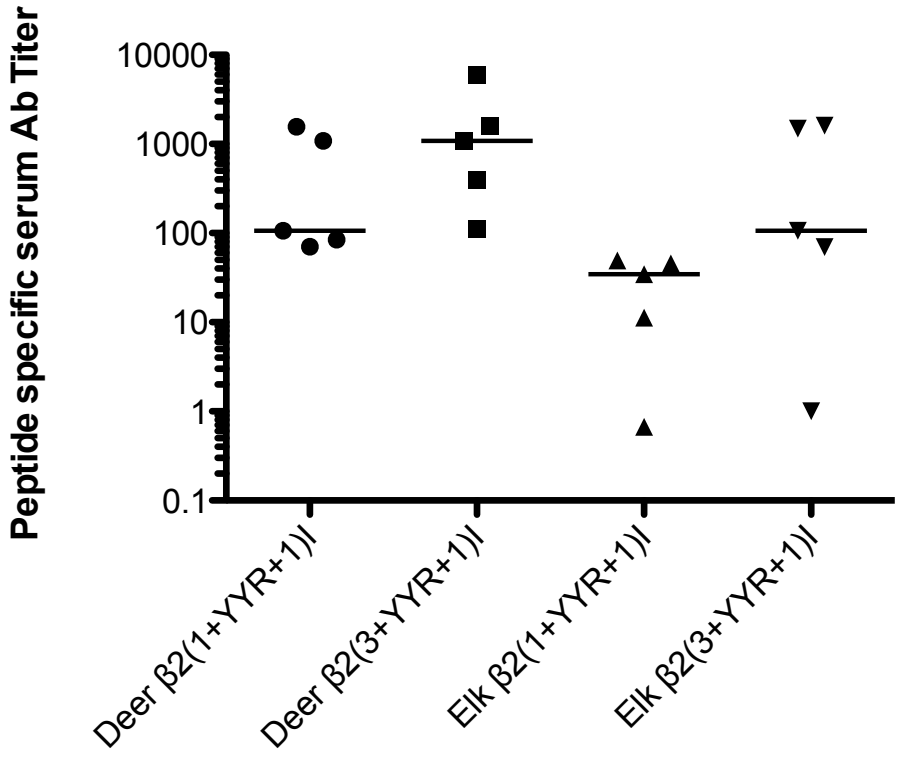

Figure 3.24: Comparison of peptide-specific serum Ab titers at week 18 for whitetail deer and elk immunized with Lkt-β2(1+YYR+1)I and Lkt-β2(3+YYR+1)I constructs. Deer and elk were vaccinated SC at 0, 6, and 12 weeks with 50 μg of the indicated Lkt chimeric protein formulated in 30% Emulsigen-D. Each dot represents the titer of individual animals within each group and the horizontal bars indicate group median values.

immunogenicity, but also to test the boundaries of the PrP^{Sc}-specific epitope. If the PrP epitope was too large, it was hypothesized that specificity for PrP^{Sc} would be lost or that PrP-specific T-reg cells may be invoked, inhibiting antibody responses. A large trial was conducted to compare the new epitope [β2(2+YYR+9)I] with previously tested epitopes. By week 16, the β2(2+YYR+9)I construct induced antibody titers ranging between 5,000 to 246,000 [**Figure 3.25**]. Analysis of peptide-specific antibody titers for all PrP epitope constructs revealed the week 16 median titers for the β2(2+YYR+9)I group was significantly higher ($p < 0.018$) than all other groups with the exception of the β2(2+YYR+2)L group which had a median titer of 17,700 [**Figure 3.26**]. While more robust immune responses had been stimulated, it was critical to determine whether specificity for PrP^{Sc} had been maintained; these results are discussed later.

To examine whether the significant increase in immunogenicity observed with β2(2+YYR+9)I was attributable to the size of the epitope or its unique amino acid sequence, another construct was tested. This PrP epitope was similar in length and molecular weight but the amino acid sequence was expanded toward the N-terminus instead [β2(9+YYR+2)I]. Two groups of mice (n=8) were vaccinated three times at three-week intervals, with either 10 μg of the Lkt-β2(9+YYR+2)I [**Figure 3.27**] or β2(2+YYR+9)I [**Figure 3.28**] formulated in 30% Emulsigen. The β2(9+YYR+2)I construct produced a slower antibody response, with titers ranging from 10,000 to 100,000 at week 7, versus week 3 for the same magnitude of response in the β2(2+YYR+9)I group. Another difference observed was in the range of individual animal antibody responses. Between weeks three and six, the variation in individual antibody responses within the β2(2+YYR+9)I group was less than the other group. By week 10, the antibody titers were significantly different ($p < 0.010$), with a median titer of 23,000 for the β2(9+YYR+2)I group and 63,000 for the β2(2+YYR+9)I group [**Figure 3.29**]. These results provided further evidence that the amino acid sequence significantly affects the immunogenicity of PrP^{C} cryptic epitopes.

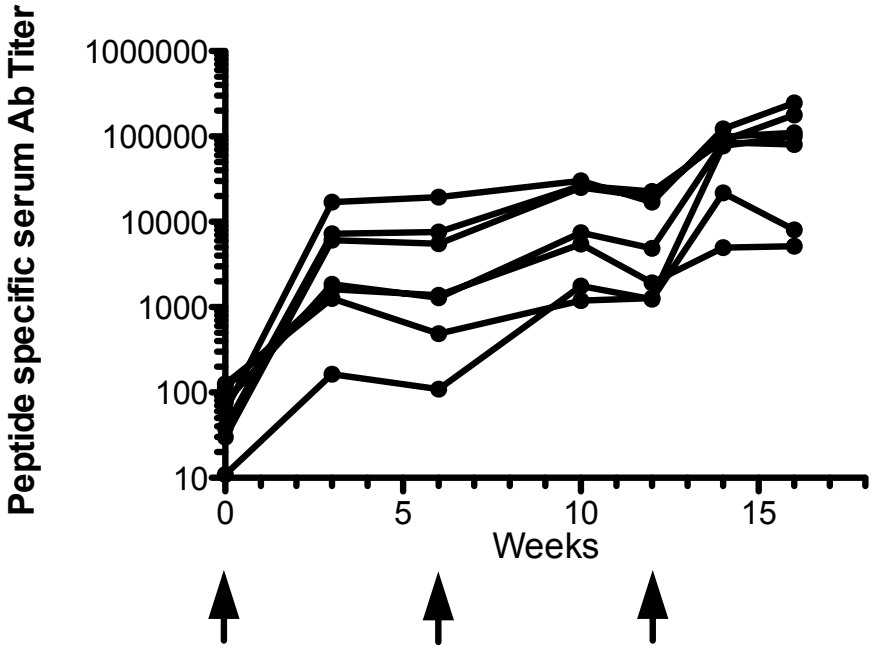

Figure 3.25: β2(2+YYR+9)I peptide-specific sheep serum Ab titers for the 50 μg Lkt-β2(2+YYR+9)I group. Sheep (n=7) were vaccinated with 50 μg Lkt produced as a genetic fusion to the β2(2+YYR+9)I epitope. Vaccines were formulated with 30% Emulsigen-D and administered SC at weeks 0, 6 and 12. Antibodies were detected using peptide-specific ELISAs and data presented represents individual animals. Arrows indicate immunization intervals.

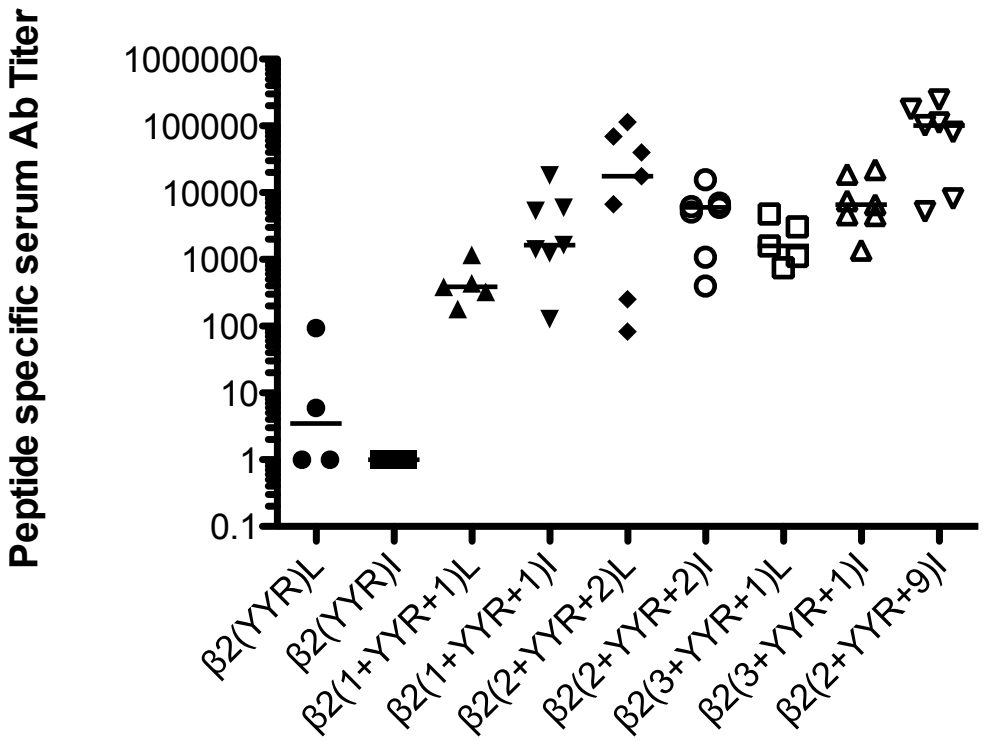

Figure 3.26: Comparison of peptide-specific sheep serum Ab titers at week 16 for nine different YYR constructs. Sheep were vaccinated SC at 0, 6, and 12 weeks with 50 μg of the indicated Lkt chimeric protein formulated in 30% Emulsigen-D. Each dot represents the titer of individual sheep within each group and the horizontal bars indicate group median values.

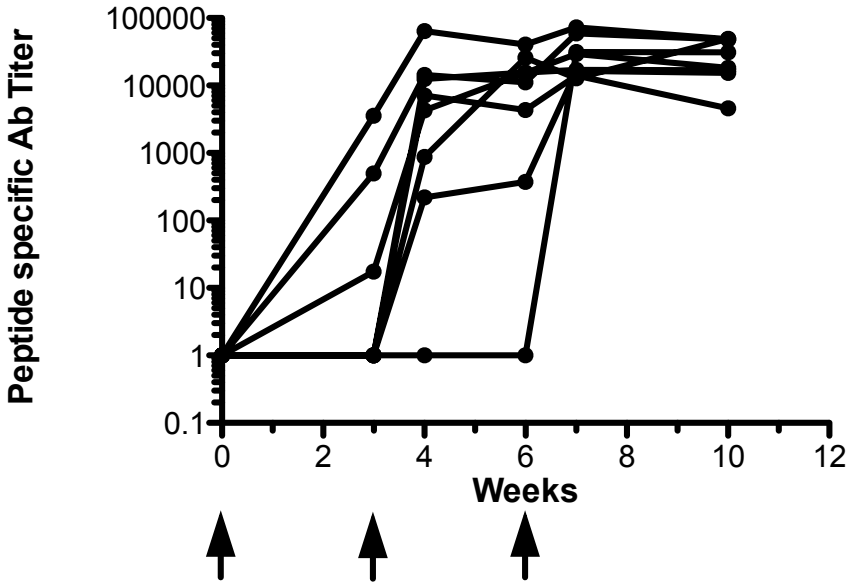

Figure 3.27: β2(9+YYR+2)I peptide-specific murine serum Ab titers for the 10 μg Lkt-β2(9+YYR+2)I group. Mice (n=8) were vaccinated with 10 μg Lkt produced as a genetic fusion to the β2(9+YYR+2)I epitope. Vaccines were formulated with 30% Emulsigen-D and administered SC at weeks 0, 3 and 6. Antibodies were detected using peptide-specific ELISAs and data presented represents individual animals. Arrows indicate immunization intervals.

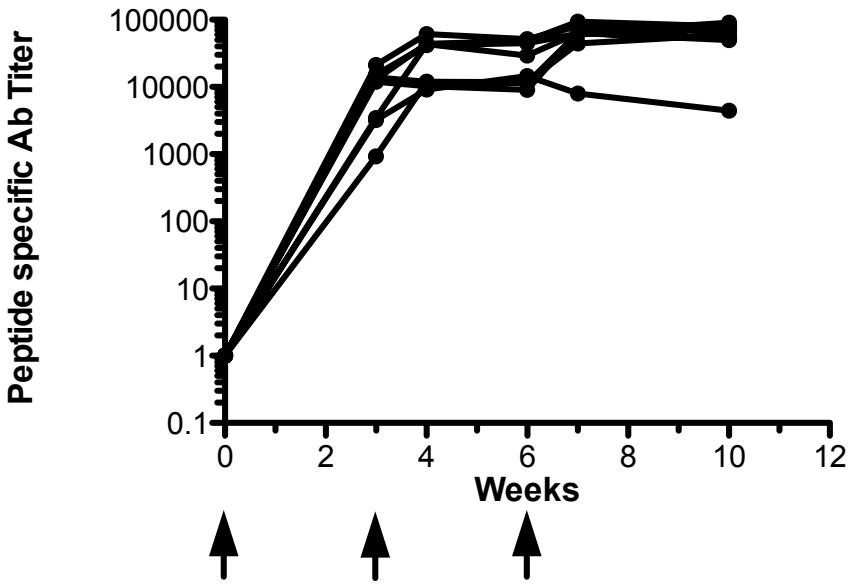

Figure 3.28: β2(2+YYR+9)I peptide-specific murine serum Ab titers for the 10 μg Lkt-β2(2+YYR+9)I. Mice (n=8) were vaccinated with 10 μg Lkt produced as a genetic fusion to the β2(2+YYR+9)I epitope. Vaccines were formulated with 30% Emulsigen-D and administered SC at weeks 0, 3 and 6. Antibodies were detected using peptide-specific ELISAs and data presented represents individual animals. Arrows indicate immunization intervals.

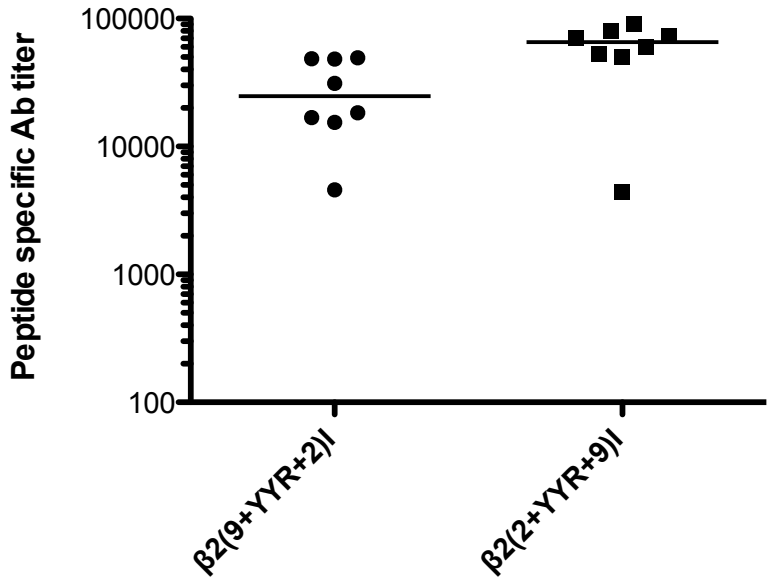

Figure 3.29: Comparison of peptide-specific murine serum Ab titers at week 10 for the 10 μg Lkt-β2(9+YYR+2)I and Lkt-β2(2+YYR+9)I groups. Mice were vaccinated SC at 0, 3, and 6 weeks with 10 μg of the indicated Lkt chimeric protein formulated in 30% Emulsigen-D. Each dot represents the titer of individual sheep within each group and the horizontal bars indicate group median values. There was a statistically significant difference between the median titers of the two groups ($p < 0.010$).

3.9.1 Immunogenicity Analysis of the Region Between Epitopes β2(2+YYR+2) and β2(2+YYR+9)

The data in Figure 3.32 revealed a significant ($p < 0.01$) increase in immunogenicity following a seven amino acid addition to the β2(2+YYR+2)I in the C-terminal direction. To better understand the structural basis for this increased immunogenicity, six new peptide epitopes were designed which increased in sized by single amino acid increments from β2(2+YYR+3)I, to β2(2+YYR+8)I. It was anticipated that there would be either an incremental increase in immunogenicity with each additional amino acid or the immunogenicity of β2(2+YYR+2)I would remain relatively constant until a threshold in peptide size was reached and immunogenicity would escalate to the level seen in β2(2+YYR+9)I. This series of constructs, including the original β2(2+YYR+2)I and β2(2+YYR+9)I, were used to vaccinate groups of C57BL/6 mice (n=8) twice with a three week interval. The original β2(2+YYR+2)I construct was the least immunogenic, with peptide-specific titers ranging between 400 to 4,000 at week 6 [**Figure 3.30**]. The next two constructs, β2(2+YYR+3)I and β2(2+YYR+4)I produced significantly greater antibody responses ($p < 0.0002$), with titers ranging between 4,500 to 85,000 (median 43,00), and 14,000 to 81,000 (median 55,898), respectively [**Figure 3.31 and 3.32**]. All mice immunized with β2(2+YYR+4)I developed high antibody titers that were more consistent than antibody responses in any other group. Interestingly, the titers for the next largest epitope, β2(2+YYR+5)I, were significantly weaker ($p < 0.0002$) than the previous two peptides, with a range between 270 to 11,300 and a median value of 906 [**Figure 3.33**]. Constructs β2(2+YYR+6)I and β2(2+YYR+7)I had comparable immunogenicity, with antibody titers ranging between 30 to 18,600 (median 13,000) and 1,000 to 55,800 (10,902), respectively [**Figure 3.34 and 3.35**]. The final construct, β2(2+YYR+8)I was moderately immunogenic with titers ranging between 10,400 to 70,100 (median 18,683) [**Figure 3.36**]. Along with β2(2+YYR+2)I, β2(2+YYR+9)I was used as a comparison construct displaying titers ranging between 3,700 to 58,000 (median 32,600) [**Figure 3.37**] a significant difference from β2(2+YYR+2), β2(2+YYR+5)I and β2(2+YYR+6)I I ($p < 0.0003$; $p < 0.0006$ and $p < 0.040$ respectively) [**Figure 3.38**]. Comparison of titers at week 10 revealed that there was no

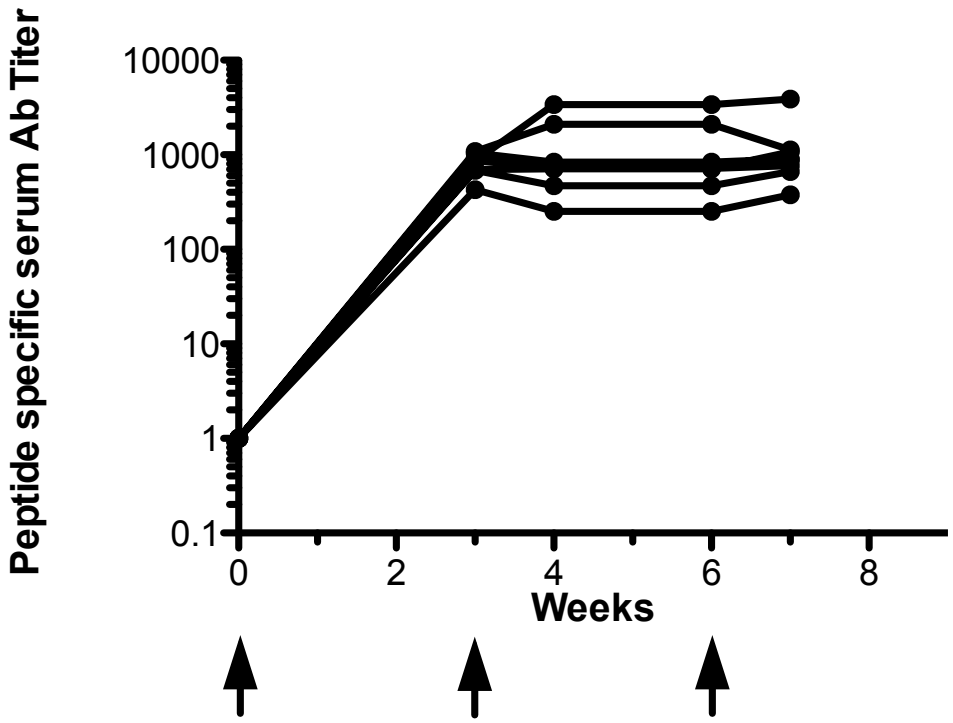

Figure 3.30: β2(2+YYR+2)I peptide-specific murine serum Ab titers for the 10 μg Lkt-β2(2+YYR+2)I group. Mice (n=8) were vaccinated with 10 μg Lkt produced as a genetic fusion to the β2(2+YYR+2)I epitope. Vaccines were formulated with 30% Emulsigen-D and administered SC at weeks 0, 3 and 6. Antibodies were detected using peptide-specific ELISAs and data presented represents individual animals. Arrows indicate immunization intervals.

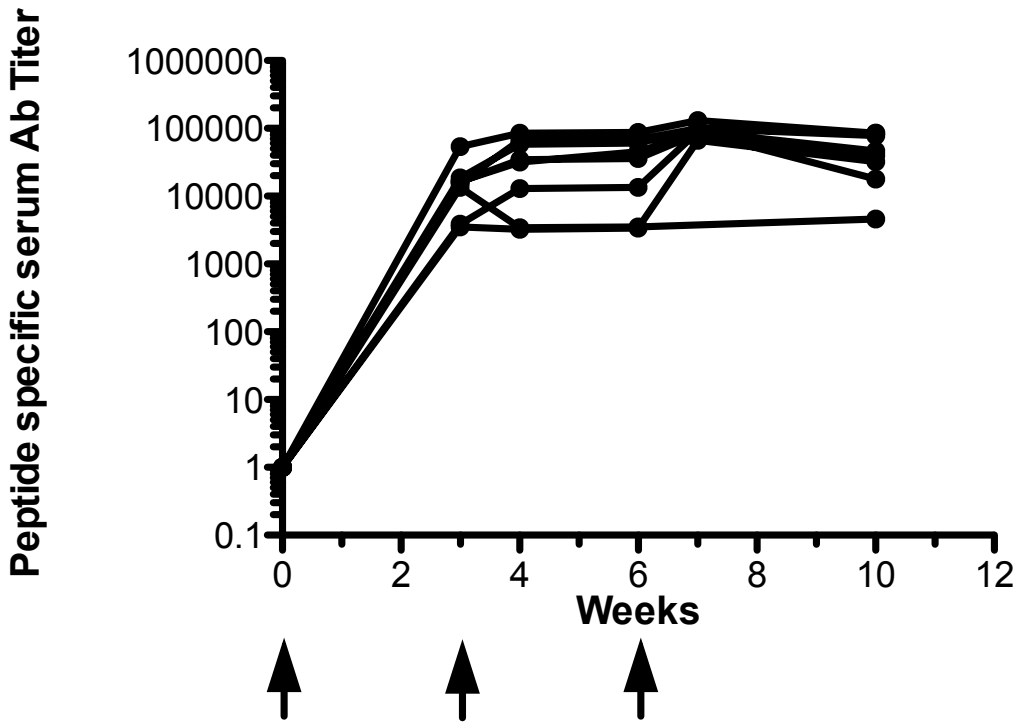

Figure 3.31: β2(2+YYR+3)I peptide-specific murine serum Ab titers for the 10 μg Lkt-β2(2+YYR+3)I group. Mice (n=8) were vaccinated with 10 μg Lkt produced as a genetic fusion to the β2(2+YYR+3)I epitope. Vaccines were formulated with 30% Emulsigen-D and administered SC at weeks 0, 3 and 6. Antibodies were detected using peptide-specific ELISAs and data presented represents individual animals. Arrows indicate immunization intervals.

.

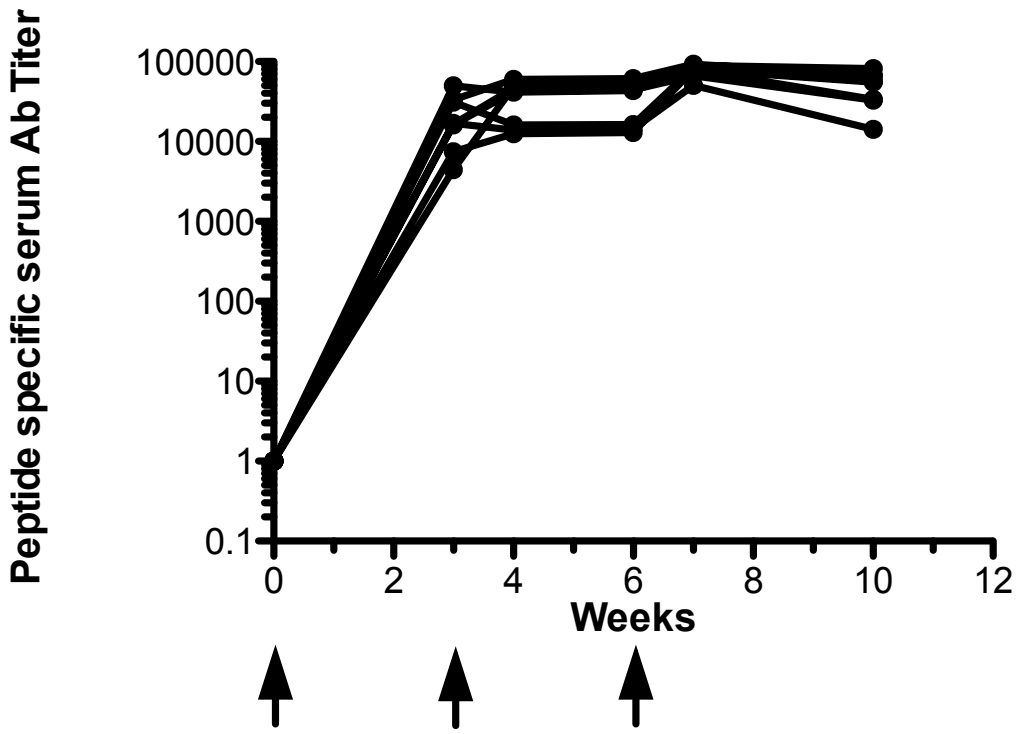

Figure 3.32: β2(2+YYR+4)I peptide-specific murine serum Ab titers for the 10 μg Lkt-β2(2+YYR+4)I group. Mice (n=8) were vaccinated with 10 μg Lkt produced as a genetic fusion to the β2(2+YYR+4)I epitope. Vaccines were formulated with 30% Emulsigen-D and administered SC at weeks 0, 3 and 6. Antibodies were detected using peptide-specific ELISAs and data presented represents individual animals. Arrows indicate immunization intervals.

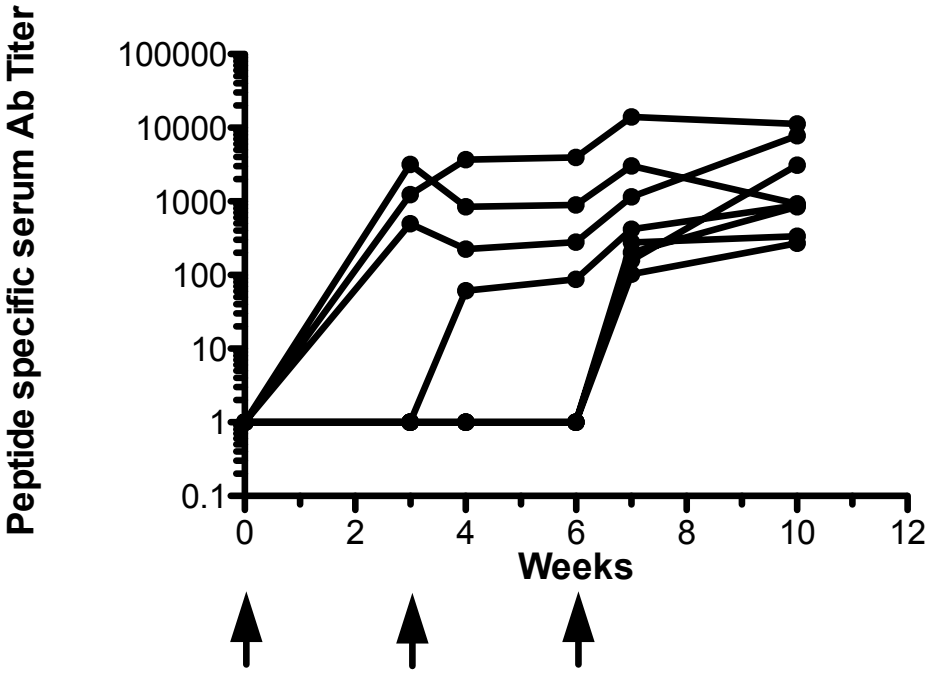

Figure 3.33: β2(2+YYR+5)I peptide-specific murine serum Ab titers for the 10 μg Lkt-β2(2+YYR+5)I group. Mice (n=8) were vaccinated with 10 μg Lkt produced as a genetic fusion to the β2(2+YYR+5)I epitope. Vaccines were formulated with 30% Emulsigen-D and administered SC at weeks 0, 3 and 6. Antibodies were detected using peptide-specific ELISAs and data presented represents individual animals. Arrows indicate immunization intervals.

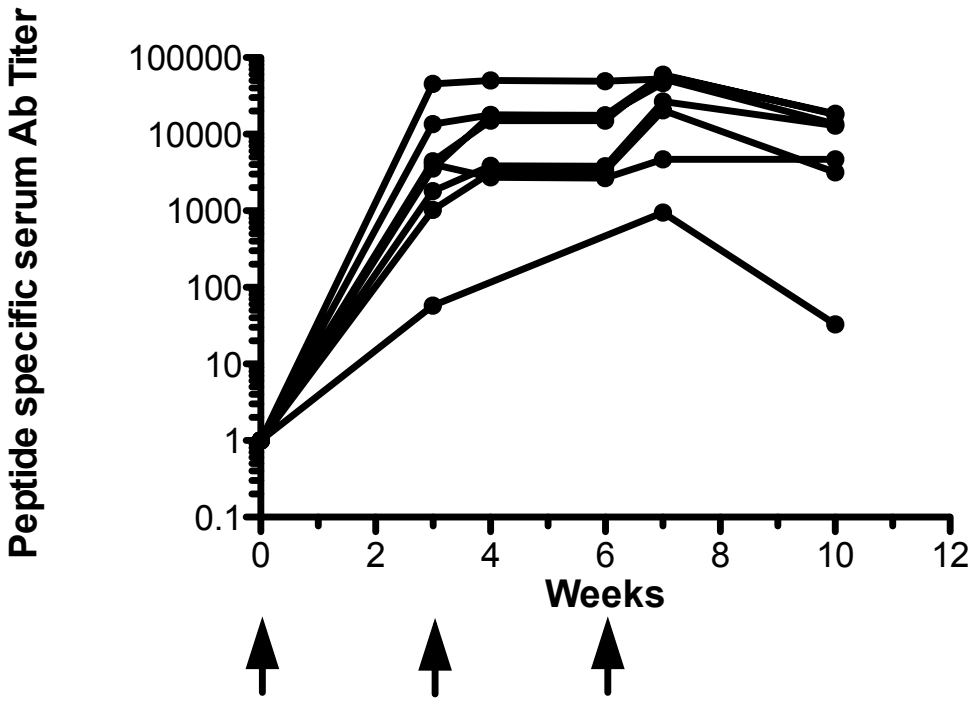

Figure 3.34: β2(2+YYR+6)I peptide-specific murine serum Ab titers for the 10 μg Lkt-β2(2+YYR+6)I group. Mice (n=8) were vaccinated with 10 μg Lkt produced as a genetic fusion to the β2(2+YYR+6)I epitope. Vaccines were formulated with 30% Emulsigen-D and administered SC at weeks 0, 3 and 6. Antibodies were detected using peptide-specific ELISAs and data presented represents individual animals. Arrows indicate immunization intervals.

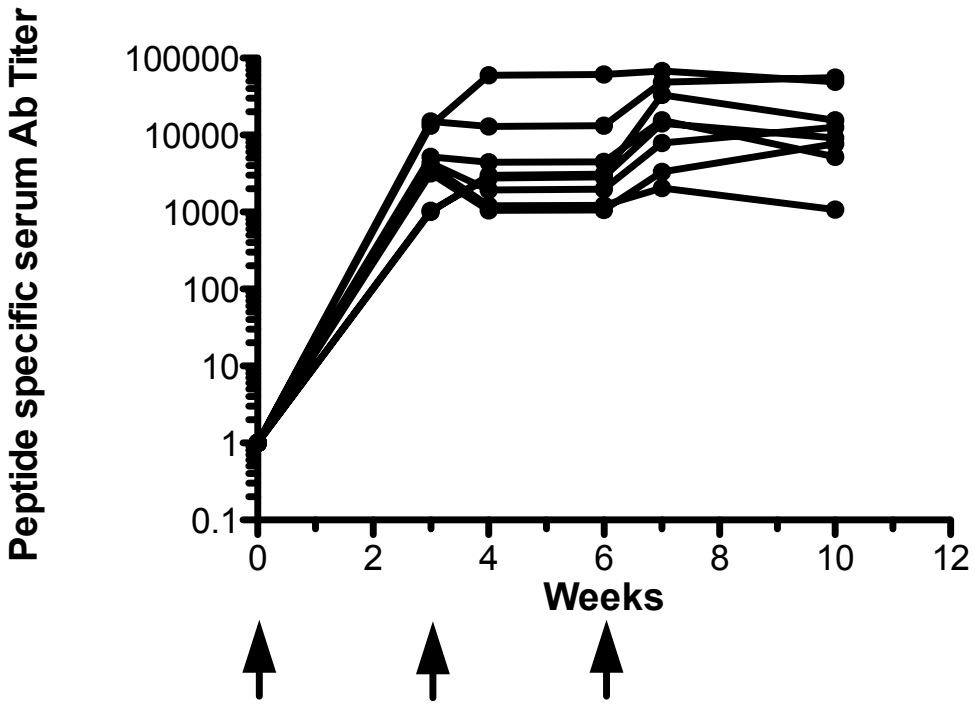

Figure 3.35: β2(2+YYR+7)I peptide-specific murine serum Ab titers for the 10 μg Lkt-β2(2+YYR+7)I group. Mice (n=8) were vaccinated with 10 μg Lkt produced as a genetic fusion to the β2(2+YYR+7)I epitope. Vaccines were formulated with 30% Emulsigen-D and administered SC at weeks 0, 3 and 6. Antibodies were detected using peptide-specific ELISAs and data presented represents individual animals. Arrows indicate immunization intervals.

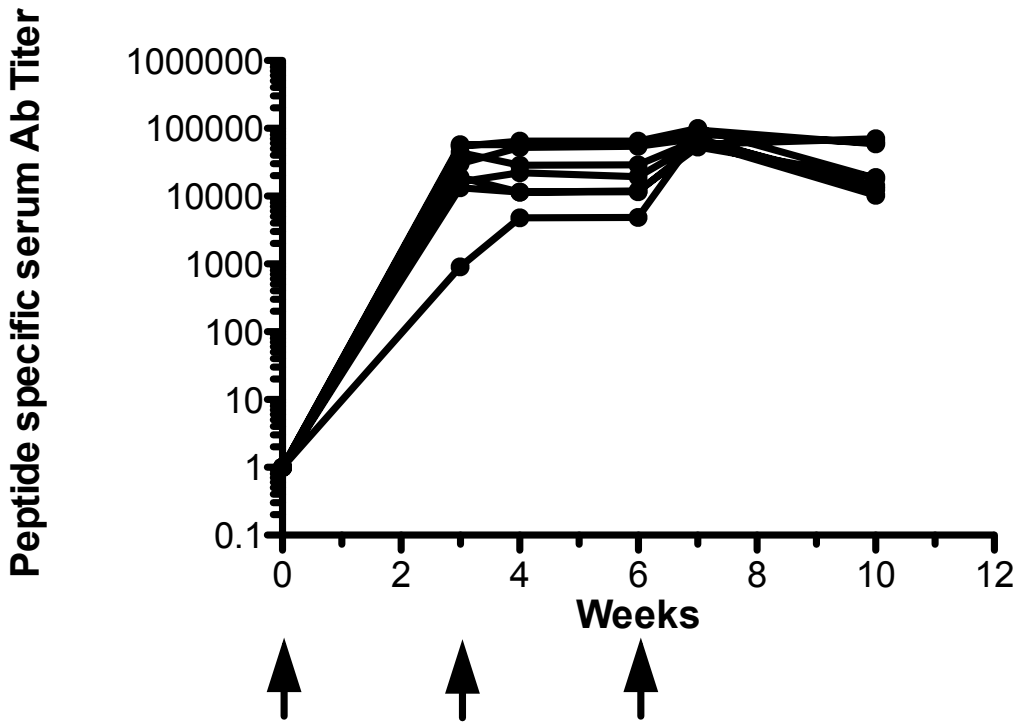

Figure 3.36: β2(2+YYR+8)I peptide-specific murine serum Ab titers for the 10 μg Lkt-β2(2+YYR+8)I group. Mice (n=8) were vaccinated with 10 μg Lkt produced as a genetic fusion to the β2(2+YYR+8)I epitope. Vaccines were formulated with 30% Emulsigen-D and administered SC at weeks 0, 3 and 6. Antibodies were detected using peptide-specific ELISAs and data presented represents individual animals. Arrows indicate immunization intervals.

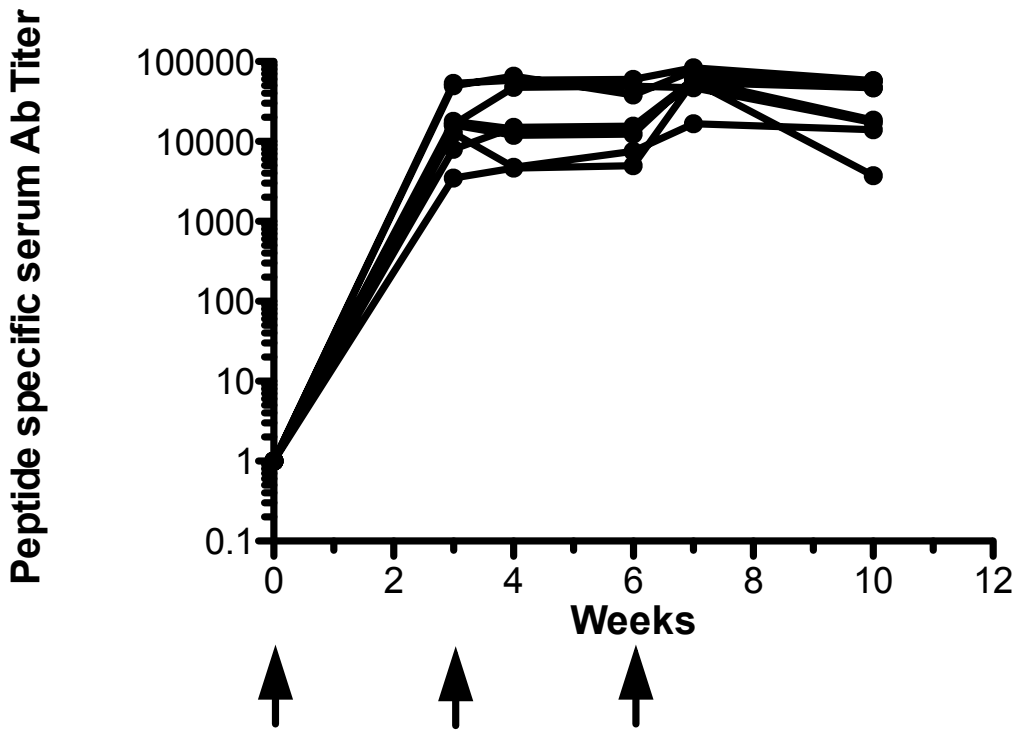

Figure 3.37: β2(2+YYR+9)I peptide-specific murine serum Ab titers for the 10 μg Lkt-β2(2+YYR+9)I group. Mice (n=8) were vaccinated with 10 μg Lkt produced as a genetic fusion to the β2(2+YYR+9)I epitope. Vaccines were formulated with 30% Emulsigen-D and administered SC at weeks 0, 3 and 6. Antibodies were detected using peptide-specific ELISAs and data presented represents individual animals. Arrows indicate immunization intervals.

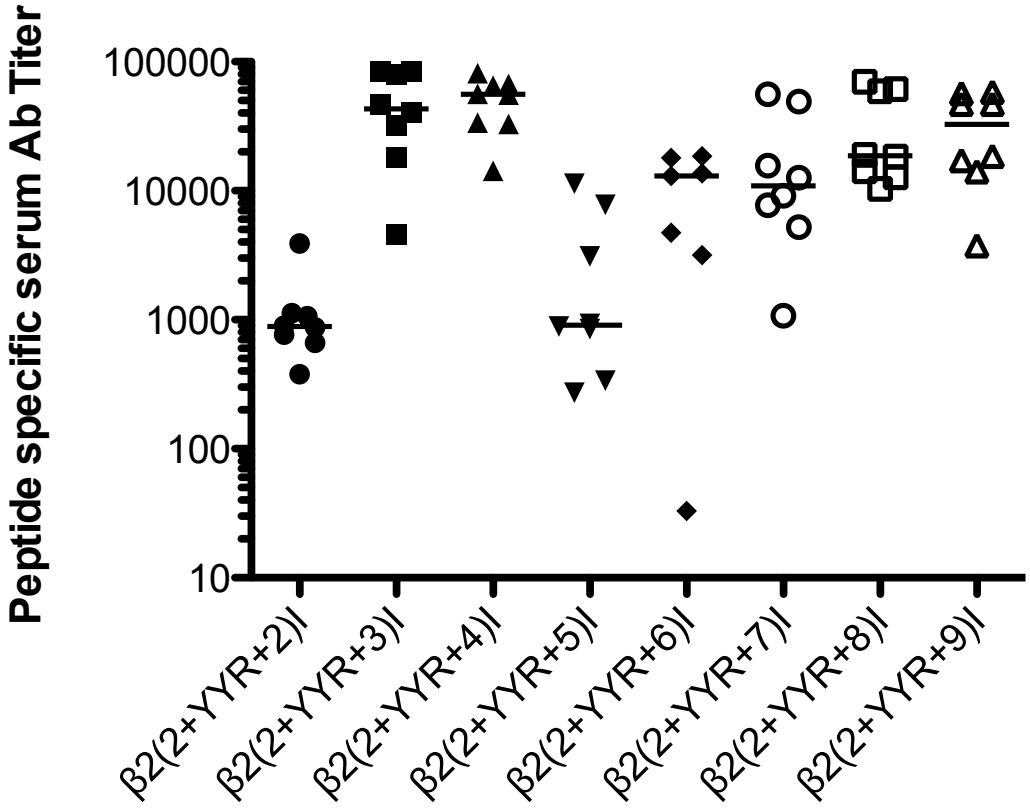

Figure 3.38: Comparison of peptide-specific murine serum Ab titers at week 10 for 8 constructs. Mice were vaccinated SC at 0, 3, and 6 weeks with 10 μg of the indicated Lkt chimeric protein formulated in 30% Emulsigen-D. Each dot represents the titer of individual sheep within each group and the horizontal bars indicate group median values. Because week 10 samples for the β2(2+YYR+8)I group were unavailable, values from week 7 were used to calculate the median titers.

statistical difference between the four most immunogenic constructs, β2(2+YYR+3)I, β2(2+YYR+4)I, β2(2+YYR+8)I and β2(2+YYR+9)I [**Figure 3.38**].

3.10 The α-Helix 1 YYR Epitope

It was suggested by Muller-Schiffmann and Korth (2008) that the best target for passive and active immunization was the region between amino acids 145 and 160. This is the α-helix 1 region containing the first of the YYR epitopes. They argued that these residues stimulate T-cell proliferation and are also a preferred B-cell epitope, resulting in significant antibody production. In addition, antibodies to this region had anti-prion activity in ScN2a cells (Muller-Schiffmann and Korth, 2008).

Taking this work into consideration, a construct was designed based on the α-helix 1 YYR region [α1(2+YYR+2)I]. The construct was fused to Lkt and used to vaccinate sheep using a 50 μg dose of chimeric protein formulated in 30% Emulsigen. This vaccine was injected at 6 week intervals. Antibody responses to this construct were very poor. One animal achieved an antibody titer of 100,000 but the highest titer among the remaining 6 animals was 1,600, with three animals failing to break 1,000 [**Figure 3.39**]. In terms of active antibody responses, this epitope on the α-helix 1 was poorly immunogenic when compared to both the β2(2+YYR+2)I and β2(2+YYR+9)I constructs. It has also been shown later that the antibodies to the α-helix 1 epitope were not PrP^{Sc}-specific [**Figure 3.41]**. Perhaps it would be possible to alter the YYR epitope on the α-helix 1 to improve its immunogenicity and PrP^{Sc}-specificity as was done with the other YYR epitope.

3.11 Presence of Antibody at Sites Pertinent to TSE Infection (Mucosal Surface, Cerebral Spinal Fluid)

Mucosal surfaces (upper respiratory and gastro-intestinal tracts) with the associated organized lymphoid tissue (tonsil, Peyer's patches, and draining lymph nodes) provide critical sites for prion entry and amplification (Heggebo *et al.*, 2003), while the brain serves as the final prion destination and site of pathology. Consequently, the main goal of prion vaccination is

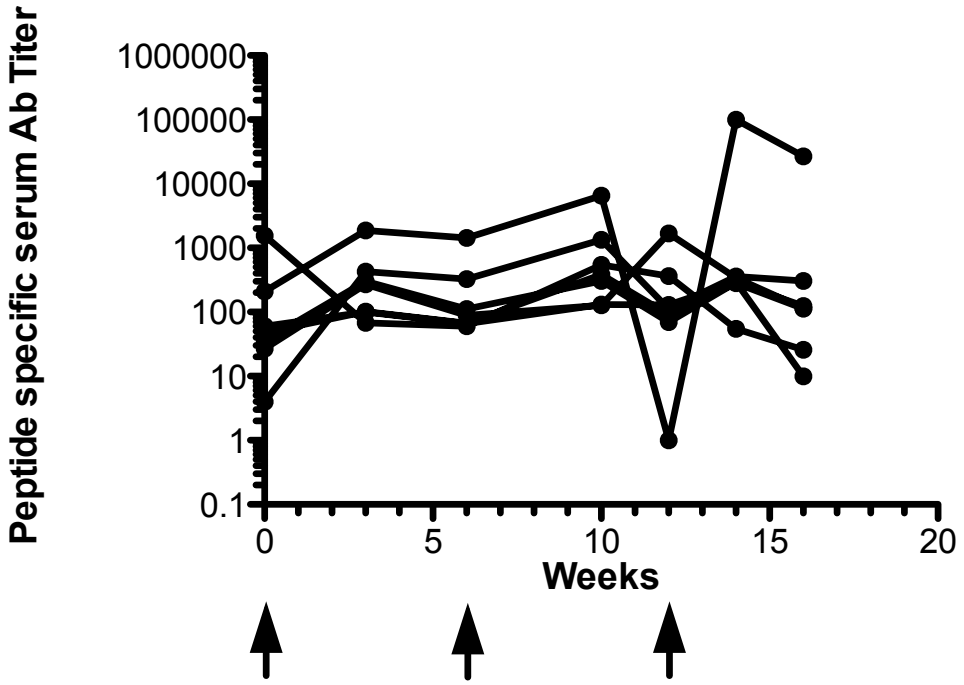

Figure 3.39: α1(2+YYR+2)I peptide-specific sheep serum Ab titers for the 50 μg Lkt-α1(2+YYR+2)I group. Sheep (n=7) were vaccinated with 50 μg Lkt produced as a genetic fusion to the α1(2+YYR+2)I epitope. Vaccines were formulated with 30% Emulsigen-D and administered SC at weeks 0, 6 and 12. Antibodies were detected using peptide-specific ELISAs and data presented represents individual animals. Arrows indicate immunization intervals.

to neutralize infectious prions before they cross the mucosa or, in cases where an animal is already infected, prevent the accumulation of proteinaceous plaques in the brain. For this to happen there must be sufficient PrP^{Sc}-specific neutralizing antibodies at mucosal surfaces and associated lymphoid tissue, as well as antibody in the CNS. Due to physiological/anatomical constraints like the blood-brain barrier, which has a permeability coefficient of 0.1×10^{-6} mL/g/s (Poduslo *et al.*, 2001), Ig concentration gradients following SC immunization are expected to be: serum > mucosa > CSF. Altering the vaccination route to a mucosal delivery system would markedly shift the Ig concentration in favour of the mucosa.

Although the concentration of PrP^{Sc}-specific antibody required for disease prevention is not known, it was important to determine the distribution of peptide-specific antibody in various body fluids following immunization with the Lkt-peptide vaccine system. At the end of the vaccine trial using the β2(2+YYR+9)I construct, five animals were sacrificed. CSF, serum and nasal secretions were collected and analyzed to determine peptide-specific titers. As expected, the serum antibody titers were highest (ranging from 1,000 - 60,000), followed by nasal secretions (250 - 20,000) and finally CSF (100 – 650) [**Figure 3.40**]. Regression analysis showed a significant correlation ($r^2 = 0.95$, $p < 0.0052$) between serum antibody titers and antibody concentrations in the CSF. Achieving high PrP^{Sc}-specific antibody titers in serum may therefore, may be critical for the prevention of prion plaque deposition in the CNS. Interestingly, immunotherapy studies for Alzheimer's have shown CSF protection against A-beta plaque formation despite low concentrations of anti-Amyloid β IgG in the CSF (Poduslo *et al.*, 2007).

Epitope-specific antibody responses were also detected in the mucosal secretions, following vaccination. There was, however, no significant correlation ($r^2 = 0.52$, $p < 0.17$) between the mucosal and serum peptide-specific antibody titers. Because parenteral vaccine administration is not an ideal way to stimulate mucosal immunity, this lack of correlation was expected.

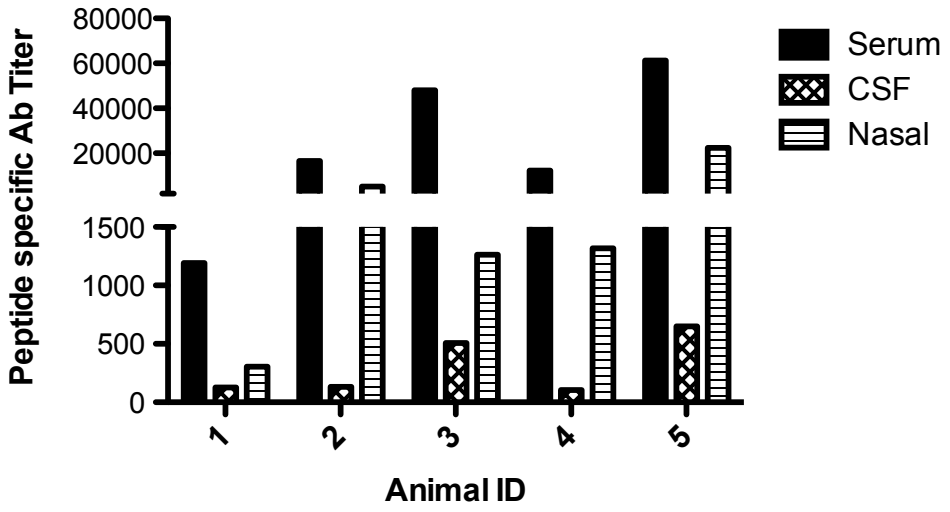

Figure 3.40: Epitope-specific serum, CSF and mucosal Ab titers at week 23. Sheep (n=5) were vaccinated with 50 μg Lkt produced as a genetic fusion to the β2(2+YYR+9)I epitope. Vaccines were formulated with 30% Emulsigen-D and administered SC at weeks 0, 6 and 12 and 21. Antibodies were detected using peptide-specific ELISAs and data is presented for individual animals.

3.12 IgG subtype determination

To better charaterize the types of IgG antibody responses our constructs were stimulating we screened mouse immune sera against anti-IgG1,-IgG2a and -IgG2b antibodies. Sera from three different groups of mice immunized with either Lkt-β2(2+YYR+2)I, Lkt-β2(9+YYR+2)I or Lkt-β2(2+YYR+9)I were analyzed using peptide ELISAs specific for the different IgG subtypes. All sera predominantly consisted of IgG1 antibodies with a median titer of 54,000 while IgG2a and IgG2b had median titers of 24 and 30 respectively [**Figure 3.41]**.

3.13 Specificity of the Immune Response for PrP^{C} and PrP^{Sc}

3.13.1 PrP^{C} ELISA

The primary reason for investigating YYR epitope alterations was to improve peptide immunogenicity without altering antibody specificity for PrP^{Sc}. It was presumed that increased antibody responses would be correlated with protective antibody concentrations at appropriate sites to achieve prion neutralization. We hypothesized that an increase in neutralizing antibody titer could be achieved without a loss in antibody specificity for PrP^{Sc}. A reduction in specificity could result in antibody binding to PrP^{C} and possibly disrupting normal function or stimulating inappropriate signalling events in neurons (Solforosi *et al.*, 2004). Antibody specificity was first analyzed by comparing the reactivity of pre-immune and immune sera with recombinant PrP^{C} in an ELISAs. None of the β-strand 2 constructs, in the 65 animals tested, induced a detectable antibody reaction with PrP^{C} [**Figure 3.42**]. One animal in the α-helix 1 group did, however, have an antibody response that cross-reacted with PrP^{C}.

3.13.2 PrP^{C} and PrP^{Sc} Immunoprecipitation

To further investigate the specificity of the expanded PrP epitopes, PrP^{Sc} immunoprecipitation assays were performed using uninfected and Rocky Mountain Laboratory (RML) Scrapie-infected mouse brain homogenates. Sera from sheep immunized with β2(2+YYR+9)I and β2(2+YYR+2)I only immunoprecipitated PrP^{Sc}, whereas sera from animals

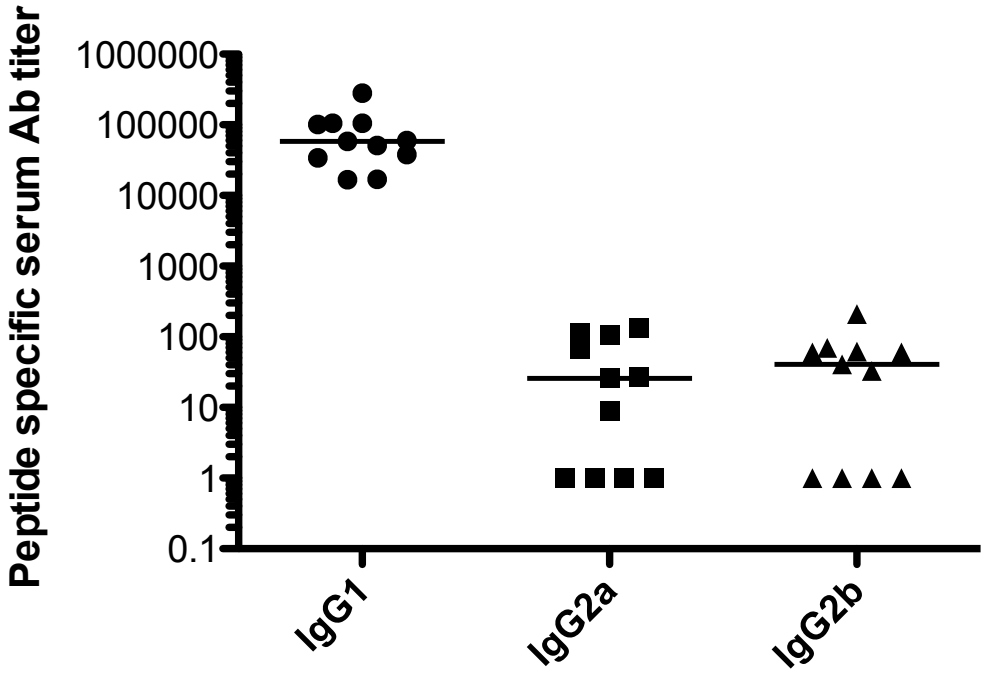

Figure 3.41: IgG antibody subtype characterization. Week 10 immune sera from mice (n=11) previously vaccinated at week 0, 3 and 6 with 10 μg of either Lkt-β2(2+YYR+2)I, Lkt-β2(9+YYR+2)I or Lkt-β2(2+YYR+9)I were screened using a peptide ELISA. The secondary antibody used in the ELISA was IgG subtype specific for IgG1, IgG2a or IgG2b. Each dot represents the titer of an indidual mouse and the bars indicate the median titers for each different IgG subtype.

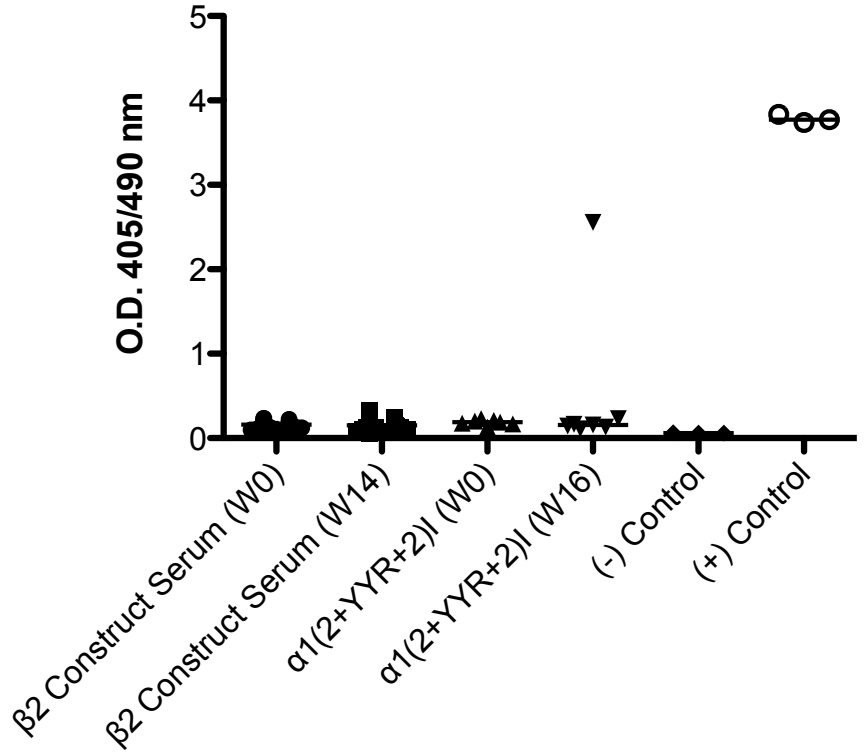

Figure 3.42: PrP^C reactivity of serum from sheep immunized with different β2-strand [β2(YYR)I, β2(1+YYR+1)I, β2(2+YYR+2)L, β2(2+YYR+2)I, β2(1+YYR+1)I x 4, β2(2+YYR+9)I] and α1 epitopes (2+YYR+2)I. Sheep (n=65) were divided into groups and then vaccinated with individual constructs at 6 week intervals. Week 0 and 14 sera from the β2 construct groups was screened while sera from the α1 group were tested at week 0 and 16. The positive control was SAF32, a PrP^C mAb.

immunized with β2(1+YYR+)I and β2(YYR)L, to a lesser degree, immunoprecipitated both PrP^{Sc} and PrP^{C} [**Figure 3.43**]. The presence of two or three bands per lane on the RML gel can be explained by the three glycosylation states (non-, mono- and diglycosylation) that exist in both cellular and infectious conformation (Aguzzi *et al.*, 2007).

The results regarding specificity differ from the PrP^{C} ELISA results in that the ELISA detected PrP^{C} reactivity only for serum specific for the α1 epitope. What was consistent, however, was that in both experiments, the antisera for the most immunogenic construct, β2(2+YYR+9)I, lacked reactivity against PrP^{C}. This confirms that it is possible to design a PrP epitope which induces strong antibody responses and maintains specificity for PrP^{Sc}.

3.14 Immunization Using Lkt-PrP^{C}

An immune response to a protein often results in preferential targeting of one or more epitopes, also known as the dominant epitopes, by different components of the acquired immune system. Another mechanism exists, known as epitope-spreading, whereby the specificity of the immune response broadens over time to include epitopes neighbouring the dominant one (Vanderlugt and Miller, 2002). With the goal of directing an immune response to a cryptic epitope on a self protein, epitope-spreading threatens the specificity of the intended response by creating alternative epitopes outside the cryptic region, potentially resulting in autoimmunity. To investigate the possible consequence of epitope spreading within the Lkt vaccine model, we conducted an experiment with the objective of breaking immune tolerance to PrP^{C}. A recombinant fusion of Lkt and full-length PrP^{C} (Lkt-PrP^{C}) was created, expressed in *E. coli*, and purified. Sheep (n=7) were immunized three times at 6 week intervals using the vaccine formulation and dose utilized for the YYR peptide vaccines. ELISA was used to screen both pre-immune and immune (week 15) sera with recombinant PrP^{C} protein, but we were unable to detect a significant change in antibody titers when comparing week 15 Lkt control sera and Lkt-PrP^{C} sera ($p < 0.23$) [**Figure 3.44**]. This inability to break PrP^{C} tolerance led to the conclusion that epitope spreading, in response to vaccination with the Lkt-YYR based constructs, would be restricted by immune tolerance.

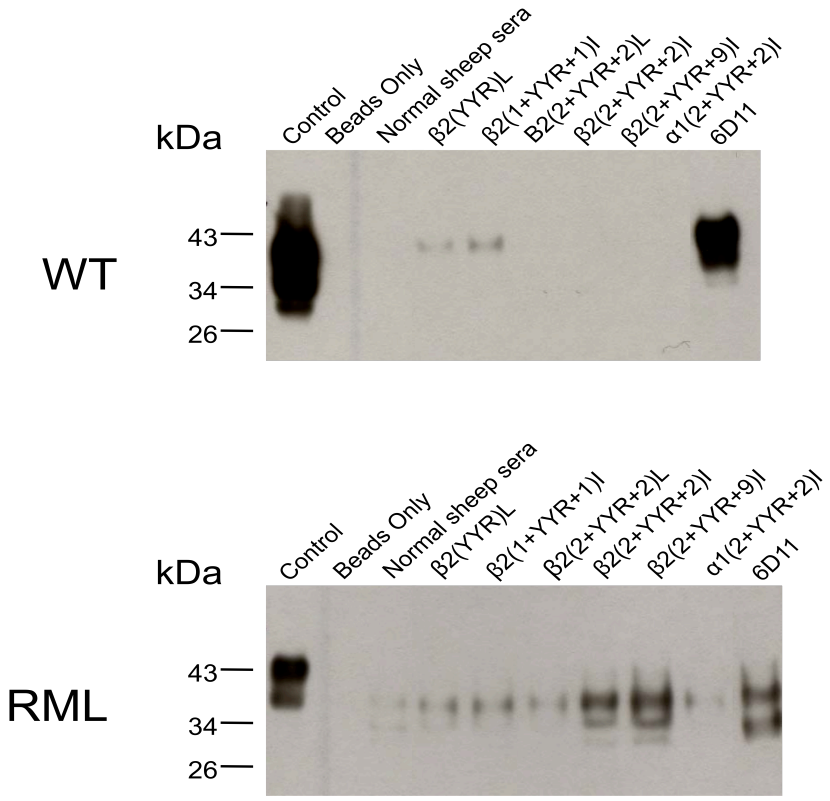

Figure 3.43: Immunoprecipitation of PrP^{Sc} and PrP^{C} using serum from sheep vaccinated with different YYR Constructs. Sera from sheep immunized with β2(YYR)L, β2(1+YYR+1)I, β2(2+YYR+2)L, β2(2+YYR+2)I, β2(2+YYR+9)I, and α1(2+YYR+2)I three times at six week intervals were evaluated for reactivity with PrP^{Sc} and PrP^{C}. Antibodies conjugated to magnetic beads were used in immunoprecipitation assays with brain homogenates of uninfected (WT) and Scrapie-infected mice (RML). 3 μL of 10% WT or RML brain homogenate was used as a PrP control for each blot. Magnetic beads or magnetic beads coated with serum from naïve sheep serve as negative controls while beads coated with 6D11, a commercially available mAb which binds both PrP^{Sc} and PrP^{C}, serves as a positive control.

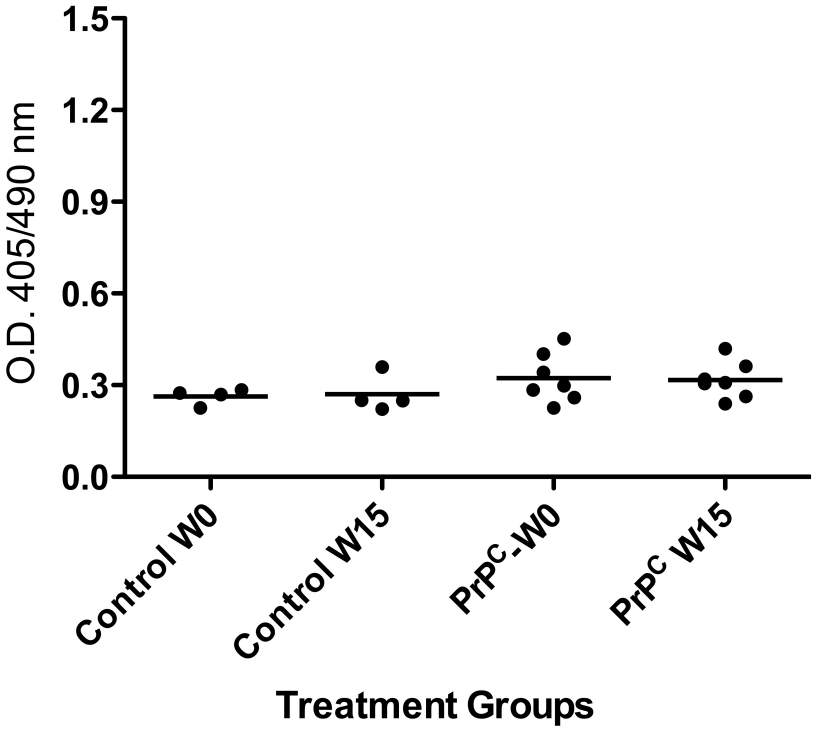

Figure 3.44: Antibodies to Lkt-PrP^C do not break tolerance against recombinant PrP^C. Scrapie-susceptible sheep (genotype ARQ) were immunized three times with either Lkt carrier (Control; n = 4) or Lkt-PrP^C (PrP^C; n = 7) at six week intervals. PrP^C-specific antibody titers were determined by ELISA using recombinant PrP^C protein. Pre-immune serum (W0) and serum collected 2 weeks after the third immunization (W15) were screened at a final dilution of 1/10. No PrP^C-specific cross-reactivity was detected.

3.15 Effectiveness of Maternal Ab Protection Following Oral Scrapie Challenge in Newborn Lambs.

A key application of this work is the ability to produce an antibody response capable of delaying the onset of Scrapie symptoms following exposure to PrP^{Sc}. Part way through this project, we had the opportunity to collaborate with a group of Scrapie immunologists in Norway (Drs. Martha Ulvund, Charles Press and Arild Espenes) affiliated with the Norwegian School of Veterinary Science. They have developed an aggressive method of experimental Scrapie inoculation which produces symptoms within a four month period. Their model is able to achieve symptoms so quickly because they inoculate the lambs as newborns. It is in the first 9 months of life, during development of the gut associated lymphoid tissue, that sheep are most susceptible to Scrapie infection (St Rose *et al.*, 2006). Throughout this period of development, the ileal Peyer's patch possesses an extensive bed of follicular dendritic cells and specialized epithelial which are actively engaged in the uptake and transcytosis of macromolecules from the gut (Heggebo *et al.*, 2000), thus efficiently facilitating the uptake of Scrapie particles.

At the time when this collaboration was established, the most effective vaccine epitope tested was Lkt-β2(2+YYR+2)I. To assess the effectiveness of Abs stimulated by this construct pregnant ewes were vaccinated with either Lkt-β2(2+YYR+2)I or just Lkt at 6 and 3 weeks prior to delivery. At birth, the lambs were immediately taken (before receiving their first colostrum feed) and inoculated with a 1 g suspension of infectious Scrapie material via a feeding tube. The lambs were returned to their mother and sibling(s) and monitored via 24 h video surveillance for signs of infection which is indicated by spontaneous scratching of the head, tail root, back, flanks and feet (Ersdal *et al.*, 2005).

The Lkt control group (n=4) were the first to demonstrate signs of illness, with two sheep presenting at 103 days post infection and the remaining two at 132 days [**Figure 3.45**]. In the Lkt-β2(2+YYR+2)I vaccinated group (n=3) two sheep became ill at 138 days and the third at 139 days [**Figure 3.45**]. Despite the small sample size, a comparison of the median onset of symptoms 117.5 day for the Lkt control group and 138 days for the vaccinated group demonstrated a statistically significant ($p < 0.019$) delay in symptoms for the vaccinated group. This suggested that the maternal IgG antibodies produced, in the Lkt-β2(2+YYR+2)I

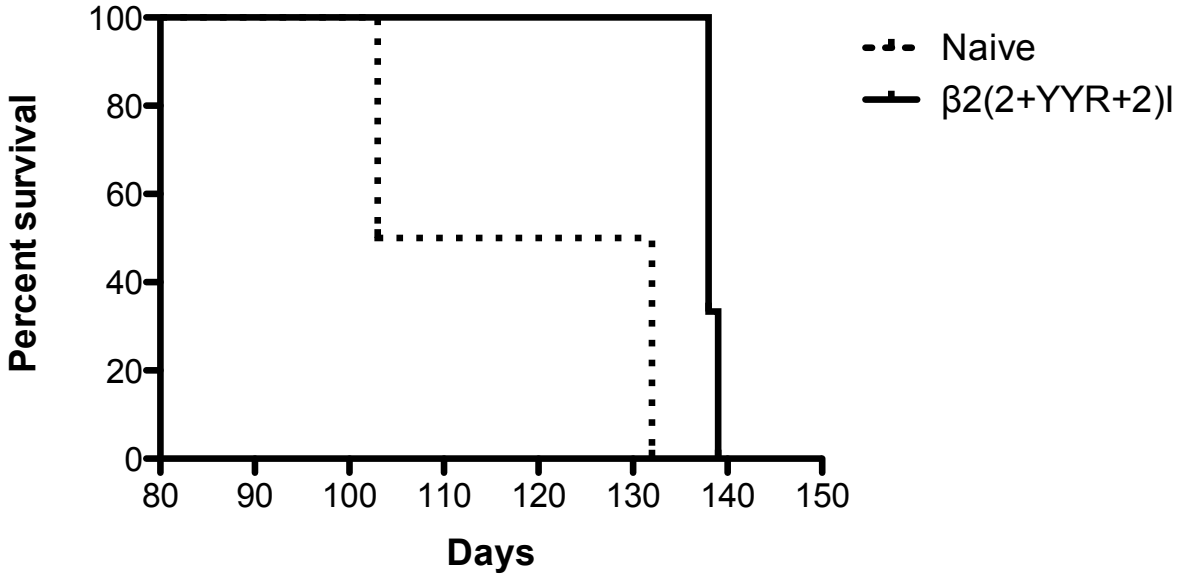

Figure 3.45: Symptoms onset following oral Scrapie challenge of newborn labs while nursing from mothers vaccinated with either Lkt or Lkt-β2(2+YYR+2)I. Two Pregnant ewes were vaccinated with Lkt and two with Lkt-β2(2+YYR+2)I. Vaccines were formulated with Emulsigen-D and administered SC at 6 and 4 weeks prior to delivery of their lambs. At birth, and prior to the first feeding, all lambs were inoculated with a 4 mL PBS suspension containing 1 g of Scrapie infected brain material, administered using a stomach tube. Lambs were continuously monitored via 24 h video surveillance for the onset of Scrapie symptoms.

vaccinated sheep, were transferred passively to the nursing lambs and interfered with the uptake of PrP^{Sc} material. This resulted in a delay of disease onset.

4.0 DISCUSSION

4.1 LKT as a Carrier Molecule

Prion diseases provide unique challenges for the development of immunotherapeutic strategies. Typical infectious agents are composed almost exclusively of biomolecules which are foreign to the body and presents developers of therapeutic agents or vaccines with a broad range of potential targets. Successful progression of prion disease is completely reliant on the presence of a ubiquitously expressed protein for which the body has developed significant immunological anergy or tolerance (Griffin and Cashman, 2005). Because the major pathogenic agent is a misfolded endogenous protein, researchers have been unable to detect PrP^{Sc}-specific immune responses at any point during disease manifestation (Bockman and Kingsbury, 1988). It has been suggested that PrP^{Sc} is too similar (immunogenically) to PrP^{C} and that tolerance mechanisms suppress an immune response, or alternatively that PrP^{Sc} is present all the time at concentrations too low to stimulate disease but high enough to establish self-tolerance (Muller-Schiffmann and Korth, 2008). This is in contrast to Alzheimer's disease research, which has shown successful immunization using the Aβ peptide in animal and human models (Orgogozo *et al.*, 2003; Schenk *et al.*, 1999), indicating that epitopes of oligomeric or multimeric Aβ are indeed immunogenic.

Immunotherapeutic strategies using full-length PrP^{C} have had limited success and generate legitimate concerns regarding the potential consequences of circulating anti-PrP^{C} antibodies. Examples of such potential outcomes are: complement-dependent lysis of cells, autoimmunity, impairment of PrP^{C} function, apoptosis of neurons, inappropriate activation of cell signalling pathways, or suppression of T-cell activation of human lymphocytes (Cashman and Caughey, 2004).

More recent methodologies have enlisted the use of specific PrP peptide fragments to stimulate anti-PrP^{Sc} antibody responses. While this may appear to be a safer strategy, due to the reduced risk of producing anti-PrP^{C} related effects, poor immunogenicity remains a significant challenge. Efforts to enhance immunogenicity have included the experimentation with different adjuvants and carrier systems. Although numerous adjuvants have been investigated, few have been licensed for use in commercial vaccine formulations (Ertl and

Lanzavecchia, 2010). For this project, we utilized a commercially available veterinary adjuvant 'Emulsigen–D' which is an oil-in-water emulsion containing the additive dimethyldioctadecylammonium bromide (a known T-cell activator) for increased immunostimulation with weak antigens.

The main function of a hapten carrier system is to stimulate T helper cell activity which can interact with hapten-specific B-cells. This is achieved when hapten-specific B-cells take up the entire protein complex and present T-cell epitopes from the carrier protein, in the context of major histocompatibility complex II molecules (Potter and Manns, 2000). To facilitate the immunogenic presentation of PrP peptides produced here, a Lkt carrier system was adapted. The Lkt carrier has previously been used to deliver self-peptide hormones such as GnRH to a variety of species (Robbins *et al.*, 2004). It was hypothesized that this system may be sufficiently immunogenic to effectively break PrP tolerance and stimulate an anti-PrP antibody response.

To validate this system a comparison was first made between the Lkt chimeric protein and the peptide chemically conjugated to the KLH delivery system. While this clearly was not an exhaustive analysis of all available carriers, based on literature searches, KLH was one of the most widely used carrier molecules in prion research. The results in mice supported the hypothesis that Lkt was a more immunogenic carrier system than KLH. The 10 μg Lkt construct was significantly more immunogenic than the 100 μg KLH model and also produced more consistent responses within the group of vaccinated mice. We also observed a dose-dependent carrier activity with Lkt, a trait that may actually prove challenging when designing a delivery strategy for wild animals. While trying to deliver a specific dose of prion vaccine orally in the wild is outside the objectives of this project, it is worth being aware of potential downstream complications in vaccine development. An initial strategy for addressing such a challenge might be drawn from research done in the 1980's which demonstrated the successful delivery of an oral rabies vaccine to wild fox populations (Engel, 1986). They used modified live rabies virus which they injected into a sponge, coated it with wax and placed in plastic pouches containing bait. The pouches could then be dropped by low-flying airplanes in areas where rabies was endemic. Because an oral PrP vaccine delivery system is likely the most feasible method of delivery for wild animal populations, it is likely that a different carrier or expression model will need to be adapted in the future. For the purposes of this study where we

are more interested in studying the characteristics of different PrP epitopes, the Lkt carrier system is perfectly suitable.

The dose dependent nature of Lkt carrier activity was investigated in both mice and sheep. As further experiments were conducted, using optimized vaccine formulations for each animal model, it became apparent that the Lkt constructs were between 3 and 6-fold more immunogenic in sheep than in mice. Although not directly investigated, one could rationalise this difference based on the knowledge that Lkt is derived from a common ruminant pathogen *P. haemolytica* (Poulsen *et al.*, 2006) and therefore may more efficiently induce an immunological response. As an example of the prevalence of pre-experimental exposure to *P. haemolytica* we screened 35 sheep at day 0 for Lkt peptide-specific titers and found that all 35 animals displayed titers ranging from 5000 to 270,000 (data not shown). It is possible that recognition of the PrP peptides is influenced by the pre-existing T-cell repertoire in each host species.

4.2 Significance of Epitope Design and Orientation on Immunogenicity

Although there has been no detectable immune response to either natural or experimental prion infection (Bockman and Kingsbury, 1988), extensive research has investigated the potential of PrP^{C} in its entirety or as smaller fragments to stimulate antibody production. Souan *et al*. isolated residues 131-150 and 211-230, because those regions contained a MHC II binding motif, which are potential T-cell epitopes. They used these fragments to vaccinate mice and later observed high T-cell proliferation. They also split PrP^{C} into 20mer peptides and used them in murine immunogenicity studies. Results showed that the regions containing the MHC II motif were again the most immunogenic, as were two other slightly less effective epitopes 31-50 and 151-170. They followed up with experiments which showed that antibodies to the 131-150 region cleared PrP^{Sc} in ScNa2 cells (Souan *et al.*, 2001). Another group created 30mer peptides and identified residues 143-172 and 156-187 as having strong T-cell proliferative effects in knock-out mice (Gregoire *et al.*, 2004). Regions extending from 145-190, encompassing the α-helix 1, β-strand 2 and α-helix 2 secondary structures, were able to stimulate both B-cell and T-cell proliferation in both PrP-knockout and wild-type mice (Muller-Schiffmann and Korth, 2008).

In a typical hapten-carrier system, the carrier molecule contains T-cell epitopes specific for a different protein than that to which the B-cell epitopes are derived. Although this combination of T and B-cell epitopes facilitates the induction of an antibody response, a limiting factor is the lack of a memory T-cell response to the protein containing the B-cell epitope. If, however, there are both T and B-cell epitopes on the hapten, as is suggested might be the case for the region encompassed by the β2(2+YYR+9)I construct (Muller-Schiffmann and Korth, 2008), then memory T-cells may be stimulated. This may help prolong the effectiveness of the vaccine by lengthening the interval of time required between booster immunizations. This would be especially beneficial for the immunization efforts in wild animal populations.

The PrP region which served as the starting point for this research was the YYR (amino acids 165-168) epitope located on the β-strand 2. It had been demonstrated previously that it was possible to generate antibodies to this region and that those antibodies were specific for the infectious PrP^{Sc} conformation (Paramithiotis *et al.*, 2003). The potential therapeutic value of this residue, however, was limited by poor immunogenicity. Using a vaccine delivery system unique to prion research, different epitope presentation methods, and epitope sequence manipulation, many vaccine constructs were created in an effort to increase the immunogenicity of the YYR epitope while maintaining its specificity for PrP^{Sc}.

As previously mentioned, an ideal vaccine epitope sequence would contain both a B and T-cell epitope to facilitate robust immune responses. In order to target a specific cryptic epitope on PrP, the sequence of the epitope being designed must directly represent the sequence at the cryptic region. In situations where multiple cryptic epitopes exist, the immunogenic potential of each may influence the decision regarding its inclusion/exclusion during vaccine design. Epitope design is further complicated by the lack of structural data for PrP^{Sc}. Although all of the expanded β-strand 2 constructs were significantly more immunogenic than the core YYR epitope [**Figure 3.26**], it was difficult to anticipate the effect of additional amino acid residues. For example, the asymmetrical expansion β2(2+YYR+9)I, which according to PrP^{C} structural modelling studies extends outside of the cryptic region to a surface-exposed area (DeMarco *et al.*, 2006), was designed to induce PrP^{C} antibodies. Interestingly, not only was it the most immunogenic construct, but it also retained PrP^{Sc} specificity. Perhaps such sequences need to lose structure in addition to being surface exposed for there to be a loss in specificity.

Upon dissecting the β2(2+YYR+9)I epitope by single amino acid residues, it was demonstrated that expanding the β2(2+YYR+2)I and β2(2+YYR+4)I epitopes by one amino acid produced a 48-fold increase and 62-fold decrease in immunogenicity, respectively [**Figure 3.38**]. This provided evidence that subtle changes in epitope sequence can have a marked effect on immunogenicity, a characteristic also observed in anti-cancer peptide vaccine development (Lazoura and Apostolopoulos, 2005). It is likely that the differing chemical and physical properties of individual amino acid's such as hydophobicity/hydrophilicity, positive or negative charge, presence/absence of bulky side-chains, influence the affinity between the epitope and B-cell receptor. The addition of an amino acid which improves the epitope/receptor affinity increases the strength of stimulating signal received by the immune cell, resulting in a more robust immune response (Partidos *et al.*, 1992).

Peptide presentation likely plays an important role in the stimulation of an immune response to a given epitope. Several groups have reported that creating tandem peptide repeats induced antigen processing more efficiently, resulting in stronger immunogenicity and increased production of neutralising antibodies (Meloen *et al.*, 1994; Qi *et al.*, 2009; Silva-Flannery *et al.*, 2009). Epitope presentations in this work consisted of either linear or inverted tandem repeats. Inverted repeats were initially used in order to replicate the YYR epitope presentation used in the paper by Paramithiotis *et al* (2003). They hypothesized that binding of the YYR mAb is dependent on the terminal arginine residue. Consequently, the CYYRRYYRYY sequence was used because arginine flanks the PrP bi-tyrosine motif at both the N and C-terminus (Paramithiotis *et al.*, 2003). As we expanded the epitopes and maintained the inverted formula, the original rationale was no longer applicable [**Figure 4.1a**]. Comparisons of linear vs. inverted orientation for β2(1+YYR+1), β2(2+YYR+2), and β2(3+YYR+1) epitopes demonstrated that the inverted presentations were equal to or significantly more immunogenic than the linear version. Consequently, follow-up constructs were designed primarily in the inverted form.

A possible explanation for the increased immunogenicity of the inverted constructs [using β2(2+YYR+9) as an example] may have to do with a longer consecutive sequence of hydrophilic amino acids (8) versus the linear construct (5) [**Figure 4.1b**]. Because B-cell

a)

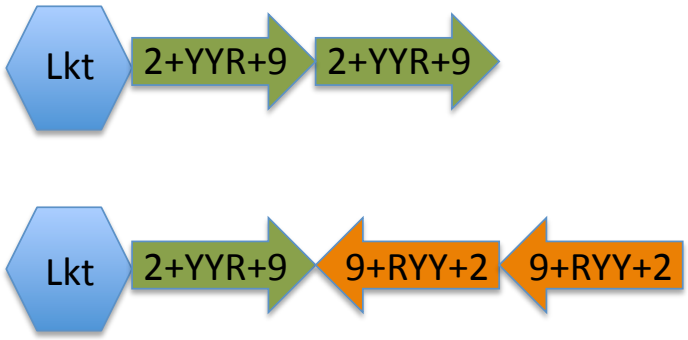

b)

Figure 4.1: Illustration of linear vs. inverted epitope presentation. a) The top construct demonstrates the linear version containing two repeated epitopes in the same forward orientation. The bottom construct demonstrates the inverted version where there is one epitope in the forward orientation followed by two epitopes which are identical to the first except for their backwards orientation. b) The top β2(2+YYR+9) sequence represents the amino acids present in the linear construct while the bottom is the sequence of the inverted construct. The red letters indicate hydrophilic amino acid residues.

epitopes are generally composed of hydrophilic amino acids (Kindt *et al.*, 2007), the inverted presentation may be more efficient in stimulating an epitope-specific B-cell response. Analyzing the linear and inverted epitope using Bepipred Linear Epitope Prediction software suggests that the linear construct contains one B-cell epitope at amino acid 7-22 while the inverted construct contains the same B-cell epitope at position 7-22 and an additional one at 27-36 (Larsen *et al.*, 2006). It may be that the later epitope is more immunogenic than the shared one or that the ELISA detects the additive effect of two different B-cell clones, one producing Ab to the linear epitope and another for the unique inverted epitope. Because the peptide used in the ELISA contains both sequences, it is possible that if the two different Abs do not interfere with each others binding, their additive effect produces a stronger signal.

Antibodies typically recognize either sequential or discontinuous/conformational epitopes. Sequential epitopes represent a linear sequence of amino acids which are correlated to a protein's primary structure. Discontinuous epitopes are composed of amino acid residues from different parts of the sequence which are brought together by folding of the protein into its native conformation. It is suggested that the conformational epitopes make up 90% of the total epitope repertoire recognized by antibodies (Barlow *et al.*, 1986). Because the peptide sequences generated for this research project ranged in length, it is likely that the Ab epitopes also varied between linear and conformational. It would be of interest to evaluate the strongly and weakly immunogenic constructs [eg. anti-β2(2+YYR+9)I and β2(YYR1)L)] to determine whether the epitopes of the induced antibodies are sequential or conformational. Because the transformation from PrP^{C} to PrP^{Sc} requires a conformational shift, it would make sense that the most effective antibodies are recognizing a conformationally specific sequence.

The quantity of specific Ab induced by an epitope following vaccination directly influences the amount of Ab which accumulates in relevant body compartments such as mucosal surfaces and CSF. Due to the small molecular size of IgG (150 kilodaltons), it easily diffuses out of the blood and into neighbouring tissues (Janeway *et al.*, 2001). Diffusion to the CNS is limited, however, by the blood-brain barrier which prevents most molecules greater than 400 daltons from passing through (Boado *et al.*, 2010). We evaluated the serum, mucosal and CNS titers from 5 animals vaccinated with the β2(2+YYR+9)I epitope. In each animal, the titers were greatest in the serum and lowest in the CNS, with an overall positive correlation between serum and CSF titers [**Figure 3.40**]. Because such a small fraction of the serum Ab

enters the CNS, achieving high body titers for as long as possible is essential and may be confounded by the presence of peripheral amyloid deposits which can act as Ab sponges (Kokjohn and Roher, 2009). There is a lack of data, however, defining what antibody titer would be sufficient for protection. Making comparisons of Ab magnitude between different researchers is difficult because there is no standardized method of presenting Ab levels. Some groups report Ab levels as ELISA optical densities at varying serum concentrations, others report Ab levels in μg/mL, while a third method assigns the Ab quantities a titer value.

An Alzheimer's immunotherapy study reported by Hu *et al*. (2008) may help provide some perspective for our results. Using an AD transgenic mouse model which develops disease at 6 months, the authors vaccinated mice with one of three different peptides, $A\beta_{1\text{-}15}$, $A\beta_{36\text{-}42}$ and $A\beta_{42}$ at 5 months of age. The initial vaccination consisted of 10-16 subcutaneous injections on the back of each mouse followed by weekly boosts beginning at seven months using an inhaled vaccine administered into the nostrils. The titers for all groups peaked at 210 days with median values of 9,600 ($A\beta_{1\text{-}15}$), 7,771 ($A\beta_{36\text{-}42}$) and 12,000 ($A\beta_{42}$) (Hu *et al.*, 2008). Clinical outcome was assessed by grading the performance of the mice in a water maze as well as post-mortem histological examination of the brains. All three vaccinated groups displayed performance improvements over the non-vaccinated control group, however the $A\beta_{1\text{-}15}$ and $A\beta_{42}$ were superior in their ability to prevent senile plaque formation which coincided with better cognitive function (Hu *et al.*, 2008). In comparison, our most immunogenic construct [β2(2+YYR+9)] achieved median titers of 63,000 in mice [**Figure 3.28**] and 100,000 in sheep [**Figure 3.25**]. While there are pathophysiologic differences between Alzheimer's and prion diseases, the results reported by Hu *et al*. suggest that our construct may be immunogenically adequate.

While titer magnitude is an important criteria for assessing potential epitopes, the Ab isotype also has implications for the ability of a humoral immune response to protect against prion disease. Although there are five different isotypes of antibodies present in the body (IgA, IgM, IgG, IgE and IgD) IgA and IgG are the most relevant for this discussion. Despite IgA representing 10-15% of the circulating immunoglobulin in serum, it is the primary form present in secretions such as tears, saliva, milk and mucus from the digestive, genitourinary and bronchial tracts (Kindt *et al.*, 2007). Production of secretory IgA by plasma cells lining the mucosal membranes can reach as high as 15 g per day in humans, more than any other isotype.

Because prion diseases are transmitted primarily by the oral route in animals (Beekes and McBride, 2007), the ability to neutralise PrP^{Sc} in the gut mucosa may play an important role in delaying disease onset (Goni *et al.*, 2005).

The other relevant class of Ab is IgG which represents 80% of the total serum immunoglobulin. This class can be further divided into 4 subtypes IgG1, IgG2, IgG3 and IgG4. IgG1 and IgG3 have the greatest affinity for Fc receptors on phagocytic cells, and are better complement activators in comparison to the other two. Also, IgG1 and IgG3 are the only immunoglobulins able to cross the placenta and therefore play a role in protecting the human fetus (Kindt *et al.*, 2007). The production of PrP-specific IgG Abs has been shown by several laboratories to be effective in delaying symptoms for peripheral Scrapie infections in mice (Goni *et al.*, 2008; Pilon *et al.*, 2007).

To better characterise the immune responses to our YYR based epitopes we conducted isotype specific ELISAs on serum from animals vaccinated with the different constructs. Regardless of the epitope used, all of the antibodies produced were predominantly IgG1 [**Figure 3.41**]. Immunization studies in AD demonstrated that IgG1 antibodies had stronger affinity for Aβ plaques but were less efficient at clearing plaques than IgG2a antibodies (Bard *et al.*, 2003). Should the same be true for prion disease, an IgG1 dominant response with high affinity for PrP^{Sc} amyloid would be advantageous for the neutralization of infectious particles and prevention of PrP isoform conversion. Although creating antibodies to clear plaques seems like an ideal strategy in neurodegenerative disease, AD research has produced conflicting results. For example, one study demonstrated a decline in plaque burden was accompanied by increased cognitive function (Janus *et al.*, 2000), whereas, a contrasting study described patients displaying cognitive improvements following vaccination without a corresponding clearance of amyloid plaques (Dodart *et al.*, 2002). Consequently, with uncertainty surrounding the relationship between amyloid accumulation and clinical symptoms, the type of IgG Ab produced by our constructs seems suitable for our downstream therapeutic goals which include preventing: the uptake of orally ingested PrP^{Sc}, the transition from peripheral PrP^{Sc} amplification to neuroinvasion, and excretion of PrP^{Sc} into the environment.

4.3 Consequence of Epitope Selection on Specificity

The identification of a cryptic epitope on PrP^{C} which becomes exposed when refolded into the infectious conformation presents an opportunity for targeted immunotherapy (Paramithiotis *et al.*, 2003). It has been suggested that stimulation of PrP^{Sc}-specific antibodies may lead to destruction and uptake of infectious particles by tingible body macrophages prior to the development of protease resistance in PrP^{Sc}. Isoform specific antibodies may also disrupt the interaction between PrP^{C} and PrP^{Sc}, thus preventing template-based misfolding of PrP^{C}. Experiments have shown that isoform conversion occurs close to or at the cell surface, indicating the potential for antibody-PrP^{Sc} interaction (Borchelt *et al.*, 1990; Caughey and Raymond, 1991). Successful interruption in the isoform conversion process would suggest that immunoprophylaxis for the prevention of disease onset in PrP^{Sc} exposed animals may be possible. In animals already infected, the presence of PrP^{Sc}-specific antibodies may slow disease progression and prevent/reduce the shedding of infectious prion material into the environment, thereby disrupting its natural transmission cycle. The epitopes designed for this project utilized prion amino acid sequences which are highly conserved across relevant species such as mice, cattle, deer, elk and humans. Consequently, an effective epitope may have a protective application across multiple species once vaccine dose and formulation have been optimized. Subtle species differences do exist however. For example at residue 174 Elk, Mule deer and Whitetail deer have asparagine while other species including sheep, mice and human, have a serine residue. This difference may influence peptide immunogenicity. Should a single amino acid difference be shown to negatively affect immunogenicity, then it would be possible to customize epitope composition for each target species.

Designing an epitope with the ability to induce antibodies discriminating between one prion isoform and another was an integral objective of this research. As is the case for most TSEs, where aggregation of the misfolded proteins makes structural analysis impossible, predictions of epitope architecture on the PrP^{Sc} molecule are challenging. In the absence of such data, decisions can be made based on biophysical models of protein misfolding (as was done for this project), simulations of different patterns of exposure, panels of randomly selected epitopes and computer modeling. Because modeling cannot accurately anticipate *in vivo*

scenarios, antibodies produced by each construct must be screened using ELISA and immunoprecipitation experiments to determine antibody specificity for either PrP^{C} or PrP^{Sc}.

The YY motif present on α-helix 1 was also shown to be surface-exposed upon conversion from PrP to PrP^{Sc} (Paramithiotis *et al.*, 2003). Although only briefly examined in this thesis work, many researchers have suggested that because this region is thought to have a key role in the conversion process, it is an ideal target for immunotherapy. The mAb 6H4, specific for amino acids 144-52 (in the bovine sequence) was able to protect against Scrapie infection in both Scrapie susceptible cells N2a and transgenic mice expressing a fragment antigen-binding region of 6H4 (Enari *et al.*, 2001; Heppner *et al.*, 2001). Interestingly, our results following vaccination with α1(2+YYR+2)I demonstrated both weak immunogenicity [**Figure 3.39**] and in one animal no PrP^{Sc}-specificity [**Figure 3.42**]. Because mAb 6H4 binds to both the infectious and cellular versions of PrP and overlaps with the α1(2+YYR+2)I epitope, is was not surprising that one animal produced an immune response lacking conformational specificity. Also in the same region, just 2 amino acids closer to the N-teminus, an Ab called 15B3-1 was described that, in contrast to the previous two epitopes, is PrP^{Sc}-specific (Korth *et al.*, 1997). A comparison of these neighbouring/overlapping α-helix 1 epitopes suggest that subtle changes in amino acid composition can have a marked effect on specificity [**Figure 4.2**].

While the specificity of an antibody response is significant from a prion immunotherapeutic perspective, there are also important implications for use in disease detection. Current diagnosis involves post-mortem analysis of brain and lymphoid tissues using immunohistochemistry or an ELISA to detect the PrP^{Sc} isoform. While these tests are accurate, there is a great need for a reliable pre-mortem diagnostic tools. The ability to diagnose prion disease from samples such as CSF, blood or urine would be ideal, but has proven challenging due to the low levels of PrP^{Sc} present in the different fluids of infected animals and the inability of current diagnostic antibodies to differentiate between PrP^{C} and PrP^{Sc} (Herbst *et al.*, 2009). The identification of an epitope [β2(2+YYR+9)I] which is not only immunogenic but PrP^{Sc}-specific, allows for its potential application as an immunotherapeutic agent as well as a diagnostic tool.

An example of a potential diagnostic application for PrP^{Sc}-specific Abs has been demonstrated by Madampage *et al.* (2010). They have utilized nanopore technology consisting

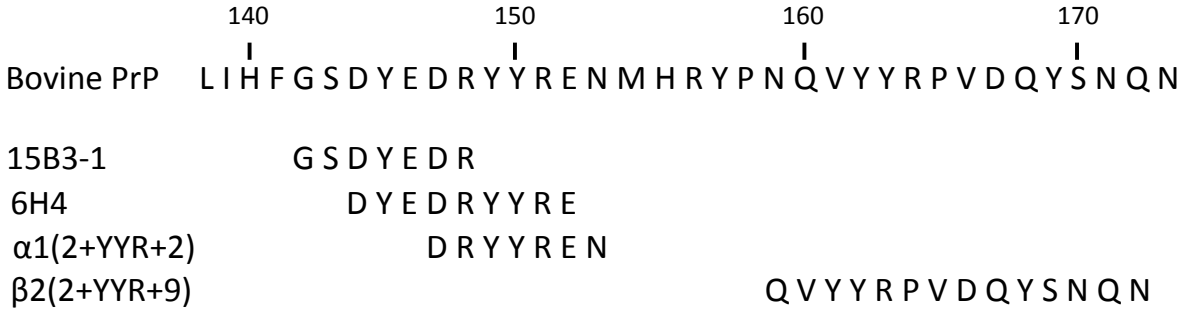

Figure 4.2: The portion of the α-helix 1 and β-strand 2 from Bovine PrP illustrating the location of the 15B3-1, 6H4, α1(2+YYR+2) and β2(2+YYR+9) epitopes in relation to each other. Only the 15B3-1 and β2(2+YYR+9) epitopes are specific for the PrP^{Sc} conformation.

of a lipid bilayer that creates a membrane barrier between two chambers filled with buffer and the toxin α-hemolysin which inserts into the membrane creating a channel. By passing a charge across the channel they can monitor the current created by ions as they pass through. If a large molecule is in close proximity to the channel or passes through it, characteristic changes in the current are detectable and are defined as "bumping" and "translocation" events, respectively (Madampage *et al.*, 2010). They demonstrated that PrP^{C} can pass through the channel despite the presence of α-helices, β-hairpins and disulphide bonds. The addition of Ab specific for a portion of the PrP molecule, when bound, prevents the translocation of PrP through the channel (Madampage *et al.*, 2010). Because structural elements of PrP are maintained in this type of analysis, conformation-specific Abs may be able to detect PrP^{Sc} at pre-clinical levels from pre-mortem serum, saliva, milk or urine samples allowing time for appropriate intervention.

4.4 Peptide Vaccination followed by *In Vivo* Scrapie Challenge

Although demonstrating immunogenicity and specificity are critical variables in the development of a prion vaccine, they become irrelevant (from a public health perspective) if there is no impact on parameters such as disease transmission, onset of symptoms or disease progression. Given the physiological nature of PrP^{Sc}, challenge trials require special level three facilities and elaborate decontamination protocols, making experiments in large species like sheep, cattle and deer costly and labour intensive. Despite this, these type of trials are essential for evaluating the therapeutic potential of constructs that have been shown to be both immunogenic and PrP^{Sc}-specific in vaccination trials.

Although the challenge experiment conducted in Norway was limited by sample size, it provided critical information necessary for the planning of future experiments. Most importantly, the results demonstrated that our YYR-based vaccine was able to delay the onset of symptoms in all three vaccinated animals. While the results were statistically significant, one may question whether a median 20 day delay of symptoms would have any detectable impact in a population of animals. It should be noted, however, that the epitope used in this particular experiment has since been altered through selective amino acid expansion [(β2(2+YYR+9)I] to achieve significant improvements in immunogenicity. As it has been

previously demonstrated that the magnitude of Ab response has a direct relationship to the level of protection provided (Goni *et al.*, 2008; Sigurdsson *et al.*, 2002), this new expanded epitope may achieve a better level of protection than the one originally tested.

Important information that would complement the results of this trial would be the Ab titers from the pregnant ewe's serum and colostrum at the time of delivery, as well as serum IgG and gut IgA Ab titers from the lambs a few days after delivery to determine the degree of maternal transfer. This would help in understanding the relationship between titer magnitude and delay in symptom onset. Immunohistochemistry analysis of gut lymphoid tissue as well as representative CNS material would facilitate a comparison of PrP^{Sc} accumulation between the vaccinated and non-vaccinated groups. It would also be of interest to monitor urine and excrement to see if vaccination has any impact on prion shedding during infection. Shedding of infectious material has a significant impact on both the spread of disease between members of a herd but also has implications on land use. Because PrP^{Sc} can survive for extended periods of time in the soil, contaminated land can be unusable for grazing purposes for as long as 16 years (Georgsson *et al.*, 2006).

4.5 Peptide-based vaccines in cancer immunotherapy

The development of cancer cells is a complicated process and is thought to be initiated by two different mechanisms: viral infection (eg. human T-cell lymphotropic virus and Epstein-Barr virus have been linked to T-cell leukemia and Burkitt's lymphoma respectively); and genetic mutations attributed to environmental insults (Lazoura and Apostolopoulos, 2005). The majority of tumor antigens identified (eg. Her2/neu, and MAGE2/3) are expressed on both normal and cancer cells, however the expression levels are much higher on the cancer cells. Because self-peptides are the target of cancer immunotherapeutic strategies, the induced immune responses can potentially initiate unwanted autoimmune reactions, as is the case for prion vaccines (Lazoura and Apostolopoulos, 2005).

The branch of the immune system most involved in the eradication of tumor cells are the cytotoxic T-cell lymphocytes (CTLs). Initially researchers focused on attaining high affinity T-cell epitopes derived from tumor associated antigens believing that these would be the most successful in producing a robust CTL response. However, *In vivo* studies indicated

these epitopes were ineffective because T-cells recognizing high affinity epitopes had been eliminated/silenced by host tolerance mechanisms. As a result lower affinity epitopes produced more effective immune responses (Lazoura and Apostolopoulos, 2005). The major complication arising from this discovery was that low affinity epitopes are much more difficult to screen for due to their inherently weak immunogenicity.

A surprising link between PrP^{Sc}-specific antibodies and cancer cells was made by Cashman *et al* in 2010. They discovered that prion proteins are misfolded on the surface of certain cancer cells, suggesting that there may be potential for prion antibodies to aid in treatment of cancer (http://www.vchri.ca/s/NewsReleases.asp?ReportID=410543). The idea of specifically targeting cancer cells without the toxic side effects produced by many commonly used chemotherapeutic agents is highly attractive.

5.0 CONCLUSIONS

Research done as a component of this thesis project, identified a highly immunogenic cryptic PrP epitope which produces PrP^{Sc}-specific titers in the serum, mucosal surfaces and CSF, a requirement which may be critical for successful immunotherapy. Endogenous peptides are inherently difficult to vaccinate against due to tolerance and the potential repercussions of an improper immune response resulting in autoimmunity. While there does not seem to be a straight forward methodology that can be used for developing a vaccine to endogenous proteins, a few key concepts have been identified. First, knowledge of protein structure helps to identify regions of the self protein that make suitable targets for an immune response. Experiments which demonstrated that bi-tyrosine motifs are exposed during the misfolding of the prion protein provided a starting point for this project. However, because there is an incomplete understanding of the PrP^{Sc} structure, anticipating which amino acid expansions would increase immunogenicity and yet retain specificity was challenging. This problem may be unique to misfolding diseases which involve protein aggregation, because determining crystal structure is not possible unless single protein molecules can be isolated.

Second, with the abundance of bioinformatic tools available, it may seem logical to analyse the prion protein amino acid sequence and use whatever antigenic epitope predictions are calculated in the vaccine. These programs operate on the logic that the most antigenic regions of a protein are surface exposed residues and predict these regions using parameters such as hydrophilicity, accessibility and flexibility (Kolaskar and Tongaonkar, 1990). This approach makes sense for proteins foreign to the immune system. For endogenous proteins, however, it is precisely these predicted surface exposed residues that are likely to invoke the strongest tolerance. Furthermore, in misfolding diseases, the epitope prediction software cannot predict what residues would be exposed in the disease conformation because its calculations are based on the amino acid sequence which is identical for PrP^{C} and PrP^{Sc}. Consequently single amino acid manipulations, once a general epitope of interest has been identified, seems to be the most effective way to optimize an epitope for immunogenicity and specificity.

Finally, the true therapeutic value of a vaccine construct can only be determined following extensive *in vivo* challenge experimentation. Regarding the epitope identified in this

work, factors such as symptom progression, prion shedding, and time of death as a result of prion disease challenge must be evaluated. While these experiments have begun in sheep, trials will eventually have to be carried out in the target species of interest, such as cervids. Building on the results from the Norway challenge trial, a new *in vivo* sheep challenge study has begun. Animals received vaccinations with the [β2(2+YYR+9)I] construct followed by an oral Scrapie challenge. Key parameters to be followed are the length of peripheral amplification, duration/severity of CNS symptoms and overall lifespan of the infected animals. Success of the vaccine would be defined as a statistically significant delay in mortality of the experimental groups compared to controls and it would need to be established what the mechanism of this delay was. Is the production of PrP^{Sc}-specific antibodies interfering with key pathological processes like prion uptake in the gastrointestinal tract, peripheral amplification, progression to the CNS or the mechanism of CNS toxicity? Other important future studies should examine methods of vaccination. Because wild cervids are the most common prion infected species in Alberta and Saskatchewan, vaccination administration would have to be capable of reaching these populations, likely as an oral formulation. Dose titrations would need to be conducted in both deer and elk as it appears that Lkt behaves in a dose-dependent manner. Because the PrP amino acid sequence in cervids differs by a few residues from the sheep sequences used in this project, creating "cervidized" constructs may further enhance immunogenicity and should be evaluated.

Despite the considerable factors that still need addressing, this work outlines the important considerations for stimulating immune responses specific for misfolded prion protein. Strategies identified here may be relevant in the search for immunotherapeutic vaccines against other protein misfolding diseases such as Alzheimer's, ALS, Huntington's, and Parkinson's Disease.

6.0 REFERENCES

Adelstein, S., Pritchard-Briscoe, H., Anderson, T.A., Crosbie, J., Gammon, G., Loblay, R.H., Basten, A., and Goodnow, C.C. (1991). Induction of self-tolerance in T cells but not B cells of transgenic mice expressing little self antigen. Science *251*, 1223-1225.

Aguzzi, A. (2006). Prion diseases of humans and farm animals: epidemiology, genetics, and pathogenesis. J Neurochem *97*, 1726-1739.

Aguzzi, A., Baumann, F., and Bremer, J. (2008a). The prion's elusive reason for being. Annu Rev Neurosci *31*, 439-477.

Aguzzi, A., and Calella, A.M. (2009). Prions: protein aggregation and infectious diseases. Physiol Rev *89*, 1105-1152.

Aguzzi, A., and Heikenwalder, M. (2006). Pathogenesis of prion diseases: current status and future outlook. Nat Rev Microbiol *4*, 765-775.

Aguzzi, A., Heikenwalder, M., and Polymenidou, M. (2007). Insights into prion strains and neurotoxicity. Nat Rev Mol Cell Biol *8*, 552-561.

Aguzzi, A., and Heppner, F.L. (2000). Pathogenesis of prion diseases: a progress report. Cell Death Differ *7*, 889-902.

Aguzzi, A., and Polymenidou, M. (2004). Mammalian prion biology: one century of evolving concepts. Cell *116*, 313-327.

Aguzzi, A., Sigurdson, C., and Heikenwaelder, M. (2008b). Molecular mechanisms of prion pathogenesis. Annu Rev Pathol *3*, 11-40.

Alonso, D.O., An, C., and Daggett, V. (2002). Simulations of biomolecules: Characterization of the early steps in the pH-induced conformational conversion of the hamster, bovine and human forms of the prion protein. Philos Transact A Math Phys Eng Sci *360*, 1165-1178.

Andreoletti, O., Berthon, P., Marc, D., Sarradin, P., Grosclaude, J., van Keulen, L., Schelcher, F., Elsen, J.M., and Lantier, F. (2000). Early accumulation of PrP^{Sc} in gut-associated lymphoid and nervous tissues of susceptible sheep from a Romanov flock with natural scrapie. J Gen Virol *81*, 3115-3126.

Bard, F., Barbour, R., Cannon, C., Carretto, R., Fox, M., Games, D., Guido, T., Hoenow, K., Hu, K., Johnson-Wood, K.*, et al.* (2003). Epitope and isotype specificities of antibodies to beta -amyloid peptide for protection against Alzheimer's disease-like neuropathology. Proc Natl Acad Sci U S A *100*, 2023-2028.

Barlow, D.J., Edwards, M.S., and Thornton, J.M. (1986). Continuous and discontinuous protein antigenic determinants. Nature *322*, 747-748.

Baron, T., and Biacabe, A.G. (2006). Origin of bovine spongiform encephalopathy. Lancet *367*, 297-298; author reply 298-299.

Barrow, P.A., Holmgren, C.D., Tapper, A.J., and Jefferys, J.G. (1999). Intrinsic physiological and morphological properties of principal cells of the hippocampus and neocortex in hamsters infected with scrapie. Neurobiol Dis *6*, 406-423.

Bartz, J.C., Bessen, R.A., McKenzie, D., Marsh, R.F., and Aiken, J.M. (2000). Adaptation and selection of prion protein strain conformations following interspecies transmission of transmissible mink encephalopathy. J Virol *74*, 5542-5547.

Basler, K., Oesch, B., Scott, M., Westaway, D., Walchli, M., Groth, D.F., McKinley, M.P., Prusiner, S.B., and Weissmann, C. (1986). Scrapie and cellular PrP isoforms are encoded by the same chromosomal gene. Cell *46*, 417-428.

Beekes, M., and McBride, P.A. (2007). The spread of prions through the body in naturally acquired transmissible spongiform encephalopathies. FEBS J *274*, 588-605.

Beghi, E., Gandolfo, C., Ferrarese, C., Rizzuto, N., Poli, G., Tonini, M.C., Vita, G., Leone, M., Logroscino, G., Granieri, E.*, et al.* (2004). Bovine spongiform encephalopathy and Creutzfeldt-Jakob disease: facts and uncertainties underlying the causal link between animal and human diseases. Neurol Sci *25*, 122-129.

Belay, E.D., Maddox, R.A., Williams, E.S., Miller, M.W., Gambetti, P., and Schonberger, L.B. (2004). Chronic wasting disease and potential transmission to humans. Emerg Infect Dis *10*, 977-984.

Bessen, R.A., and Marsh, R.F. (1994). Distinct PrP properties suggest the molecular basis of strain variation in transmissible mink encephalopathy. J Virol *68*, 7859-7868.

Biacabe, A.G., Morignat, E., Vulin, J., Calavas, D., and Baron, T.G. (2008). Atypical bovine spongiform encephalopathies, France, 2001-2007. Emerg Infect Dis *14*, 298-300.

Boado, R.J., Lu, J.Z., Hui, E.K., and Pardridge, W.M. (2010). IgG-single chain Fv fusion protein therapeutic for Alzheimer's disease: Expression in CHO cells and pharmacokinetics and brain delivery in the rhesus monkey. Biotechnol Bioeng *105*, 627-635.

Bockman, J.M., and Kingsbury, D.T. (1988). Immunological analysis of host and agent effects on Creutzfeldt-Jakob disease and scrapie prion proteins. J Virol *62*, 3120-3127.

Borchelt, D.R., Scott, M., Taraboulos, A., Stahl, N., and Prusiner, S.B. (1990). Scrapie and cellular prion proteins differ in their kinetics of synthesis and topology in cultured cells. J Cell Biol *110*, 743-752.

Borchelt, D.R., Taraboulos, A., and Prusiner, S.B. (1992). Evidence for synthesis of scrapie prion proteins in the endocytic pathway. J Biol Chem *267*, 16188-16199.

Bosque, P.J., Ryou, C., Telling, G., Peretz, D., Legname, G., DeArmond, S.J., and Prusiner, S.B. (2002). Prions in skeletal muscle. Proc Natl Acad Sci U S A *99*, 3812-3817.

Bounhar, Y., Zhang, Y., Goodyer, C.G., and LeBlanc, A. (2001). Prion protein protects human neurons against Bax-mediated apoptosis. J Biol Chem *276*, 39145-39149.

Bouzamondo-Bernstein, E., Hopkins, S.D., Spilman, P., Uyehara-Lock, J., Deering, C., Safar, J., Prusiner, S.B., Ralston, H.J., 3rd, and DeArmond, S.J. (2004). The neurodegeneration sequence in prion diseases: evidence from functional, morphological and ultrastructural studies of the GABAergic system. J Neuropathol Exp Neurol *63*, 882-899.

Brown, D.R., Schmidt, B., Groschup, M.H., and Kretzschmar, H.A. (1998). Prion protein expression in muscle cells and toxicity of a prion protein fragment. Eur J Cell Biol *75*, 29-37.

Brown, D.R., Wong, B.S., Hafiz, F., Clive, C., Haswell, S.J., and Jones, I.M. (1999). Normal prion protein has an activity like that of superoxide dismutase. Biochem J *344 Pt 1*, 1-5.

Brown, H.R., Goller, N.L., Rudelli, R.D., Merz, G.S., Wolfe, G.C., Wisniewski, H.M., and Robakis, N.K. (1990). The mRNA encoding the scrapie agent protein is present in a variety of non-neuronal cells. Acta Neuropathol *80*, 1-6.

Brown, P., Preece, M., Brandel, J.P., Sato, T., McShane, L., Zerr, I., Fletcher, A., Will, R.G., Pocchiari, M., Cashman, N.R*., et al.* (2000). Iatrogenic Creutzfeldt-Jakob disease at the millennium. Neurology *55*, 1075-1081.

Browning, S.R., Mason, G.L., Seward, T., Green, M., Eliason, G.A., Mathiason, C., Miller, M.W., Williams, E.S., Hoover, E., and Telling, G.C. (2004). Transmission of prions from mule deer and elk with chronic wasting disease to transgenic mice expressing cervid PrP. J Virol *78*, 13345-13350.

Bruce, M., Chree, A., McConnell, I., Foster, J., Pearson, G., and Fraser, H. (1994). Transmission of bovine spongiform encephalopathy and scrapie to mice: strain variation and the species barrier. Philos Trans R Soc Lond B Biol Sci *343*, 405-411.

Bruijn, L.I., Miller, T.M., and Cleveland, D.W. (2004). Unraveling the mechanisms involved in motor neuron degeneration in ALS. Annu Rev Neurosci *27*, 723-749.

Brunswick, M., Finkelman, F.D., Highet, P.F., Inman, J.K., Dintzis, H.M., and Mond, J.J. (1988). Picogram quantities of anti-Ig antibodies coupled to dextran induce B cell proliferation. J Immunol *140*, 3364-3372.

Cappai, R., and Collins, S.J. (2004). Structural biology of prions. Contrib Microbiol *11*, 14-32.

Cardinale, A., Filesi, I., Vetrugno, V., Pocchiari, M., Sy, M.S., and Biocca, S. (2005). Trapping prion protein in the endoplasmic reticulum impairs PrP^{C} maturation and prevents PrP^{Sc} accumulation. J Biol Chem *280*, 685-694.

Cashman, N.R., and Caughey, B. (2004). Prion diseases--close to effective therapy? Nat Rev Drug Discov *3*, 874-884.

Caughey, B., Kocisko, D.A., Raymond, G.J., and Lansbury, P.T., Jr. (1995). Aggregates of scrapie-associated prion protein induce the cell-free conversion of protease-sensitive prion protein to the protease-resistant state. Chem Biol *2*, 807-817.

Caughey, B., and Raymond, G.J. (1991). The scrapie-associated form of PrP is made from a cell surface precursor that is both protease- and phospholipase-sensitive. J Biol Chem *266*, 18217-18223.

Chesebro, B., Trifilo, M., Race, R., Meade-White, K., Teng, C., LaCasse, R., Raymond, L., Favara, C., Baron, G., Priola, S.*, et al.* (2005). Anchorless prion protein results in infectious amyloid disease without clinical scrapie. Science *308*, 1435-1439.

Chiarini, L.B., Freitas, A.R., Zanata, S.M., Brentani, R.R., Martins, V.R., and Linden, R. (2002). Cellular prion protein transduces neuroprotective signals. Embo J *21*, 3317-3326.

Choi, S.I., Ju, W.K., Choi, E.K., Kim, J., Lea, H.Z., Carp, R.I., Wisniewski, H.M., and Kim, Y.S. (1998). Mitochondrial dysfunction induced by oxidative stress in the brains of hamsters infected with the 263 K scrapie agent. Acta Neuropathol *96*, 279-286.

Collee, G.J., Bradley, R., and Liberski, P.P. (2006). Variant CJD (vCJD) and bovine spongiform encephalopathy (BSE): 10 and 20 years on: part 2. Folia Neuropathologica *44*, 102-110.

Collinge, J. (1999). Variant Creutzfeldt-Jakob disease. Lancet *354*, 317-323.

Collinge, J. (2001). Prion diseases of humans and animals: their causes and molecular basis. Annu Rev Neurosci *24*, 519-550.

Collinge, J., and Clarke, A.R. (2007). A general model of prion strains and their pathogenicity. Science *318*, 930-936.

Collins, S.J., Lawson, V.A., and Masters, C.L. (2004). Transmissible spongiform encephalopathies. Lancet *363*, 51-61.

Comber, T. (1772). Real Improvements in Agriculture, First edn (London: Nicoll, W.).

Conway, K.A., Harper, J.D., and Lansbury, P.T. (1998). Accelerated in vitro fibril formation by a mutant alpha-synuclein linked to early-onset Parkinson disease. Nat Med *4*, 1318-1320.

Coulthart, M.B., and Cashman, N.R. (2001). Variant Creutzfeldt-Jakob disease: a summary of current scientific knowledge in relation to public health. Cmaj *165*, 51-58.

Creutzfeldt, H.G. (1989). On a particular focal disease of the central nervous system (preliminary communication), 1920. Alzheimer Dis Assoc Disord *3*, 3-25.

Criado, J.R., Sanchez-Alavez, M., Conti, B., Giacchino, J.L., Wills, D.N., Henriksen, S.J., Race, R., Manson, J.C., Chesebro, B., and Oldstone, M.B. (2005). Mice devoid of prion protein have cognitive deficits that are rescued by reconstitution of PrP in neurons. Neurobiol Dis *19*, 255-265.

Cuille, P., and Chelle, L. (1936). Pathologie animale - La malade dite tremblante du mouton est-elle inocuable? Comptes rendous hebdomadaires des seances de l'Acadamie des Sciences *203*, 1552-1554.

Cuille, P., and Chelle, L. (1938). Le tremblante du mouton est-elle determinee par un virus filtrable? Comptes rendous hebdomadaires des seances de l'Acadamie des Sciences *203*, 1687-1688.

Deleault, N.R., Harris, B.T., Rees, J.R., and Supattapone, S. (2007). Formation of native prions from minimal components in vitro. Proc Natl Acad Sci U S A *104*, 9741-9746.

DeMarco, M.L., Silveira, J., Caughey, B., and Daggett, V. (2006). Structural properties of prion protein protofibrils and fibrils: an experimental assessment of atomic models. Biochemistry *45*, 15573-15582.

Diarra-Mehrpour, M., Arrabal, S., Jalil, A., Pinson, X., Gaudin, C., Pietu, G., Pitaval, A., Ripoche, H., Eloit, M., Dormont, D., and Chouaib, S. (2004). Prion protein prevents human breast carcinoma cell line from tumor necrosis factor alpha-induced cell death. Cancer Res *64*, 719-727.

Dickinson, A.G., and Fraser, H. (1969). Genetical control of the concentration of ME7 scrapie agent in mouse spleen. J Comp Pathol *79*, 363-366.

Dodart, J.C., Bales, K.R., Gannon, K.S., Greene, S.J., DeMattos, R.B., Mathis, C., DeLong, C.A., Wu, S., Wu, X., Holtzman, D.M., and Paul, S.M. (2002). Immunization reverses memory deficits without reducing brain Abeta burden in Alzheimer's disease model. Nat Neurosci *5*, 452-457.

Donnelly, C.A., Ferguson, N.M., Ghani, A.C., and Anderson, R.M. (2002). Implications of BSE infection screening data for the scale of the British BSE epidemic and current European infection levels. Proc Biol Sci *269*, 2179-2190.

Dormont, D. (2003). Approaches to prophylaxis and therapy. Br Med Bull *66*, 281-292.

Duffy, P., Wolf, J., Collins, G., DeVoe, A.G., Streeten, B., and Cowen, D. (1974). Letter: Possible person-to-person transmission of Creutzfeldt-Jakob disease. N Engl J Med *290*, 692-693.

Editorial-team (2007). Fourth case of transfusion-associated vCJD infection in the United Kingdom. Euro Surveill *12*, E070118 070114.

El-Agnaf, O.M., Salem, S.A., Paleologou, K.E., Curran, M.D., Gibson, M.J., Court, J.A., Schlossmacher, M.G., and Allsop, D. (2006). Detection of oligomeric forms of alpha-synuclein protein in human plasma as a potential biomarker for Parkinson's disease. FASEB J *20*, 419-425.

Emadi, S., Kasturirangan, S., Wang, M.S., Schulz, P., and Sierks, M.R. (2009). Detecting morphologically distinct oligomeric forms of alpha-synuclein. J Biol Chem *284*, 11048-11058.

Enari, M., Flechsig, E., and Weissmann, C. (2001). Scrapie prion protein accumulation by scrapie-infected neuroblastoma cells abrogated by exposure to a prion protein antibody. Proc Natl Acad Sci U S A *98*, 9295-9299.

Engel, J. (1986). New vaccine delivery methods may turn tide against rabies. CMAJ *135*, 379-380.

Ersdal, C., Ulvund, M.J., Espenes, A., Benestad, S.L., Sarradin, P., and Landsverk, T. (2005). Mapping PrP^{Sc} propagation in experimental and natural scrapie in sheep with different PrP genotypes. Vet Pathol *42*, 258-274.

Ertl, H.C., and Lanzavecchia, A. (2010). Current Opinion in Immunology. Vaccines. Introduction. Curr Opin Immunol *22*, 355-357.

Everest, D.J., Waterhouse, S., Kelly, T., Velo-Rego, E., and Sauer, M.J. (2007). Effectiveness of capillary electrophoresis fluoroimmunoassay of blood Prp^{Sc} for evaluation of scrapie pathogenesis in sheep. J Vet Diagn Invest *19*, 552-557.

Falsig, J., Nilsson, K.P., Knowles, T.P., and Aguzzi, A. (2008). Chemical and biophysical insights into the propagation of prion strains. Hfsp J *2*, 332-341.

Fournier, J.G., Escaig-Haye, F., Billette de Villemeur, T., and Robain, O. (1995). Ultrastructural localization of cellular prion protein (PrP^{C}) in synaptic boutons of normal hamster hippocampus. C R Acad Sci III *318*, 339-344.

Fraser, H.M., Gunn, A., Jeffcoate, S.L., and Holland, D.T. (1974). Effect of active immunization to luteinizing hormone releasing hormone on serum and pituitary gonadotrophins, testes and accessory sex organs in the male rat. J Endocrinol *63*, 399-406.

Gabizon, R., McKinley, M.P., Groth, D., and Prusiner, S.B. (1988). Immunoaffinity purification and neutralization of scrapie prion infectivity. Proc Natl Acad Sci U S A *85*, 6617-6621.

Gajdusek, D.C. (1977). Unconventional viruses and the origin and disappearance of kuru. Science *197*, 943-960.

Gajdusek, D.C., Gibbs, C.J., and Alpers, M. (1966). Experimental transmission of a Kuru-like syndrome to chimpanzees. Nature *209*, 794-796.

Gajdusek, D.C., and Zigas, V. (1957). Degenerative disease of the central nervous system in New Guinea; the endemic occurrence of kuru in the native population. N Engl J Med *257*, 974-978.

Garfin, D.E., Stites, D.P., Zitnik, L.A., and Prusiner, S.B. (1978). Suppression of polyclonal B cell activation in scrapie-infected C3H/HeJ mice. J Immunol *120*, 1986-1990.

Georgsson, G., Sigurdarson, S., and Brown, P. (2006). Infectious agent of sheep scrapie may persist in the environment for at least 16 years. J Gen Virol *87*, 3737-3740.

Gerstmann, J., Straussler, E., and Scheinker, I. (1936). Uber eine eigenartige hereditar-familiare Erkrankung des Zentralnervensystems. Zugleich ein Beirtag zur Frage des vorzeitigen lokalen Alterns. Zeitschrift fur die gesamte Neurologie und Pscychiatry *154*, 736-762.

Ghochikyan, A. (2009). Rationale for peptide and DNA based epitope vaccines for Alzheimer's disease immunotherapy. CNS Neurol Disord Drug Targets *8*, 128-143.

Ghosh, S., and Jackson, D.C. (1999). Antigenic and immunogenic properties of totally synthetic peptide-based anti-fertility vaccines. Int Immunol *11*, 1103-1110.

Gibbs, C.J., Jr., Gajdusek, D.C., Asher, D.M., Alpers, M.P., Beck, E., Daniel, P.M., and Matthews, W.B. (1968). Creutzfeldt-Jakob disease (spongiform encephalopathy): transmission to the chimpanzee. Science *161*, 388-389.

Gilch, S., Wopfner, F., Renner-Muller, I., Kremmer, E., Bauer, C., Wolf, E., Brem, G., Groschup, M.H., and Schatzl, H.M. (2003). Polyclonal anti-PrP auto-antibodies induced with dimeric PrP interfere efficiently with PrP^{Sc} propagation in prion-infected cells. J Biol Chem *278*, 18524-18531.

Glatzel, M., Heppner, F.L., Albers, K.M., and Aguzzi, A. (2001). Sympathetic innervation of lymphoreticular organs is rate limiting for prion neuroinvasion. Neuron *31*, 25-34.

Glatzel, M., Ott, P.M., Linder, T., Gebbers, J.O., Gmur, A., Wust, W., Huber, G., Moch, H., Podvinec, M., Stamm, B., and Aguzzi, A. (2003). Human prion diseases: epidemiology and integrated risk assessment. Lancet Neurol *2*, 757-763.

Goldmann, W., Hunter, N., Smith, G., Foster, J., and Hope, J. (1994). PrP genotype and agent effects in scrapie: change in allelic interaction with different isolates of agent in sheep, a natural host of scrapie. J Gen Virol *75 (Pt 5)*, 989-995.

Goni, F., Knudsen, E., Schreiber, F., Scholtzova, H., Pankiewicz, J., Carp, R., Meeker, H.C., Rubenstein, R., Brown, D.R., Sy, M.S.*, et al.* (2005). Mucosal vaccination delays or prevents prion infection via an oral route. Neuroscience *133*, 413-421.

Goni, F., Prelli, F., Schreiber, F., Scholtzova, H., Chung, E., Kascsak, R., Brown, D.R., Sigurdsson, E.M., Chabalgoity, J.A., and Wisniewski, T. (2008). High titers of mucosal and systemic anti-PrP antibodies abrogate oral prion infection in mucosal-vaccinated mice. Neuroscience *153*, 679-686.

Gossert, A.D., Bonjour, S., Lysek, D.A., Fiorito, F., and Wuthrich, K. (2005). Prion protein NMR structures of elk and of mouse/elk hybrids. Proc Natl Acad Sci U S A *102*, 646-650.

Graner, E., Mercadante, A.F., Zanata, S.M., Forlenza, O.V., Cabral, A.L., Veiga, S.S., Juliano, M.A., Roesler, R., Walz, R., Minetti, A.*, et al.* (2000). Cellular prion protein binds laminin and mediates neuritogenesis. Brain Res Mol Brain Res *76*, 85-92.

Gregoire, S., Bergot, A.S., Feraudet, C., Carnaud, C., Aucouturier, P., and Rosset, M.B. (2005). The murine B cell repertoire is severely selected against endogenous cellular prion protein. J Immunol *175*, 6443-6449.

Gregoire, S., Logre, C., Metharom, P., Loing, E., Chomilier, J., Rosset, M.B., Aucouturier, P., and Carnaud, C. (2004). Identification of two immunogenic domains of the prion protein (PrP) which activate class II-restricted T cells and elicit antibody responses against the native molecule. J Leukoc Biol *76*, 125-134.

Griffin, J.K., and Cashman, N.R. (2005). Progress in prion vaccines and immunotherapies. Expert Opin Biol Ther *5*, 97-110.

Grosset, A., Moskowitz, K., Nelsen, C., Pan, T., Davidson, E., and Orser, C.S. (2005). Rapid presymptomatic detection of PrP^{Sc} via conformationally responsive palindromic PrP peptides. Peptides *26*, 2193-2200.

Hadlow, W.J. (1959). Scrapie and Kuru. Lancet *2*, 289-290.

Haigh, C.L., Wright, J.A., and Brown, D.R. (2007). Regulation of prion protein expression by noncoding regions of the Prnp gene. J Mol Biol *368*, 915-927.

Halliwell, B. (2006). Oxidative stress and neurodegeneration: where are we now? J Neurochem *97*, 1634-1658.

Hanan, E., Goren, O., Eshkenazy, M., and Solomon, B. (2001a). Immunomodulation of the human prion peptide 106-126 aggregation. Biochem Biophys Res Commun *280*, 115-120.

Hanan, E., Priola, S.A., and Solomon, B. (2001b). Antiaggregating antibody raised against human PrP 106-126 recognizes pathological and normal isoforms of the whole prion protein. Cell Mol Neurobiol *21*, 693-703.

Handisurya, A., Gilch, S., Winter, D., Shafti-Keramat, S., Maurer, D., Schatzl, H.M., and Kirnbauer, R. (2007). Vaccination with prion peptide-displaying papillomavirus-like particles induces autoantibodies to normal prion protein that interfere with pathologic prion protein production in infected cells. FEBS J *274*, 1747-1758.

Harrison, M.D., and Dameron, C.T. (1999). Molecular mechanisms of copper metabolism and the role of the Menkes disease protein. J Biochem Mol Toxicol *13*, 93-106.

Heggebo, R., Press, C.M., Gunnes, G., Lie, K.I., Tranulis, M.A., Ulvund, M., Groschup, M.H., and Landsverk, T. (2000). Distribution of prion protein in the ileal Peyer's patch of scrapie-free lambs and lambs naturally and experimentally exposed to the scrapie agent. J Gen Virol *81*, 2327-2337.

Heggebo, R., Press, C.M., Gunnes, G., Ulvund, M.J., Tranulis, M.A., and Lsverk, T. (2003). Detection of PrP^{Sc} in lymphoid tissues of lambs experimentally exposed to the scrapie agent. J Comp Pathol *128*, 172-181.

Heikenwalder, M., Zeller, N., Seeger, H., Prinz, M., Klohn, P.C., Schwarz, P., Ruddle, N.H., Weissmann, C., and Aguzzi, A. (2005). Chronic lymphocytic inflammation specifies the organ tropism of prions. Science *307*, 1107-1110.

Heppner, F.L., and Aguzzi, A. (2004). Recent developments in prion immunotherapy. Curr Opin Immunol *16*, 594-598.

Heppner, F.L., Musahl, C., Arrighi, I., Klein, M.A., Rulicke, T., Oesch, B., Zinkernagel, R.M., Kalinke, U., and Aguzzi, A. (2001). Prevention of scrapie pathogenesis by transgenic expression of anti-prion protein antibodies. Science *294*, 178-182.

Herbst, A., McIlwain, S., Schmidt, J.J., Aiken, J.M., Page, C.D., and Li, L. (2009). Prion disease diagnosis by proteomic profiling. J Proteome Res *8*, 1030-1036.

Hooper, N.M., and Turner, A.J. (2008). A new take on prions: preventing Alzheimer's disease. Trends Biochem Sci *33*, 151-155.

Hope, J., Morton, L.J., Farquhar, C.F., Multhaup, G., Beyreuther, K., and Kimberlin, R.H. (1986). The major polypeptide of scrapie-associated fibrils (SAF) has the same size, charge distribution and N-terminal protein sequence as predicted for the normal brain protein (PrP). Embo J *5*, 2591-2597.

Horiuchi, M., and Caughey, B. (1999). Specific binding of normal prion protein to the scrapie form via a localized domain initiates its conversion to the protease-resistant state. EMBO J *18*, 3193-3203.

Houston, F., Goldmann, W., Chong, A., Jeffrey, M., Gonzalez, L., Foster, J., Parnham, D., and Hunter, N. (2003). Prion diseases: BSE in sheep bred for resistance to infection. Nature *423*, 498.

Hsiao, K., Baker, H.F., Crow, T.J., Poulter, M., Owen, F., Terwilliger, J.D., Westaway, D., Ott, J., and Prusiner, S.B. (1989). Linkage of a prion protein missense variant to Gerstmann-Straussler syndrome. Nature *338*, 342-345.

Hu, J., Li, G., Wang, H., Lin, X., and Yao, Z. (2008). Prevention of pathological change and cognitive degeneration of Tg2576 mice by inoculating Abeta(1-15) vaccine. Sci China C Life Sci *51*, 743-750.

Huang, F.P., Farquhar, C.F., Mabbott, N.A., Bruce, M.E., and MacPherson, G.G. (2002). Migrating intestinal dendritic cells transport PrP^{Sc} from the gut. J Gen Virol *83*, 267-271.

Humphrey, J.H. (1981). Tolerogenic or immunogenic activity of hapten-conjugated polysaccharides correlated with cellular localization. Eur J Immunol *11*, 212-220.

Hundt, C., Peyrin, J.M., Haik, S., Gauczynski, S., Leucht, C., Rieger, R., Riley, M.L., Deslys, J.P., Dormont, D., Lasmezas, C.I., and Weiss, S. (2001). Identification of interaction domains of the prion protein with its 37-kDa/67-kDa laminin receptor. EMBO J *20*, 5876-5886.

Hur, K., Kim, J.I., Choi, S.I., Choi, E.K., Carp, R.I., and Kim, Y.S. (2002). The pathogenic mechanisms of prion diseases. Mech Ageing Dev *123*, 1637-1647.

Ikeda, T., Horiuchi, M., Ishiguro, N., Muramatsu, Y., Kai-Uwe, G.D., and Shinagawa, M. (1995). Amino acid polymorphisms of PrP with reference to onset of scrapie in Suffolk and Corriedale sheep in Japan. J Gen Virol *76 (Pt 10)*, 2577-2581.

Ingrosso, L., Vetrugno, V., Cardone, F., and Pocchiari, M. (2002). Molecular diagnostics of transmissible spongiform encephalopathies. Trends Mol Med *8*, 273-280.

Inoue, S., Tanaka, M., Horiuchi, M., Ishiguro, N., and Shinagawa, M. (1997). Characterization of the bovine prion protein gene: the expression requires interaction between the promoter and intron. J Vet Med Sci *59*, 175-183.

Ishibashi, D., Yamanaka, H., Yamaguchi, N., Yoshikawa, D., Nakamura, R., Okimura, N., Yamaguchi, Y., Shigematsu, K., Katamine, S., and Sakaguchi, S. (2007). Immunization with recombinant bovine but not mouse prion protein delays the onset of disease in mice inoculated with a mouse-adapted prion. Vaccine *25*, 985-992.

Iwai, A., Masliah, E., Yoshimoto, M., Ge, N., Flanagan, L., de Silva, H.A., Kittel, A., and Saitoh, T. (1995). The precursor protein of non-A beta component of Alzheimer's disease amyloid is a presynaptic protein of the central nervous system. Neuron *14*, 467-475.

Jakob, A. (1921). Uber eigenartige Erkrankungen des Zentralnervensystems mit bemerkswerten anatomischen Befunden (spastische Pseudosklerose-Encephalomyelopathie mit dissemeirten Degenerationsherden). Vorlaufige Mitteilung. Z. Ges. Neurol. Psychiatry *64*, 147-228.

Janeway, C., Travers, P., and Walport, M. (2001). Immunobiology: The immume system in Health and Disease, 5th edn (New York: Garland Science).

Janus, C., Pearson, J., McLaurin, J., Mathews, P.M., Jiang, Y., Schmidt, S.D., Chishti, M.A., Horne, P., Heslin, D., French, J.*, et al.* (2000). A beta peptide immunization reduces behavioural impairment and plaques in a model of Alzheimer's disease. Nature *408*, 979-982.

Jeffrey, M., Goodsir, C.M., Race, R.E., and Chesebro, B. (2004). Scrapie-specific neuronal lesions are independent of neuronal PrP expression. Ann Neurol *55*, 781-792.

Jeffrey, M., Halliday, W.G., Bell, J., Johnston, A.R., MacLeod, N.K., Ingham, C., Sayers, A.R., Brown, D.A., and Fraser, J.R. (2000). Synapse loss associated with abnormal PrP precedes neuronal degeneration in the scrapie-infected murine hippocampus. Neuropathol Appl Neurobiol *26*, 41-54.

Jinshu, X., Jingjing, L., Duan, P., Zheng, Z., Ding, M., Jie, W., Rongyue, C., and Zhuoyi, H. (2004). The immunogenicity of recombinant and dimeric gonadotrophin-releasing hormone vaccines incorporating a T-helper epitope and GnRH or repeated GnRH units. J Immunol Methods *289*, 111-122.

Johnstone, R.W., Ruefli, A.A., and Lowe, S.W. (2002). Apoptosis: a link between cancer genetics and chemotherapy. Cell *108*, 153-164.

Kao, R.R., Gravenor, M.B., Baylis, M., Bostock, C.J., Chihota, C.M., Evans, J.C., Goldmann, W., Smith, A.J., and McLean, A.R. (2002). The potential size and duration of an epidemic of bovine spongiform encephalopathy in British sheep. Science *295*, 332-335.

Kascsak, R.J., Rubenstein, R., Merz, P.A., Tonna-DeMasi, M., Fersko, R., Carp, R.I., Wisniewski, H.M., and Diringer, H. (1987). Mouse polyclonal and monoclonal antibody to scrapie-associated fibril proteins. J Virol *61*, 3688-3693.

Kasper, K.C., Bowman, K., Stites, D.P., and Prusiner, S.B. (1981). Toward development of assays for scrapie-specific antibodies. In Hamster Immune Responses in Infectious and Oncological Diseases, J.W. Streilein, D.A. Hart, J. Stein-Streilein, W.R. Duncan, and R.E. Billingham, eds. (New York: Plenum Press), pp. 401-413.

Kasper, K.C., Stites, D.P., Bowman, K.A., Panitch, H., and Prusiner, S.B. (1982). Immunological studies of scrapie infection. J Neuroimmunol *3*, 187-201.

Kazantsev, A.G., and Kolchinsky, A.M. (2008). Central role of alpha-synuclein oligomers in neurodegeneration in Parkinson disease. Arch Neurol *65*, 1577-1581.

Khosravani, H., Zhang, Y., Tsutsui, S., Hameed, S., Altier, C., Hamid, J., Chen, L., Villemaire, M., Ali, Z., Jirik, F.R., and Zamponi, G.W. (2008). Prion protein attenuates excitotoxicity by inhibiting NMDA receptors. J Cell Biol *181*, 551-565.

Kim, C.L., Karino, A., Ishiguro, N., Shinagawa, M., Sato, M., and Horiuchi, M. (2004a). Cell-surface retention of PrP^{C} by anti-PrP antibody prevents protease-resistant PrP formation. J Gen Virol *85*, 3473-3482.

Kim, C.L., Umetani, A., Matsui, T., Ishiguro, N., Shinagawa, M., and Horiuchi, M. (2004b). Antigenic characterization of an abnormal isoform of prion protein using a new diverse panel of monoclonal antibodies. Virology *320*, 40-51.

Kindt, T., Goldsby, R., and Osborne, B. (2007). Immunology, 6th edn (New York: W.H. Freeman and Company).

Kirnbauer, R., Booy, F., Cheng, N., Lowy, D.R., and Schiller, J.T. (1992). Papillomavirus L1 major capsid protein self-assembles into virus-like particles that are highly immunogenic. Proc Natl Acad Sci U S A *89*, 12180-12184.

Kirschbaum, W. (1924). Zwei eigenartige Erkrankungen des Zentralnervensystems nach Art der spatischen Pseudoskerlose (Jakob). Zeitschrift fur die gesamte Neurologie und Pscychiatry *92*, 175-220.

Kitamoto, T., Muramoto, T., Mohri, S., Doh-Ura, K., and Tateishi, J. (1991). Abnormal isoform of prion protein accumulates in follicular dendritic cells in mice with Creutzfeldt-Jakob disease. J Virol *65*, 6292-6295.

Klatzo, I., Gajdusek, D.C., and Zigas, V. (1959). Pathology of Kuru. Lab Invest *8*, 799-847.

Klitzman, R.L., Alpers, M.P., and Gajdusek, D.C. (1984). The natural incubation period of kuru and the episodes of transmission in three clusters of patients. Neuroepidemiology *3*, 3-20.

Koch, C.A., Anderson, D., Moran, M.F., Ellis, C., and Pawson, T. (1991). SH2 and SH3 domains: elements that control interactions of cytoplasmic signaling proteins. Science *252*, 668-674.

Kokjohn, T.A., and Roher, A.E. (2009). Antibody responses, amyloid-beta peptide remnants and clinical effects of AN-1792 immunization in patients with AD in an interrupted trial. CNS Neurol Disord Drug Targets *8*, 88-97.

Kolaskar, A.S., and Tongaonkar, P.C. (1990). A semi-empirical method for prediction of antigenic determinants on protein antigens. FEBS Lett *276*, 172-174.

Koller, M.F., Grau, T., and Christen, P. (2002). Induction of antibodies against murine full-length prion protein in wild-type mice. J Neuroimmunol *132*, 113-116.

Konold, T., Lee, Y.H., Stack, M.J., Horrocks, C., Green, R.B., Chaplin, M., Simmons, M.M., Hawkins, S.A., Lockey, R., Spiropoulos, J.*, et al.* (2006). Different prion disease phenotypes result from inoculation of cattle with two temporally separated sources of sheep scrapie from Great Britain. BMC Vet Res *2*, 31.

Korth, C., Stierli, B., Streit, P., Moser, M., Schaller, O., Fischer, R., Schulz-Schaeffer, W., Kretzschmar, H., Raeber, A., Braun, U.*, et al.* (1997). Prion (PrPSc)-specific epitope defined by a monoclonal antibody. Nature *390*, 74-77.

Korth, C., Streit, P., and Oesch, B. (1999). Monoclonal antibodies specific for the native, disease-associated isoform of the prion protein. Methods Enzymol *309*, 106-122.

Kretzschmar, H.A., Prusiner, S.B., Stowring, L.E., and DeArmond, S.J. (1986). Scrapie prion proteins are synthesized in neurons. Am J Pathol *122*, 1-5.

Krieg, A.M., Yi, A.K., Matson, S., Waldschmidt, T.J., Bishop, G.A., Teasdale, R., Koretzky, G.A., and Klinman, D.M. (1995). CpG motifs in bacterial DNA trigger direct B-cell activation. Nature *374*, 546-549.

Krug, A., Towarowski, A., Britsch, S., Rothenfusser, S., Hornung, V., Bals, R., Giese, T., Engelmann, H., Endres, S., Krieg, A.M., and Hartmann, G. (2001). Toll-like receptor expression reveals CpG DNA as a unique microbial stimulus for plasmacytoid dendritic cells which synergizes with CD40 ligand to induce high amounts of IL-12. Eur J Immunol *31*, 3026-3037.

Kruger, D., Thomzig, A., Lenz, G., Kampf, K., McBride, P., and Beekes, M. (2009). Faecal shedding, alimentary clearance and intestinal spread of prions in hamsters fed with scrapie. Vet Res *40*, 4.

Kurschner, C., and Morgan, J.I. (1995). The cellular prion protein (PrP) selectively binds to Bcl-2 in the yeast two-hybrid system. Brain Res Mol Brain Res *30*, 165-168.

Kurschner, C., and Morgan, J.I. (1996). Analysis of interaction sites in homo- and heteromeric complexes containing Bcl-2 family members and the cellular prion protein. Brain Res Mol Brain Res *37*, 249-258.

Larsen, J.E., Lund, O., and Nielsen, M. (2006). Improved method for predicting linear B-cell epitopes. Immunome Res *2*, 2.

Lasmezas, C.I., Deslys, J.P., Robain, O., Jaegly, A., Beringue, V., Peyrin, J.M., Fournier, J.G., Hauw, J.J., Rossier, J., and Dormont, D. (1997). Transmission of the BSE agent to mice in the absence of detectable abnormal prion protein. Science *275*, 402-405.

Lazoura, E., and Apostolopoulos, V. (2005). Insights into peptide-based vaccine design for cancer immunotherapy. Current Medicinal Chemistry *12*, 1481-1494.

Li, L., Napper, S., and Cashman, N.R. (2010). Immunotherapy for prion diseases: opportunities and obstacles. Immunotherapy *2*, 269-282.

Liu, T., Li, R., Wong, B.S., Liu, D., Pan, T., Petersen, R.B., Gambetti, P., and Sy, M.S. (2001). Normal cellular prion protein is preferentially expressed on subpopulations of murine hemopoietic cells. J Immunol *166*, 3733-3742.

Llewelyn, C.A., Hewitt, P.E., Knight, R.S., Amar, K., Cousens, S., Mackenzie, J., and Will, R.G. (2004). Possible transmission of variant Creutzfeldt-Jakob disease by blood transfusion. Lancet *363*, 417-421.

Madampage, C.A., Andrievskaia, O., and Lee, J.S. (2010). Nanopore detection of antibody prion interactions. Anal Biochem *396*, 36-41.

Mallucci, G., Dickinson, A., Linehan, J., Klohn, P.C., Brandner, S., and Collinge, J. (2003). Depleting neuronal PrP in prion infection prevents disease and reverses spongiosis. Science *302*, 871-874.

Manns, J., Barker, C., and Attah-Poku, S. (1997). The design, production, purification, and testing of a chimeric antigen protein to be used as an immunosterilant in domestic animals. Can J Chem *75*, 829-833.

Mattson, M.P. (2004). Pathways towards and away from Alzheimer's disease. Nature *430*, 631-639.

Meloen, R.H., Casal, J.I., Dalsgaard, K., and Langeveld, J.P. (1995). Synthetic peptide vaccines: success at last. Vaccine *13*, 885-886.

Meloen, R.H., Turkstra, J.A., Lankhof, H., Puijk, W.C., Schaaper, W.M., Dijkstra, G., Wensing, C.J., and Oonk, R.B. (1994). Efficient immunocastration of male piglets by immunoneutralization of GnRH using a new GnRH-like peptide. Vaccine *12*, 741-746.

Meslin, F., Hamai, A., Gao, P., Jalil, A., Cahuzac, N., Chouaib, S., and Mehrpour, M. (2007). Silencing of prion protein sensitizes breast adriamycin-resistant carcinoma cells to TRAIL-mediated cell death. Cancer Res *67*, 10910-10919.

Milhavet, O., and Lehmann, S. (2002). Oxidative stress and the prion protein in transmissible spongiform encephalopathies. Brain Res Brain Res Rev *38*, 328-339.

Miller, M.W., Williams, E.S., McCarty, C.W., Spraker, T.R., Kreeger, T.J., Larsen, C.T., and Thorne, E.T. (2000). Epizootiology of chronic wasting disease in free-ranging cervids in Colorado and Wyoming. J Wildl Dis *36*, 676-690.

Mishra, R.S., Basu, S., Gu, Y., Luo, X., Zou, W.Q., Mishra, R., Li, R., Chen, S.G., Gambetti, P., Fujioka, H., and Singh, N. (2004). Protease-resistant human prion protein and ferritin are cotransported across Caco-2 epithelial cells: implications for species barrier in prion uptake from the intestine. J Neurosci *24*, 11280-11290.

Mond, J.J., Vos, Q., Lees, A., and Snapper, C.M. (1995). T cell independent antigens. Curr Opin Immunol *7*, 349-354.

Morel, E., Fouquet, S., Chateau, D., Yvernault, L., Frobert, Y., Pincon-Raymond, M., Chambaz, J., Pillot, T., and Rousset, M. (2004). The cellular prion protein PrP^{C} is expressed in human enterocytes in cell-cell junctional domains. J Biol Chem *279*, 1499-1505.

Mouillet-Richard, S., Ermonval, M., Chebassier, C., Laplanche, J.L., Lehmann, S., Launay, J.M., and Kellermann, O. (2000). Signal transduction through prion protein. Science *289*, 1925-1928.

Muller-Schiffmann, A., and Korth, C. (2008). Vaccine approaches to prevent and treat prion infection : progress and challenges. BioDrugs *22*, 45-52.

Nazor, K.E., Kuhn, F., Seward, T., Green, M., Zwald, D., Purro, M., Schmid, J., Biffiger, K., Power, A.M., Oesch, B*., et al.* (2005). Immunodetection of disease-associated mutant PrP, which accelerates disease in GSS transgenic mice. EMBO J *24*, 2472-2480.

Neutra, M.R. (1999). M cells in antigen sampling in mucosal tissues. Curr Top Microbiol Immunol *236*, 17-32.

Nicoll, J.A., Wilkinson, D., Holmes, C., Steart, P., Markham, H., and Weller, R.O. (2003). Neuropathology of human Alzheimer disease after immunization with amyloid-beta peptide: a case report. Nat Med *9*, 448-452.

Nikles, D., Bach, P., Boller, K., Merten, C.A., Montrasio, F., Heppner, F.L., Aguzzi, A., Cichutek, K., Kalinke, U., and Buchholz, C.J. (2005). Circumventing tolerance to the prion protein (PrP): vaccination with PrP-displaying retrovirus particles induces humoral immune responses against the native form of cellular PrP. J Virol *79*, 4033-4042.

Nordlund, A., and Oliveberg, M. (2008). SOD1-associated ALS: a promising system for elucidating the origin of protein-misfolding disease. HFSP J *2*, 354-364.

Orgogozo, J.M., Gilman, S., Dartigues, J.F., Laurent, B., Puel, M., Kirby, L.C., Jouanny, P., Dubois, B., Eisner, L., Flitman, S.*, et al.* (2003). Subacute meningoencephalitis in a subset of patients with AD after Abeta42 immunization. Neurology *61*, 46-54.

Paltrinieri, S., Comazzi, S., Spagnolo, V., Rondena, M., Ponti, W., and Ceciliani, F. (2004). Bovine Doppel (Dpl) and prion protein (PrP) expression on lymphoid tissue and circulating leukocytes. J Histochem Cytochem *52*, 1639-1645.

Pan, K.M., Baldwin, M., Nguyen, J., Gasset, M., Serban, A., Groth, D., Mehlhorn, I., Huang, Z., Fletterick, R.J., Cohen, F.E., and et al. (1993). Conversion of alpha-helices into beta-sheets features in the formation of the scrapie prion proteins. Proc Natl Acad Sci U S A *90*, 10962-10966.

Paramithiotis, E., Pinard, M., Lawton, T., LaBoissiere, S., Leathers, V.L., Zou, W.Q., Estey, L.A., Lamontagne, J., Lehto, M.T., Kondejewski, L.H.*, et al.* (2003). A prion protein epitope selective for the pathologically misfolded conformation. Nat Med *9*, 893-899.

Parry, H.B. (1962). Scrapie: a transmissible and hereditary disease of sheep. Heredity *17*, 75-105.

Partidos, C., Stanley, C., and Steward, M. (1992). The effect of orientation of epitopes on the immunogenicity of chimeric synthetic peptides representing measles virus protein sequences. Mol Immunol *29*, 651-658.

Pauly, P.C., and Harris, D.A. (1998). Copper stimulates endocytosis of the prion protein. J Biol Chem *273*, 33107-33110.

Peden, A.H., Head, M.W., Ritchie, D.L., Bell, J.E., and Ironside, J.W. (2004). Preclinical vCJD after blood transfusion in a PRNP codon 129 heterozygous patient. Lancet *364*, 527-529.

Peretz, D., Scott, M.R., Groth, D., Williamson, R.A., Burton, D.R., Cohen, F.E., and Prusiner, S.B. (2001a). Strain-specified relative conformational stability of the scrapie prion protein. Protein Sci *10*, 854-863.

Peretz, D., Williamson, R.A., Kaneko, K., Vergara, J., Leclerc, E., Schmitt-Ulms, G., Mehlhorn, I.R., Legname, G., Wormald, M.R., Rudd, P.M., *et al.* (2001b). Antibodies inhibit prion propagation and clear cell cultures of prion infectivity. Nature *412*, 739-743.

Perrier, V., Solassol, J., Crozet, C., Frobert, Y., Mourton-Gilles, C., Grassi, J., and Lehmann, S. (2004). Anti-PrP antibodies block PrP^{Sc} replication in prion-infected cell cultures by accelerating PrP^{C} degradation. J Neurochem *89*, 454-463.

Peters, P.J., Mironov, A., Jr., Peretz, D., van Donselaar, E., Leclerc, E., Erpel, S., DeArmond, S.J., Burton, D.R., Williamson, R.A., Vey, M., and Prusiner, S.B. (2003). Trafficking of prion proteins through a caveolae-mediated endosomal pathway. J Cell Biol *162*, 703-717.

Pilon, J., Loiacono, C., Okeson, D., Lund, S., Vercauteren, K., Rhyan, J., and Miller, L. (2007). Anti-prion activity generated by a novel vaccine formulation. Neurosci Lett *429*, 161-164.

Poduslo, J.F., Curran, G.L., Wengenack, T.M., Malester, B., and Duff, K. (2001). Permeability of proteins at the blood-brain barrier in the normal adult mouse and double transgenic mouse model of Alzheimer's disease. Neurobiol Dis *8*, 555-567.

Poduslo, J.F., Ramakrishnan, M., Holasek, S.S., Ramirez-Alvarado, M., Kandimalla, K.K., Gilles, E.J., Curran, G.L., and Wengenack, T.M. (2007). In vivo targeting of antibody fragments to the nervous system for Alzheimer's disease immunotherapy and molecular imaging of amyloid plaques. J Neurochem *102*, 420-433.

Polymenidou, M., Heppner, F.L., Pellicioli, E.C., Urich, E., Miele, G., Braun, N., Wopfner, F., Schatzl, H.M., Becher, B., and Aguzzi, A. (2004). Humoral immune response to native eukaryotic prion protein correlates with anti-prion protection. Proc Natl Acad Sci U S A *101 Suppl 2*, 14670-14676.

Potter AA, and Manns JG (2000). GnRH-leukotoxin chimeras. (USA, University of Saskatchewan).

Potter, A.A., and Manns, J.G. (2000). GnRH-leukotoxin chimeras. (USA, University of Saskatchewan).

Poulsen, L.L., Reinert, T.M., Sand, R.L., Bisgaard, M., Christensen, H., Olsen, J.E., Stuen, S., and Bojesen, A.M. (2006). Occurrence of haemolytic Mannheimia spp. in apparently healthy sheep in Norway. Acta Vet Scand *47*, 70.

Prinz, M., Montrasio, F., Furukawa, H., van der Haar, M.E., Schwarz, P., Rulicke, T., Giger, O.T., Hausler, K.G., Perez, D., Glatzel, M., and Aguzzi, A. (2004). Intrinsic resistance of oligodendrocytes to prion infection. J Neurosci *24*, 5974-5981.

Prusiner, S.B. (1982). Novel proteinaceous infectious particles cause scrapie. Science *216*, 136-144.

Prusiner, S.B. (1998). Prions. Proc Natl Acad Sci U S A *95*, 13363-13383.

Prusiner, S.B., Garfin, D.E., Cochran, S.P., Baringer, J.R., Hadlow, W.J., Eklund, C.M., and Race, R.E. (1978). Evidence for hydrophobic domains on the surface of the scrapie agent. Trans Am Neurol Assoc *103*, 62-64.

Prusiner, S.B., Garfin, D.E., Cochran, S.P., McKinley, M.P., Groth, D.F., Hadlow, W.J., Race, R.E., and Eklund, C.M. (1980). Experimental scrapie in the mouse: electrophoretic and sedimentation properties of the partially purified agent. J Neurochem *35*, 574-582.

Prusiner, S.B., Groth, D., Serban, A., Koehler, R., Foster, D., Torchia, M., Burton, D., Yang, S.L., and DeArmond, S.J. (1993). Ablation of the prion protein (PrP) gene in mice prevents scrapie and facilitates production of anti-PrP antibodies. Proc Natl Acad Sci U S A *90*, 10608-10612.

Prusiner, S.B., McKinley, M.P., Groth, D.F., Bowman, K.A., Mock, N.I., Cochran, S.P., and Masiarz, F.R. (1981). Scrapie agent contains a hydrophobic protein. Proc Natl Acad Sci U S A *78*, 6675-6679.

Puig, S., and Thiele, D.J. (2002). Molecular mechanisms of copper uptake and distribution. Curr Opin Chem Biol *6*, 171-180.

Purcell, A.W., McCluskey, J., and Rossjohn, J. (2007). More than one reason to rethink the use of peptides in vaccine design. Nat Rev Drug Discov *6*, 404-414.

Purcell, A.W., Zeng, W., Mifsud, N.A., Ely, L.K., Macdonald, W.A., and Jackson, D.C. (2003). Dissecting the role of peptides in the immune response: theory, practice and the application to vaccine design. J Pept Sci *9*, 255-281.

Qi, Y., Zhang, B.Q., Shen, Z., and Chen, Y.H. (2009). Candidate vaccine focused on a classical Swine Fever virus epitope induced antibodies with neutralizing activity. Viral Immunol *22*, 205-213.

Quaglio, E., Chiesa, R., and Harris, D.A. (2001). Copper converts the cellular prion protein into a protease-resistant species that is distinct from the scrapie isoform. J Biol Chem *276*, 11432-11438.

Race, R., Raines, A., Raymond, G.J., Caughey, B., and Chesebro, B. (2001). Long-term subclinical carrier state precedes scrapie replication and adaptation in a resistant species: analogies to bovine spongiform encephalopathy and variant Creutzfeldt-Jakob disease in humans. J Virol *75*, 10106-10112.

Race, R.E., Priola, S.A., Bessen, R.A., Ernst, D., Dockter, J., Rall, G.F., Mucke, L., Chesebro, B., and Oldstone, M.B. (1995). Neuron-specific expression of a hamster prion protein minigene in transgenic mice induces susceptibility to hamster scrapie agent. Neuron *15*, 1183-1191.

Raeber, A.J., Race, R.E., Brandner, S., Priola, S.A., Sailer, A., Bessen, R.A., Mucke, L., Manson, J., Aguzzi, A., Oldstone, M.B*., et al.* (1997). Astrocyte-specific expression of hamster prion protein (PrP) renders PrP knockout mice susceptible to hamster scrapie. Embo J *16*, 6057-6065.

Raggo, C., Habermehl, M., Babiuk, L.A., and Griebel, P. (2000). The *in vivo* effects of recombinant bovine herpesvirus-1 expressing bovine interferon-gamma. J Gen Virol *81*, 2665-2673.

Rakhit, R., Robertson, J., Vande Velde, C., Horne, P., Ruth, D.M., Griffin, J., Cleveland, D.W., Cashman, N.R., and Chakrabartty, A. (2006). An immunological epitope selective for pathological monomer-misfolded SOD1 in ALS. Nat Med *13*, 754-759.

Riek, R., Hornemann, S., Wider, G., Billeter, M., Glockshuber, R., and Wuthrich, K. (1996). NMR structure of the mouse prion protein domain PrP(121-321). Nature *382*, 180-182.

Robbins, S.C., Jelinski, M.D., and Stotish, R.L. (2004). Assessment of the immunological and biological efficacy of two different doses of a recombinant GnRH vaccine in domestic male and female cats (Felis catus). J Reprod Immunol *64*, 107-119.

Roberson, E.D., and Mucke, L. (2006). 100 years and counting: prospects for defeating Alzheimer's disease. Science *314*, 781-784.

Rosset, M.B., Ballerini, C., Gregoire, S., Metharom, P., Carnaud, C., and Aucouturier, P. (2004). Breaking immune tolerance to the prion protein using prion protein peptides plus oligodeoxynucleotide-CpG in mice. J Immunol *172*, 5168-5174.

Rosset, M.B., Sacquin, A., Lecollinet, S., Chaigneau, T., Adam, M., Crespeau, F., and Eloit, M. (2009). Dendritic cell-mediated-immunization with xenogenic PrP and adenoviral vectors breaks tolerance and prolongs mice survival against experimental scrapie. PLoS One *4*, e4917.

Saa, P., Castilla, J., and Soto, C. (2006). Ultra-efficient replication of infectious prions by automated protein misfolding cyclic amplification. J Biol Chem *281*, 35245-35252.

Saborio, G.P., Permanne, B., and Soto, C. (2001). Sensitive detection of pathological prion protein by cyclic amplification of protein misfolding. Nature *411*, 810-813.

Safar, J., Wille, H., Itri, V., Groth, D., Serban, H., Torchia, M., Cohen, F.E., and Prusiner, S.B. (1998). Eight prion strains have PrP(Sc) molecules with different conformations. Nat Med *4*, 1157-1165.

Sambrook, J., and Russell, D. (2001). Molecular cloning: A laboratory manual (Coldspring Harbor, NY: Cold Spring Harbor Laboratory Press).

Sandberg, M.K., Wallen, P., Wikstrom, M.A., and Kristensson, K. (2004). Scrapie-infected GT1-1 cells show impaired function of voltage-gated N-type calcium channels (Ca(v) 2.2) which is ameliorated by quinacrine treatment. Neurobiol Dis *15*, 143-151.

Schally, A.V., Arimura, A., and Kastin, A.J. (1973). Hypothalamic regulatory hormones. Science *179*, 341-350.

Schenk, D., Barbour, R., Dunn, W., Gordon, G., Grajeda, H., Guido, T., Hu, K., Huang, J., Johnson-Wood, K., Khan, K., *et al.* (1999). Immunization with amyloid-beta attenuates Alzheimer-disease-like pathology in the PDAPP mouse. Nature *400*, 173-177.

Schmerr, M.J., Cutlip, R.C., and Jenny, A. (1998). Capillary isoelectric focusing of the scrapie prion protein. J Chromatogr A *802*, 135-141.

Schmerr, M.J., Goodwin, K.R., Cutlip, R.C., and Jenny, A.L. (1996). Improvements in a competition assay to detect scrapie prion protein by capillary electrophoresis. J Chromatogr B Biomed Appl *681*, 29-35.

Schmerr, M.J., and Jenny, A. (1998). A diagnostic test for scrapie-infected sheep using a capillary electrophoresis immunoassay with fluorescent-labeled peptides. Electrophoresis *19*, 409-414.

Schneider, K., Fangerau, H., Michaelsen, B., and Raab, W.H. (2008). The early history of the transmissible spongiform encephalopathies exemplified by scrapie. Brain Res Bull *77*, 343-355.

Schwarz, A., Kratke, O., Burwinkel, M., Riemer, C., Schultz, J., Henklein, P., Bamme, T., and Baier, M. (2003). Immunisation with a synthetic prion protein-derived peptide prolongs survival times of mice orally exposed to the scrapie agent. Neurosci Lett *350*, 187-189.

Seeger, H., Heikenwalder, M., Zeller, N., Kranich, J., Schwarz, P., Gaspert, A., Seifert, B., Miele, G., and Aguzzi, A. (2005). Coincident scrapie infection and nephritis lead to urinary prion excretion. Science *310*, 324-326.

Serpell, L.C., Berriman, J., Jakes, R., Goedert, M., and Crowther, R.A. (2000). Fiber diffraction of synthetic alpha-synuclein filaments shows amyloid-like cross-beta conformation. Proc Natl Acad Sci U S A *97*, 4897-4902.

Shaw, B.F., and Valentine, J.S. (2007). How do ALS-associated mutations in superoxide dismutase 1 promote aggregation of the protein? Trends Biochem Sci *32*, 78-85.

Shyng, S.L., Heuser, J.E., and Harris, D.A. (1994). A glycolipid-anchored prion protein is endocytosed via clathrin-coated pits. J Cell Biol *125*, 1239-1250.

Shyng, S.L., Huber, M.T., and Harris, D.A. (1993). A prion protein cycles between the cell surface and an endocytic compartment in cultured neuroblastoma cells. J Biol Chem *268*, 15922-15928.

Shyu, W.C., Kao, M.C., Chou, W.Y., Hsu, Y.D., and Soong, B.W. (2000). Heat shock modulates prion protein expression in human NT-2 cells. Neuroreport *11*, 771-774.

Sigurdson, C.J., and Aguzzi, A. (2007). Chronic wasting disease. Biochim Biophys Acta *1772*, 610-618.

Sigurdsson, B. (1954). Rida, a chronic encephalitis of sheep: with general remarks on infections which develop slowly and some of their special characteristics. British Veterinary Journal *110*, 341-354.

Sigurdsson, E.M., Brown, D.R., Daniels, M., Kascsak, R.J., Kascsak, R., Carp, R., Meeker, H.C., Frangione, B., and Wisniewski, T. (2002). Immunization delays the onset of prion disease in mice. Am J Pathol *161*, 13-17.

Sigurdsson, E.M., Sy, M.S., Li, R., Scholtzova, H., Kascsak, R.J., Kascsak, R., Carp, R., Meeker, H.C., Frangione, B., and Wisniewski, T. (2003). Anti-prion antibodies for prophylaxis following prion exposure in mice. Neurosci Lett *336*, 185-187.

Silva-Flannery, L.M., Cabrera-Mora, M., Dickherber, M., and Moreno, A. (2009). Polymeric linear Peptide chimeric vaccine-induced antimalaria immunity is associated with enhanced in vitro antigen loading. Infect Immun *77*, 1798-1806.

Solforosi, L., Criado, J.R., McGavern, D.B., Wirz, S., Sanchez-Alavez, M., Sugama, S., DeGiorgio, L.A., Volpe, B.T., Wiseman, E., Abalos, G.*, et al.* (2004). Cross-linking cellular prion protein triggers neuronal apoptosis in vivo. Science *303*, 1514-1516.

Solomon, B. (2004). Alzheimer's disease and immunotherapy. Curr Alzheimer Res *1*, 149-163.

Sorgato, M.C., and Bertoli, A. (2009). From cell protection to death: may Ca2+ signals explain the chameleonic attributes of the mammalian prion protein? Biochem Biophys Res Commun *379*, 171-174.

Soto, C. (2004). Diagnosing prion diseases: needs, challenges and hopes. Nat Rev Microbiol *2*, 809-819.

Souan, L., Tal, Y., Felling, Y., Cohen, I.R., Taraboulos, A., and Mor, F. (2001). Modulation of proteinase-K resistant prion protein by prion peptide immunization. Eur J Immunol *31*, 2338-2346.

Spudich, A., Frigg, R., Kilic, E., Kilic, U., Oesch, B., Raeber, A., Bassetti, C.L., and Hermann, D.M. (2005). Aggravation of ischemic brain injury by prion protein deficiency: role of ERK-1/-2 and STAT-1. Neurobiol Dis *20*, 442-449.

St Rose, S.G., Hunter, N., Matthews, L., Foster, J.D., Chase-Topping, M.E., Kruuk, L.E., Shaw, D.J., Rhind, S.M., Will, R.G., and Woolhouse, M.E. (2006). Comparative evidence for a link between Peyer's patch development and susceptibility to transmissible spongiform encephalopathies. BMC Infect Dis *6*, 5.

Stites, D.P., Garfin, D.E., and Prusiner, S.B. (1979). The immunology of scrapie. In Slow Transmissible Diseases of the Nervous System, S.B. Prusiner, and W.J. Hadlow, eds. (New York: Academic Press), pp. 211-221.

Tang, Y., Zhang, L., Yuan, J., Akbulut, H., Maynard, J., Linton, P.J., and Deisseroth, A. (2004). Multistep process through which adenoviral vector vaccine overcomes anergy to tumor-associated antigens. Blood *104*, 2704-2713.

Tanji, K., Saeki, K., Matsumoto, Y., Takeda, M., Hirasawa, K., Doi, K., Matsumoto, Y., and Onodera, T. (1995). Analysis of PrP^{C} mRNA by *in situ* hybridization in brain, placenta, uterus and testis of rats. Intervirology *38*, 309-315.

Tiegs, S.L., Russell, D.M., and Nemazee, D. (1993). Receptor editing in self-reactive bone marrow B cells. J Exp Med *177*, 1009-1020.

Tobler, I., Gaus, S.E., Deboer, T., Achermann, P., Fischer, M., Rulicke, T., Moser, M., Oesch, B., McBride, P.A., and Manson, J.C. (1996). Altered circadian activity rhythms and sleep in mice devoid of prion protein. Nature *380*, 639-642.

Trevitt, C.R., and Collinge, J. (2006). A systematic review of prion therapeutics in experimental models. Brain *129*, 2241-2265.

Turner, G. (1795). Extracts from a "general" view of the agriculture of the country of Gloucester; with observations on the means of its improvements; drawn up for the consideration of the board of agriculture. Bath and West England Society 7.

van Keulen, L.J., Bossers, A., and van Zijderveld, F. (2008). TSE pathogenesis in cattle and sheep. Vet Res *39*, 24.

van Keulen, L.J., Schreuder, B.E., Meloen, R.H., Mooij-Harkes, G., Vromans, M.E., and Langeveld, J.P. (1996). Immunohistochemical detection of prion protein in lymphoid tissues of sheep with natural scrapie. J Clin Microbiol *34*, 1228-1231.

van Keulen, L.J., Schreuder, B.E., Vromans, M.E., Langeveld, J.P., and Smits, M.A. (2000). Pathogenesis of natural scrapie in sheep. Arch Virol Suppl, 57-71.

Van Loveren, H., Van Amsterdam, J.G., Vandebriel, R.J., Kimman, T.G., Rumke, H.C., Steerenberg, P.S., and Vos, J.G. (2001). Vaccine-induced antibody responses as parameters of the influence of endogenous and environmental factors. Environ Health Perspect *109*, 757-764.

Vana, K., Zuber, C., Nikles, D., and Weiss, S. (2007). Novel aspects of prions, their receptor molecules, and innovative approaches for TSE therapy. Cell Mol Neurobiol *27*, 107-128.

Vanderlugt, C.L., and Miller, S.D. (2002). Epitope spreading in immune-mediated diseases: implications for immunotherapy. Nat Rev Immunol *2*, 85-95.

Vetrugno, V., Cardinale, A., Filesi, I., Mattei, S., Sy, M.S., Pocchiari, M., and Biocca, S. (2005). KDEL-tagged anti-prion intrabodies impair PrP lysosomal degradation and inhibit scrapie infectivity. Biochem Biophys Res Commun *338*, 1791-1797.

Volles, M.J., and Lansbury, P.T., Jr. (2003). Zeroing in on the pathogenic form of alpha-synuclein and its mechanism of neurotoxicity in Parkinson's disease. Biochemistry *42*, 7871-7878.

Volles, M.J., Lee, S.J., Rochet, J.C., Shtilerman, M.D., Ding, T.T., Kessler, J.C., and Lansbury, P.T., Jr. (2001). Vesicle permeabilization by protofibrillar alpha-synuclein: implications for the pathogenesis and treatment of Parkinson's disease. Biochemistry *40*, 7812-7819.

Waggoner, D.J., Bartnikas, T.B., and Gitlin, J.D. (1999). The role of copper in neurodegenerative disease. Neurobiol Dis *6*, 221-230.

Walsh, D.M., and Selkoe, D.J. (2007). A beta oligomers - a decade of discovery. J Neurochem *101*, 1172-1184.

Walter, E.D., Chattopadhyay, M., and Millhauser, G.L. (2006). The affinity of copper binding to the prion protein octarepeat domain: evidence for negative cooperativity. Biochemistry *45*, 13083-13092.

Weise, J., Sandau, R., Schwarting, S., Crome, O., Wrede, A., Schulz-Schaeffer, W., Zerr, I., and Bahr, M. (2006). Deletion of cellular prion protein results in reduced Akt activation, enhanced postischemic caspase-3 activation, and exacerbation of ischemic brain injury. Stroke *37*, 1296-1300.

Weissmann, C. (2004). The state of the prion. Nat Rev Microbiol *2*, 861-871.

Wells, G.A., Scott, A.C., Johnson, C.T., Gunning, R.F., Hancock, R.D., Jeffrey, M., Dawson, M., and Bradley, R. (1987). A novel progressive spongiform encephalopathy in cattle. Vet Rec *121*, 419-420.

Westergard, L., Christensen, H.M., and Harris, D.A. (2007). The cellular prion protein (PrP(C)): its physiological function and role in disease. Biochim Biophys Acta *1772*, 629-644.

White, A.R., Enever, P., Tayebi, M., Mushens, R., Linehan, J., Brandner, S., Anstee, D., Collinge, J., and Hawke, S. (2003). Monoclonal antibodies inhibit prion replication and delay the development of prion disease. Nature *422*, 80-83.

Wilesmith, J.W., Wells, G.A., Cranwell, M.P., and Ryan, J.P. (1988). Bovine spongiform encephalopathy: epidemiological studies. Vet Rec *123*, 638-644.

Will, R. (1999). New variant Creutzfeldt-Jakob disease. Biomed Pharmacother *53*, 9-13.

Will, R.G., Ironside, J.W., Zeidler, M., Cousens, S.N., Estibeiro, K., Alperovitch, A., Poser, S., Pocchiari, M., Hofman, A., and Smith, P.G. (1996). A new variant of Creutzfeldt-Jakob disease in the UK. Lancet *347*, 921-925.

Williams, E.S. (2005). Chronic wasting disease. Vet Pathol *42*, 530-549.

Williams, E.S., and Young, S. (1980). Chronic wasting disease of captive mule deer: a spongiform encephalopathy. J Wildl Dis *16*, 89-98.

Williams, E.S., and Young, S. (1993). Neuropathology of chronic wasting disease of mule deer (Odocoileus hemionus) and elk (Cervus elaphus nelsoni). Vet Pathol *30*, 36-45.

Wimo, A., Winblad, B., and Jonsson, L. (2007). An estimate of the total worldwide societal costs of dementia in 2005. Alzheimers Dement *3*, 81-91.

Zeidler, M., Stewart, G.E., Barraclough, C.R., Bateman, D.E., Bates, D., Burn, D.J., Colchester, A.C., Durward, W., Fletcher, N.A., Hawkins, S.A.*, et al.* (1997). New variant Creutzfeldt-Jakob disease: neurological features and diagnostic tests. Lancet *350*, 903-907.

Zinkernagel, R.M., and Hengartner, H. (2001). Regulation of the immune response by antigen. Science *293*, 251-253.

Zou, W.Q., and Cashman, N.R. (2002). Acidic pH and detergents enhance *in vitro* conversion of human brain PrP^{C} to a PrP^{Sc}-like form. J Biol Chem *277*, 43942-43947.

7.0 APPENDIX A

Tables describing the amino acid and nucleotide sequence for all constructs designed as a part of the thesis work.

Construct	β2(YYR)I
Amino Acid Sequence	GSYYRRYYRYYSGSYYRRYYRYYGSSYYRRYYRYYSGSYYR RYYRYYGSSHHHHHH
Nucleotide Sequence	GGA TCC TAC TAT CGT CGC TAT TAC CGT TAT TAC AGC GGT TCT TAC TAT CGC CGC TAT TAC CGT TAT TAC GGC TCT AGC TAC TAT CGT CGC TAT TAC CGT TAT TAC AGC GGT AGC TAC TAT CGC CGC TAT TAC CGT TAT TAC GGT TCT AGC CAC CAC CAC CAC CAC CAC TGA CCA TGG

Construct	β2(1+YYR+1)L
Amino Acid Sequence	GSVYYRPSGSVYYRPGSSVYYRPSGSVYYRPSGSVYYRPGSSVY YRPSGSVYYRPSGSVYYRPGSSHHHHHH
Nucleotide Sequence	GGA TCC GTT TAC TAT CGT CCT AGC GGT TCT GTG TAC TAT CGC CCG GGC TCT AGC GTT TAC TAT CGT CCG AGC GGT AGC GTC TAC TAT CGC CCT AGC GGT TCT GTC TAC TAT CGT CCG GGC TCT AGC GTT TAC TAT CGC CCT AGC GGT TCT GTT TAC TAT CGT CCG AGC GGT TCT GTC TAC TAT CGC CCT GGT TCT AGC CAC CAC CAC CAC CAC CAC TGA CCA TGG

Construct	β2(1+YYR+1)I
Amino Acid Sequence	GSVYYRPPRYYVPRYYVSGSVYYRPPRYYVPRYYVGSSVYYRP PRYYVPRYYVSGSVYYRPPRYYVPRYYVGSSHHHHHH
Nucleotide Sequence	GGA TCC GTT TAC TAT CGT CCT CCG CGC TAT TAC GTT CCT CGC TAT TAC GTG AGC GGT TCT GTG TAC TAT CGC CCG CCT CGC TAT TAC GTG CCG CGC TAT TAC GTT GGC TCT AGC GTT TAC TAT CGT CCT CCG CGC TAT TAC GTT CCT CGC TAT TAC GTG AGC GGT AGC GTG TAC TAT CGC CCG CCT CGC TAT TAC GTG CCG CGC TAT TAC GTT GGT TCT AGC CAC CAC CAC CAC CAC CAC TGA CCA TGG

Construct	β2(2+YYR+2)L
Amino Acid Sequence	GSQVYYRPVSGSQVYYRPVGSSQVYYRPVSGSQVYYRPVGSSQ VYYRPVSGSQVYYRPVGSSQVYYRPVSGSQVYYRPVGSSHHHH HH
Nucleotide Sequence	GGA TCC CAA GTT TAC TAT CGT CCT GTT AGC GGT TCT CAA GTT TAC TAT CGT CCT GTT GGT TCT AGC CAA GTT TAC TAT CGT CCT GTT AGC GGT TCT CAA GTT TAC TAT CGT CCT GTT GGT TCT AGC CAA GTT TAC TAT CGT CCT GTT AGC GGT TCT CAA GTT TAC TAT CGT CCT GTT GGT TCT AGC CAA GTT TAC TAT CGT CCT GTT AGC GGT TCT CAA GTT TAC TAT CGT CCT GTT GGT TCT AGC CAC CAC CAC CAC CAC CAC TGA CCA TGG

Construct	β2(2+YYR+2)I
Amino Acid Sequence	GSQVYYRPVVPRYYVQVPRYYVQSGSQVYYRPVVPRYYVQVP RYYVQGSSQVYYRPVVPRYYVQVPRYYVQSGSQVYYRPVVPR YYVQVPRYYVQGSSHHHHHH
Nucleotide Sequence	GGA TCC CAA GTT TAC TAT CGT CCT GTT GTC CCT CGT TAT TAC GTT CAA GTT CCT CGT TAT TAC GTT CAA AGC GGT TCT CAA GTT TAC TAT CGT CCT GTT GTC CCT CGT TAT TAC GTT CAA GTT CCT CGT TAT TAC GTT CAA GGT TCT AGC CAA GTT TAC TAT CGT CCT GTT GTC CCT CGT TAT TAC GTT CAA GTT CCT CGT TAT TAC GTT CAA AGC GGT TCT CAA GTT TAC TAT CGT CCT GTT GTC CCT CGT TAT TAC GTT CAA GTT CCT CGT TAT TAC GTT CAA GGT TCT AGC CAC CAC CAC CAC CAC CAC TGA CCA TGG

Construct	β2(3+YYR+1)L
Amino Acid Sequence	GSNQVYYRPSGSNQVYYRPGSSNQVYYRPSGSNQVYYRPGSSN QVYYRPSGSNQVYYRPGSSNQVYYRPSGSNQVYYRPGSSHHHH HH
Nucleotide Sequence	GGA TCC AAT CAA GTT TAC TAT CGT CCT AGC GGT TCT AAT CAA GTT TAC TAT CGT CCT GGT TCT AGC AAT CAA GTT TAC TAT CGT CCT AGC GGT TCT AAT CAA GTT TAC TAT CGT CCT GGT TCT AGC AAT CAA GTT TAC TAT CGT CCT AGC GGT TCT AAT CAA GTT TAC TAT CGT CCT GGT TCT AGC AAT CAA GTT TAC TAT CGT CCT AGC GGT TCT AAT CAA GTT TAC TAT CGT CCT GGT TCT AGC CAC CAC CAC CAC CAC CAC TGA CCA TGG

Construct	β2(3+YYR+1)I
Amino Acid Sequence	GSNQVYYRPPRYYVQNPRYYVQNSGSNQVYYRPPRYYVQNPR YYVQNGSSNQVYYRPPRYYVQNPRYYVQNSGSNQVYYRPPRY YVQNPRYYVQNGSSHHHHHH
Nucleotide Sequence	GGA TCC AAT CAA GTT TAC TAT CGT CCT CCG CGT TAT TAC GTT CAA AAT CCT CGT TAT TAC GTT CAA AAT AGC GGT TCT AAT CAA GTT TAC TAT CGT CCT CCG CGT TAT TAC GTT CAA AAT CCT CGT TAT TAC GTT CAA AAT GGT TCT AGC AAT CAA GTT TAC TAT CGT CCT CCG CGT TAT TAC GTT CAA AAT CCT CGT TAT TAC GTT CAA AAT AGC GGT TCT AAT CAA GTT TAC TAT CGT CCT CCG CGT TAT TAC GTT CAA AAT CCT CGT TAT TAC GTT CAA AAT GGT TCT AGC CAC CAC CAC CAC CAC CAC TGA CCA TGG

Construct	β2(2+YYR+3)I
Amino Acid Sequence	GSQVYYRPVDDVPRYYVQDVPRYYVQSGSQVYYRPVDDVPRY YVQDVPRYYVQGSSQVYYRPVDDVPRYYVQDVPRYYVQSGSQ VYYRPVDDVPRYYVQDVPRYYVQSGSHHHHHH
Nucleotide Sequence	GGA TCC CAA GTT TAC TAT CGT CCT GTT GAT GAT GTA CCG CGC TAT TAC GTT CAG GAT GTC CCT CGC TAT TAC GTG CAG AGC GGT TCT CAA GTG TAC TAT CGC CCG GTC GAT GAT GTA CCT CGC TAT TAC GTG CAA GAT GTT CCG CGC TAT TAC GTT CAG GGC TCT AGC CAG GTT TAC TAT CGT CCT GTC GAT GAT GTG CCG CGC TAT TAC GTT CAG GAT GTA CCT CGC TAT TAC GTG CAA AGC GGT AGC CAG GTG TAC TAT CGC CCG GTC GAT GAT GTT CCT CGC TAT TAC GTG CAA GAT GTA CCG CGC TAT TAC GTT CAG GGT TCT AGC CAC CAC CAC CAC CAC CAC TGA CCA TGG

Construct	β2(2+YYR+4)I
Amino Acid Sequence	GSQVYYRPVDQQDVPRYYVQQDVPRYYVQSGSQVYYRPVDQ QDVPRYYVQQDVPRYYVQGSSQVYYRPVDQQDVPRYYVQQD VPRYYVQSGSQVYYRPVDQQDVPRYYVQQDVPRYYVQGSSHH HHHH
Nucleotide Sequence	GGA TCC CAA GTT TAC TAT CGT CCT GTT GAT CAG CAG GAT GTA CCG CGC TAT TAC GTT CAG CAG GAT GTC CCT CGC TAT TAC GTG CAG AGC GGT TCT CAA GTG TAC TAT CGC CCG GTC GAT CAG CAG GAT GTA CCT CGC TAT TAC GTG CAA CAG GAT GTT CCG CGC TAT TAC GTT CAG GGC TCT AGC CAG GTT TAC TAT CGT CCT GTC GAT CAG CAG GAT GTG CCG CGC TAT TAC GTT CAG CAG GAT GTA CCT CGC TAT TAC GTG CAA AGC GGT AGC CAG GTG TAC TAT CGC CCG GTC GAT CAG CAG GAT GTT CCT CGC TAT TAC GTG CAA CAG GAT GTA CCG CGC TAT TAC GTT CAG GGT TCT AGC CAC CAC CAC CAC CAC CAC TGA CCA TGG

Construct	β2(2+YYR+5)I
Amino Acid Sequence	GSQVYYRPVDQYYQDVPRYYVQYQDVPRYYVQSGSQVYYRPV DQYYQDVPRYYVQYQDVPRYYVQGSSQVYYRPVDQYYQDVPR YYVQYQDVPRYYVQSGSQVYYRPVDQYYQDVPRYYVQYQDV PRYYVQGSSHHHHHH
Nucleotide Sequence	GGA TCC CAA GTT TAC TAT CGT CCT GTT GAT CAG TAT TAT CAG GAT GTA CCG CGC TAT TAC GTT CAG TAT CAG GAT GTC CCT CGC TAT TAC GTG CAG AGC GGT TCT CAA GTG TAC TAT CGC CCG GTC GAT CAG TAT TAT CAG GAT GTA CCT CGC TAT TAC GTG CAA TAT CAG GAT GTT CCG CGC TAT TAC GTT CAG GGC TCT AGC CAG GTT TAC TAT CGT CCT GTC GAT CAG TAT TAT CAG GAT GTG CCG CGC TAT TAC GTT CAG TAT CAG GAT GTA CCT CGC TAT TAC GTG CAA AGC GGT AGC CAG GTG TAC TAT CGC CCG GTC GAT CAG TAT TAT CAG GAT GTT CCT CGC TAT TAC GTG CAA TAT CAG GAT GTA CCG CGC TAT TAC GTT CAG GGT TCT AGC CAC CAC CAC CAC CAC CAC TGA CCA TGG

Construct	β2(2+YYR+6)I
Amino Acid Sequence	GSQVYYRPVDQYSSYQDVPRYYVQSYQDVPRYYVQSGSQVYY RPVDQYSSYQDVPRYYVQSYQDVPRYYVQGSSQVYYRPVDQY SSYQDVPRYYVQSYQDVPRYYVQSGSQVYYRPVDQYSSYQDV PRYYVQSYQDVPRYYVQGSSHHHHHH
Nucleotide Sequence	GGA TCC CAA GTT TAC TAT CGT CCT GTT GAT CAG TAT AGT AGT TAT CAG GAT GTA CCG CGC TAT TAC GTT CAG AGT TAT CAG GAT GTC CCT CGC TAT TAC GTG CAG AGC GGT TCT CAA GTG TAC TAT CGC CCG GTC GAT CAG TAT AGT AGT TAT CAG GAT GTA CCT CGC TAT TAC GTG CAA AGT TAT CAG GAT GTT CCG CGC TAT TAC GTT CAG GGC TCT AGC CAG GTT TAC TAT CGT CCT GTC GAT CAG TAT AGT AGT TAT CAG GAT GTG CCG CGC TAT TAC GTT CAG AGT TAT CAG GAT GTA CCT CGC TAT TAC GTG CAA AGC GGT AGC CAG GTG TAC TAT CGC CCG GTC GAT CAG TAT AGT AGT TAT CAG GAT GTT CCT CGC TAT TAC GTG CAA AGT TAT CAG GAT GTA CCG CGC TAT TAC GTT CAG GGT TCT AGC CAC CAC CAC CAC CAC CAC TGA CCA TGG

Construct	β2(2+YYR+7)I
Amino Acid Sequence	GSQVYYRPVDQYSNNSYQDVPRYYVQNSYQDVPRYYVQSGSQ VYYRPVDQYSNNSYQDVPRYYVQNSYQDVPRYYVQGSSQVYY RPVDQYSNNSYQDVPRYYVQNSYQDVPRYYVQSGSQVYYRPV DQYSNNSYQDVPRYYVQNSYQDVPRYYVQGSSHHHHHH
Nucleotide Sequence	GGA TCC CAA GTT TAC TAT CGT CCT GTT GAT CAG TAT AGT AAC AAC AGT TAT CAG GAT GTA CCG CGC TAT TAC GTT CAG AAC AGT TAT CAG GAT GTC CCT CGC TAT TAC GTG CAG AGC GGT TCT CAA GTG TAC TAT CGC CCG GTC GAT CAG TAT AGT AAC AAC AGT TAT CAG GAT GTA CCT CGC TAT TAC GTG CAA AAC AGT TAT CAG GAT GTT CCG CGC TAT TAC GTT CAG GGC TCT AGC CAG GTT TAC TAT CGT CCT GTC GAT CAG TAT AGT AAC AAC AGT TAT CAG GAT GTG CCG CGC TAT TAC GTT CAG AAC AGT TAT CAG GAT GTA CCT CGC TAT TAC GTG CAA AGC GGT AGC CAG GTG TAC TAT CGC CCG GTC GAT CAG TAT AGT AAC AAC AGT TAT CAG GAT GTT CCT CGC TAT TAC GTG CAA AAC AGT TAT CAG GAT GTA CCG CGC TAT TAC GTT CAG GGT TCT AGC CAC CAC CAC CAC CAC CAC TGA CCA TGG

Construct	β2(2+YYR+8)I
Amino Acid Sequence	GSQVYYRPVDQYSNQQNSYQDVPRYYVQQNSYQDVPRYYVQS GSQVYYRPVDQYSNQQNSYQDVPRYYVQQNSYQDVPRYYVQG SSQVYYRPVDQYSNQQNSYQDVPRYYVQQNSYQDVPRYYVQS GSQVYYRPVDQYSNQQNSYQDVPRYYVQQNSYQDVPRYYVQG SSHHHHHH
Nucleotide Sequence	GGA TCC CAA GTT TAC TAT CGT CCT GTT GAT CAG TAT AGT AAC CAG CAG AAC AGT TAT CAG GAT GTA CCG CGC TAT TAC GTT CAG CAG AAC AGT TAT CAG GAT GTC CCT CGC TAT TAC GTG CAG AGC GGT TCT CAA GTG TAC TAT CGC CCG GTC GAT CAG TAT AGT AAC CAG CAG AAC AGT TAT CAG GAT GTA CCT CGC TAT TAC GTG CAA CAG AAC AGT TAT CAG GAT GTT CCG CGC TAT TAC GTT CAG GGC TCT AGC CAG GTT TAC TAT CGT CCT GTC GAT CAG TAT AGT AAC CAG CAG AAC AGT TAT CAG GAT GTG CCG CGC TAT TAC GTT CAG CAG AAC AGT TAT CAG GAT GTA CCT CGC TAT TAC GTG CAA AGC GGT AGC CAG GTG TAC TAT CGC CCG GTC GAT CAG TAT AGT AAC CAG CAG AAC AGT TAT CAG GAT GTT CCT CGC TAT TAC GTG CAA CAG AAC AGT TAT CAG GAT GTA CCG CGC TAT TAC GTT CAG GGT TCT AGC CAC CAC CAC CAC CAC CAC TGA CCA TGG

Construct	β2(2+YYR+9)I
Amino Acid Sequence	GSQVYYRPVDQYSNQNNQNSYQDVPRYYVQNQNSYQDVPRY YVQSGSQVYYRPVDQYSNQNNQNSYQDVPRYYVQNQNSYQD VPRYYVQGSSQVYYRPVDQYSNQNNQNSYQDVPRYYVQNQNS YQDVPRYYVQSGSQVYYRPVDQYSNQNNQNSYQDVPRYYVQ NQNSYQDVPRYYVQSGSHHHHHH
Nucleotide Sequence	GGA TCC CAA GTA TAT TAT CGT CCG GTG GAT CAG TAT AGC AAC CAG AAC AAC CAG AAC AGC TAC CAG GAT GTG CCG CGT TAC TAC GTT CAG AAC CAG AAC TCT TAT CAA GAT GTA CCG CGT TAC TAC GTG CAG TCC GGC AGC CAA GTG TAC TAC CGC CCG GTT GAT CAG TAC AGC AAC CAA AAC AAC CAG AAC AGC TAT CAA GAC GTA CCG CGT TAT TAC GTT CAA AAC CAG AAC TCC TAC CAG GAT GTA CCG CGT TAC TAC GTT CAG GGT TCC TCT CAG GTG TAT TAT CGT CCG GTT GAC CAG TAT TCT AAC CAA AAC AAC CAG AAT TCT TAC CAG GAC GTG CCG CGC TAC TAC GTA CAG AAT CAG AAC TCC TAC CAG GAC GTG CCG CGC TAT TAC GTT CAG TCT GGT TCC CAG GTG TAC TAT CGT CCA GTG GAC CAG TAC TCC AAC CAG AAC AAC CAG AAT TCT TAC CAG GAT GTT CCG CGC TAC TAC GTT CAG AAT CAG AAC AGC TAC CAG GAC GTT CCA CGT TAT TAT GTT CAG GGT TCT AGC CAC CAC CAC CAC CAC CAC TGA CCA TGG

Construct	β2(9+YYR+2)I
Amino Acid Sequence	GSNMYRYPNQVYYRPVVPRYYVQNPYRYMNVPRYYVQNPYR YMNSGSNMYRYPNQVYYRPVVPRYYVQNPYRYMNVPRYYVQ NPYRYMNGSSNMYRYPNQVYYRPVVPRYYVQNPYRYMNVPR YYVQNPYRYMNSGSNMYRYPNQVYYRPVVPRYYVQNPYRYM NVPRYYVQNPYRYMNSGSHHHHHH
Nucleotide Sequence	GGA TCC AAC ATG TAC CGT TAC CCT AAC CAG GTG TAT TAT CGT CCG GTA GTT CCA CGT TAC TAT GTG CAG AAC CCG TAT CGC TAC ATG AAT GTT CCG CGT TAC TAT GTC CAG AAC CCA TAC CGT TAC ATG AAC TCT GGT TCC AAT ATG TAC CGT TAC CCG AAC CAG GTC TAC TAC CGT CCG GTT GTG CCA CGT TAC TAC GTG CAG AAT CCG TAC CGC TAC ATG AAC GTA CCT CGT TAC TAC GTT CAG AAC CCG TAT CGT TAT ATG AAC GGC AGC TCT AAC ATG TAC CGT TAT CCG AAC CAG GTT TAT TAC CGT CCG GTA GTT CCG CGC TAT TAC GTA CAA AAC CCG TAT CGT TAC ATG AAC GTC CCG CGC TAC TAT GTT CAG AAC CCG TAC CGT TAT ATG AAC TCC GGT TCT AAC ATG TAC CGC TAT CCG AAC CAG GTT TAC TAC CGC CCT GTG GTT CCG CGC TAT TAC GTT CAG AAC CCA TAT CGC TAC ATG AAC GTG CCG CGT TAT TAC GTA CAA AAT CCG TAC CGT TAC ATG AAC GGT TCT AGC CAC CAC CAC CAC CAC CAC TGA CCA TGG

Construct	α1(2+YYR+2)I
Amino Acid Sequence	GSDRYYRENNERYYRDNERYYRDSGSDRYYRENNERYYRDNE RYYRDGSSDRYYRENNERYYRDNERYYRDSGSDRYYRENNER YYRDNERYYRDGSSHHHHHH
Nucleotide Sequence	GGA TCC GAT CGT TAC TAT CGC GAA AAC AAT GAG CGT TAC TAC CGT GAC AAC GAA CGC TAT TAC CGT GAT TCT GGC TCC GAC CGT TAC TAT CGT GAA AAC AAC GAA CGT TAC TAT CGT GAT AAC GAG CGC TAC TAC CGC GAC GGT AGC TCT CAT GAT CGT TAC TAT CGC GAA AAC AAT GAG CGT TAC TAC CGT GAC AAC GAA CGC TAT TAC CGT GAT TCT GGC TCC GAC CGT TAC TAT CGT GAA AAC AAC GAA CGT TAC TAT CGT GAT AAC GAG CGC TAC TAC CGC GAC GGT AGC TCT CAT CAC CAC CAC CAC CAC TGA CCA TGG